The Effects of Polymer-Mediated Immunocamouflage on Allorecognition of Blood Cells

by

DANA PRICE

B.Sc., The University of Alberta, 2004

A THESIS SUBMITTED IN PARTIAL FULFILLMENT OF

THE REQUIREMENTS FOR THE DEGREE OF

DOCTOR OF PHILOSOPHY

in

THE FACULTY OF GRADUATE AND POSTDOCTORAL STUDIES

(Pathology and Laboratory Medicine)

THE UNIVERSITY OF BRITISH COLUMBIA

(Vancouver)

December, 2014

Abstract

Allorecognition initiates the adverse events of red blood cell (RBC) alloimunization and tissue rejection. Current clinical approaches utilize tissue matching (HLA and blood typing) and immunosuppressive agents to attenuate allorecognition. These practices, however, lead to inventory and drug toxicity issues. Immunocamouflage of cell surfaces by the covalent grafting of methoxypoly(ethylene glycol) (mPEG; PEGylation) has potential utility for prevention of allorecognition. Previous studies have demonstrated the efficacy of immune cell and tissue immunocamouflage both *in vitro* and *in vivo*. However, the use of alternative polymers and the consequences of surface modification during allorecognition events have not been fully defined. To this end, we compared the traditionally utilized mPEG, to a novel polymer species polyethyloxazoline (PEOZ) to explore the effects of polymer grafting to human RBC and leukocytes (WBC) on cell structure, function, viability, as well as allorecognition. PEOZ has attributes that make it an attractive alternative to mPEG, and from a cellular bioengineering perspective, the low viscosity and decreased hydrophilicity of PEOZ could offer some biological and therapeutic advantages. Our studies showed that although PEOZ mediated significant immunocamouflage of cells, mPEG demonstrated improved efficacy in RBC studies. However, PEOZ would be useful for the immunocamouflage of cells, especially for patients that exhibit anti-PEG antibodies. Furthermore, we assessed the consequences of mPEG surface modification to WBC interactions and intracellular events during allorecognition. Our results demonstrated significant camouflage of surface proteins; decreased cell interactions; reduced NFκB activation, which resulted in decreased inflammatory cytokines such as IL2 and IL2Rα expression; and minimal effects to cell viability in modified cells during allogeneic challenge. The global camouflage of cells may decrease activation of numerous pathways and events responsible for cell proliferation during allorecognition. This makes PEGylation a viable non-toxic alternative to current immunosuppressive therapies. These findings demonstrated the

therapeutic potential of both traditional mPEG and novel polymer alternatives. Furthermore, this work defined several mechanisms responsible for the decreased alloresponse of immunocamouflaged cells. Our results showed the clear potential for polymer-based bioengineering to modulate the immune response to allogeneic cells and would be useful for the prevention of allorecognition in transplantation and transfusion medicine.

Preface

Chapters 2, 3 and 5 contain content published in a manuscript entitled “Comparative efficacy of blood cell immunocamouflage by membrane grafting of methoxypoly(ethylene glycol) and polyethyloxazoline”. Kyluik-Price DL, Li L, and Scott MD. *Biomaterials*. 2014 Jan; 35:412-422. Material has been used with permission from applicable source. Monocyte monolayer assay (MMA) experiments, demonstrating immunocamouflage of RhD+ opsonized red blood cells, were performed by Dr. Li Li.

Ethics approval for studies presented in Chapters 3 and 4 was obtained from The University of British Columbia. Certificate#: H02-70215 entitled “Transfusion of Antigenically Modified Erythrocytes”.

Table of Contents

List of Tables

List of Figures

List of Acronyms and Abbreviations

7-AAD	7-amino-actinomycin D
ANOVA	Analysis of variance
AP1	Activator protein 1
APC	Antigen presenting cell
BCA	Bicinchoninic acid assay
BCR	B cell receptor
BSA	Bovine serum albumin
°C	Degrees Celsius
CD	Cluster of differentiation
cDNA	Complementary deoxyribonucleic acid
CDR	Complemetarity determining region
CFSE	Carboxyfluorescein diacetate succinimidyl ester
CSF	Colony stimulating factor
Ct	Threshold cycle
CTLA	Cytotoxic T-lymphocyte-associated antigen
DC	Dendritic cell
DNA	Deoxyribonucleic acid
EASIA	Enzyme amplified sensitivity immuno assay
F3	Tissue factor
Fc	Fragment crystallizable region
FDA	Food and Drug Administration
FITC	Fluorescein isothiocyanate
GVHD	Graft *versus* host disease
GM-CSF	Granulocyte-macrophage colony stimulating factor
HEPES	4-(2-hydroxyethyl)-1-piperazineethanesulfonic acid
HLA	Human leukocyte antigen
HPG	Hyperbranched polyglycerol
ICAM	Intercellular adhesion molecule
Ig	Immunoglobulin
IL	Interleukin
IFN	Interferon
k	Kell

K	Lysine
kDa	Kilodalton
LFA	Lymphocyte function associated antigen
MCF	Mean cell fluorescence
MMA	Monocyte monolayer assay
µg	Microgram
µm	Micrometer
mg	Milligram
MHC	Major histocompatibility complex
Min	Minutes
MLR	Mixed lymphocyte reaction
mM	Millimolar
MoDC	Monocyte derived dendritic cells
mPEG	Methoxypoly(ethylene glycol)
mRNA	Messenger ribonucleic acid
mTOR	Mammalian target of rapamycin
MW	Molecular weight
NFAT	Nuclear factor of activated T cells
NHS	N-hydroxy succinimide
NFκB	Nuclear Factor-κB
NK cell	Natural killer cell
nm	Nanometers
OD	Optical density
PBMC	Peripheral blood mononuclear cells
PBS	Phosphate buffered saline
PD	Programmed death
PE	R-Phycoerythrin
PEG	Polyethylene glycol
PerCP	Peridinin chlorophyll
PEOZ	Polyethyloxazoline
PG	Polyglycerol
POZ	Polyoxazoline
PPC	Percent Positive Cells
pRBC	Packed red blood cells

qPCR	Quantitative polymerase chain reaction
RBC	Red blood cells
R_F	Flory radius
Rh	Rhesus factor
RIPA	Radioimmunoprecipitation assay buffer
RNA	Ribonucleic acid
SEM	Standard error mean
SDS-PAGE	Sodium dodecyl sulfate polyacrylamide gel electrophoresis
SPA	Succinimidyl propionate
STAT	Signal transducers and activators of transcription
SVA	Succinimidyl valerate
Tc	Cytotoxic T cells
TCR	T cell receptor
TGF	Transforming growth factor
Th	Helper T cell
TNF	Tumor necrosis factor
Treg	Regulatory T cell
WBC	White blood cells

Acknowledgements

First, I would like to thank my amazing and loving husband, family, and friends who have been so encouraging and supportive throughout this journey. To my supervisor Dr. Mark Scott- who has guided me through this project- thank you for your mentorship, encouragement, and great sense of humor. I would like to thank Dr. David Walker, for your insights, enthusiasm, support, and for encouraging me to enter graduate studies. I would also like to acknowledge my fellow lab members, past and present, which have made this process so enjoyable because of their friendship and helpful discussions. A special thank you to Dr. Yevgeniya Le, Dr. Duncheng Wang, Wendy Toyofuku, and members of the Devine Lab for your technical expertise and valuable suggestions. Finally, I would like to thank my thesis supervisory committee Dr. Maria Gyongyossy-Issa, Dr. Bruce Verchere, Dr. Marc Horwitz and Dr. Hélène Côté for your guidance and expert advice. Without your support, I would not have succeeded with this project.

Dedication

To my wonderful husband Stephen.

1 CHAPTER 1- Introduction

1.1 Overview

Blood transfusions and organ transplants date back hundreds of years, but due to unpredictable and often fatal outcomes, transplantation of blood and tissues was not established as a therapeutic reality until the beginning of the 20th century. Advances in immunology and immunosuppressant drug therapies were major developments that contributed to greater transfusion and transplantation success. However, modern transfusion and transplantation is still hindered by immunological rejection of foreign cells and tissues. This is due to both the antigenic diversity of human cells, which impedes tissue matching; and the complex nature of the immune response after recognition of foreign tissues, which requires the use of broadly acting and toxic immunosuppressant drugs. Together, these factors result in poor long-term outcomes for the transplanted cells and tissues as well as for the patients. Therefore, new methods of preventing recognition and rejection of foreign tissues are needed. The covalent attachment of non-toxic, non-immunogenic polymers to proteins and other small molecules has been used successfully to prevent immune recognition, resulting in increased circulation and decreased antigenicity. More recently, this technology has been applied to intact cells and tissues resulting in the immunocamouflage of cells by preventing immune recognition of foreign tissue components. This approach may prove useful in transfusion and transplantation medicine.

1.2 Transfusion and Transplantation

1.2.1 History

Transplantation is defined as the transfer of tissues or cells from one individual to another, which includes transfusion components (RBC, platelets), tissues or organs. The earliest transplantations were blood transfusions, followed by tissues and solid organs. The

development of transfusion and transplantation medicine has initiated, paralleled and been the consequence of advancement in other areas of science. For example, organ removal and transplantation became a successful strategy for investigating immunological processes and the function of organs. Conversely, the progression of surgical methodologies and the discovery of immune processes paved the way for the modernization of transfusion and transplantation medicine.

The discovery of blood circulation in the 17th century by William Harvey prompted greater interest in blood transfusion. Harvey's observations led to the hypothesis that the heart was responsible for circulating blood throughout the body *via* venous and arteriole circulatory systems [1,2]. This discovery stimulated the first attempts at animal blood transfusions by Richard Lower [3,4] and human blood transfusions by Jean Baptiste Denis [5] in the 1660's. Although these early transfusions (using sheep blood) were unsuccessful, they provided valuable information concerning interspecies compatibility and evidence of the danger of interspecies transfusions. In 1668 Denis conducted serial transfusions of calf blood into humans, which is now recognized as the first-recorded description of hemolytic transfusion response due to interspecies incompatibility [6], although the risks of interspecies transfusions were not officially accepted until the late 19th century [6,7]. Due to the lack of success, the practice of transfusion was largely halted until 1818 when James Blundell successfully performed the first human-to-human blood transfusion to treat postpartum hemorrhage [8]. However, severe transfusion reactions still occurred even with the use of human blood.

Safer transfusions awaited the discovery of major blood group antigens (A, B and O) by Karl Landsteiner in 1901 [9]. The identification of blood groups and implementation of cross matching, proposed by Ludvig Hektoen [10], helped to prevent some of the severe reactions observed in previous patients. This led to the first successful human blood transfusion using ABO typed and cross-matched blood by Reuben Ottenburg [11]. Despite the use of cross

matching, transfusion failures persisted until the introduction of sterile methodologies and anticoagulation agents.

The identification of bacterial/fungal contamination in 1865 by Pasteur resulted in the development of sterilization and aseptic methods preventing many of the common infections associated with transfusion [6]. This was followed by the introduction of sodium citrate in 1915, providing a practical means to prevent coagulation of donor blood, and made indirect transfusion possible [12]. Moreover, the discovery of the Rh blood group system in 1940 by Karl Landsteiner, Alexander Wiener, and Philip Levine led to further improvements in transfusion safety [13]. These events paved the way for modern transfusions, leading to the establishment of blood banks and national blood collection centers by the 1940's, approximately 300 years after the first documented blood transfusion.

Like blood transfusions, tissue transplantation has its origins in the late 19th century when early reports of skin grafts and bone transplantations emerged, yet it was not until 1936 that the first solid organ transplant was reported using a cadaveric kidney [14]. Early transplants failed in part due to lack of surgical techniques and suitable organ preservation. However, after cellular, humoral, and complement constituents of the immune response were discovered in the late 19th century, evidence emerged that it was the immune response that was a major impediment to transfusion and transplantation success.

Modern transplantation immunology is typically dated back to experiments performed by Peter Medawar in the 1940's. Medawar hypothesized that the rejection of skin allografts was an immunological phenomenon [15,16]. Medawar's work demonstrated the potency of the "host *vs* graft" response, and features of the cell-mediated events were later expanded on by Mitchison [17]. Subsequently, Gorer and Snell described the major histocompatibility complex (MHC) for the genetic locus that encodes antigens involved in allograft rejection and cell-mediated immunity in mice [18,19]. By the late 1950's the first human MHC antigens (human leukocyte antigens [HLA]) were discovered by Dausset and van Rood [20,21]. During the next two

decades virtually all of the common HLA antigens were identified, further elucidating the role they play in tissue rejection.

The first successful organ transplant arose by avoiding the immune response when Joseph Murray successfully transplanted the first kidney from identical twins in 1954 [22]. This was followed by a series of twin transplants around the world. Until HLA matching became more commonplace [23], methods to inhibit the immune response were needed to overcome rejection of mismatched foreign tissue, increasing transplantation utility. Progress came with the introduction of immunosuppressive drugs. The first drug azathioprine, and its derivative mercaptopurine, enabled the transplant of unrelated donor kidneys, resulting in the first cadaveric kidney to be successfully transplanted in 1962 [24]. This was followed by the first lung (1963) [25], pancreas (1966) [26], liver (1967) [27] and heart (1967) [28] transplants. The utilization of donor-matched tissues and the discovery of additional immunosuppressive agents such as cyclosporine (1972) [29,30] and later tacrolimus (1984) [31] increased transplantation success, and graft survival, with > 80% of kidneys surviving to 1 year [32]. Furthermore, the discovery of organ and tissue preservation solution allowed increased organ to transplant time and decreased tissue destruction [33-35].

1.2.2 Types of Transplantations and Outcomes

Both the number and types of tissues that could be transfused or transplanted rose with the advent of blood and tissue matching, immunosuppressive agents, and superior surgical techniques. Currently transplanted solid organs include heart, lung, liver, pancreas and intestine, as well as tissue such as bone marrow, red blood cells, platelets, corneas, bone, tendons, heart valves, blood vessels, and skin. In the past decade, the demands for transfusions and transplantations have grown, resulting in the expansion of national and international programs and facilities involved in the recruitment, procurement, testing and distribution of cells, tissues and organs.

Although national transfusion and transplantation centers facilitate matching and efficient utilization of donor tissues, there remains a continued imbalance between the supply and number of patients requiring therapy. This imbalance is due to several factors, including the quantity of blood donors and healthy organs as well as locating suitably matched tissues. For example, the World Health Organization estimates that 108 million units of blood were collected in 2012, but over half of the blood collected was in high income countries resulting in global supply shortages and delayed access to safe blood in countries with low donation rates [36]. Similarly 114,690 solid organs were transplanted in 2012, which met only 10% of the global need [37]. There remains an estimated 200,000 people on the wait-list worldwide for kidneys alone. In Canada, over 1 million units of blood were collected and 2,100 solid organs were transplanted in 2011 and 2010, respectively [38,39].

In addition to supply, constraints in finding suitably matched tissues remains a significant problem. For example, chronically transfused individuals can become sensitized to multiple blood group antigens, making it difficult to find matched blood units. Similarly, finding suitably matched organs is problematic due to the genetic diversity of tissue antigens. Although the rate of acute rejection has decreased over the last two decades [40] with improved immunosuppressive regimes, drugs are less effective against chronic rejection. In addition, immunosuppressive drugs are often toxic and lead to increased rates of infection and decreased graft survival. For example, the 5-year failure rate for solid organs is 26.2% for kidneys, 21.3% for liver and 50.5% for intestines. Furthermore, there is a 19% post-transplant mortality rate for heart transplants and the median survival for all lung transplant recipients is only 5.3 years [40].

1.3 The Antigenic Properties of Human Cells

As previously discussed, rejection of organs and tissues remains a major obstacle in transfusion and transplantation medicine. Rejection occurs when immune cells recognize cells

or tissues as foreign. This occurs, in large part, due to the antigenic diversity of human cells. An antigen is defined as any molecule or part of a molecule that is recognized specifically by immune cells. Alloantigens are antigens that differ between the same species and an alloreactive response is generated against alloantigens. It is the recognition (allorecognition) of alloantigens on transplanted organs or tissues that leads to the immune response, resulting in allograft rejection.

1.3.1 Blood Group Antigens

Blood group antigens are inherited protein or carbohydrate structures on the outer surface of red blood cells (RBC) that can be recognized by the immune system of antigen negative individuals. After exposure to antigen positive blood, antigen negative recipients can become alloimmunized and produce antibodies to the foreign blood antigens. The first alloantigens to be described were the ABO blood group antigens, which are carbohydrates found on glycoproteins and glycolipids. The majority of RBC antigens, however, are found on integral membrane proteins. These proteins are structurally diverse, consisting of single-pass, multi-pass, or proteins attached by a glycophosphatidylinositol anchor **(Table 1.1)**. Furthermore, blood antigen bearing structures often appear as complexes on the RBC membrane and interact with other membrane or cytoskeleton components.

The RBC represents a complex immunogen, containing a vast number of subtly different alloantigens. At present there are over 300 blood group antigens recognized by the International Society for Blood Transfusion, belonging to 33 blood group systems, with several implicated in transplantation reactions **(Table 1.1)**. The majority of protein antigens found on the RBC consist of a single amino acid polymorphism, whereas a minority consist of a protein being present or absent (*i.e.,* RhD). Conversely, carbohydrate antigens are not determined directly by polymorphic genes, but by genes encoding transferase enzymes that catalyze the final stage of the oligosaccharide chain present on cell surfaces.

While biochemical and molecular studies have defined the biological function of several molecules that express blood group antigens **(Table 1.1)**, many functions remain unknown. Carbohydrates such as A, B and H, contribute the cell surface glycocalyx which plays a role in the flow dynamics of the RBC. Other blood antigen proteins are identified as membrane transporters, adhesions, chemokine receptors, enzymes, or are involved in the structure of the cytoskeleton. The biological significance of antigenic variation (polymorphism) of blood group proteins and carbohydrates is largely unknown. There is little evidence to suggest that the presence or absence of many of the allelic variants or antigens confers any significant advantage. However, for blood groups exploited by pathological microorganisms as receptors for entry, the absence or alteration of blood group antigens could be beneficial and may have played a role in the evolution of blood group polymorphisms. Moreover, the distribution of blood group antigens is not uniform; geographical location and ethnic group influence the frequency of blood group antigens.

The ability of foreign blood group antigens to stimulate an immune response is affected in part by the location and number of determinants on the membrane (**Table 1.1)**. The expression of blood group antigens on a typical RBC vary, for example there are approximately 8-10 x 10^5 A or B antigens on an adult RBC and only 3-18 x 10^3 Kell antigens [41]. Furthermore, not all blood group antigens are found exclusively on the RBC. For example, A and B antigens are present on most tissues, making blood group matching not only essential for transfusion but also for solid organ and tissue transplantation.

The immune response is also influenced by the number of exposures to mismatched blood as well as the disease state of the recipient. While some antigens require no prior exposure (A and B), others, such as RhD, have high immunization rates with 80% of individuals mounting an effective immune response after a single exposure [42,43]. The high incidence of RhD immunization is reflected in current transfusion practice, as RhD is the only non-ABO antigen universally tested. Other clinically relevant blood group antigens, such as Kell, stimulate

antibody responses in approximately 10% of individuals [41,44], while Kidd, Duffy, and MNS result in lower incidences of antibody formation. However, immunogenicity does not always correlate with hemolytic reaction potential, and can result in mild to severe hemolytic responses in a variety of non-ABO/RhD antigens.

Studies of multi-transfused patients report up to 30% alloimmunization, which is highest in sickle cell disease patients [45]. Multiple antigen specificities are also common in alloimmunized patients [46], with studies indicating as high as 46% in sickle cell and 35% in thalassemia patients [47]. This may be due in part to the disease state of the patient as well as the genetic disparity between patient and donor phenotype. For example, in many countries blood group antigens Duffy (FYa and FYb), Kidd (JKb), and MNS (S) are less frequent in predominantly black sickle cell patient populations than in the primarily white donor population. Indeed, these are the antibodies most often found in sickle cell patients [48-51].

Table 1.1 Common Blood Group Antigens

Blood Group	No. of Antigens	Structure	Function	Copies: Adult RBC	Distribution in Other Tissues	Alloresponse
ABO (ABO)	4	Carbohydrate	Enzyme/ Glycocalyx	8-10 x 10^5	Epithelial and endothelial, secreted, platelets, lymphocytes	TR: immediate/ delayed intra/extra vascular HDN: no
MNS (MNS)	46	Single-Pass Protein	Receptor/ Transport	3-10 x 10^5	Renal epithelium and endothelium	TR: no-moderate (rare) HDN: no-severe (rare)
P1PK (P1PK)	3	Carbohydrate	Receptor/ Glycocalyx	5 x 10^5	Lymphocytes, granulocytes, monocytes, platelets	TR: no-moderate/ delayed (rare) HDN: no
Rh (RH)	54	Multi-Pass Protein	Transporter/ Structure	1-2 x 10^5	May be erythroid specific	TR: mild-severe/ immediate or delayed HDN: mild-severe
Lutheran (LU)	20	Single-Pass Protein	Adhesion	1.5-4 x 10^3	Brain, heart, kidney, liver, lung, muscle, pancreas, colon, stomach, skin	TR: no-moderate HDN: no-mild

Blood Group	No. of Antigens	Structure	Function	Copies: Adult RBC	Distribution in Other Tissues	Alloresponse
Kell (KEL)	35	Single-Pass Protein	Enzyme	3.5-18 x 10^3	Bone marrow, fetal liver, small amounts in brain and muscle	TR: mild-severe/delayed or hemolytic HDN: mild-severe
Duffy (FY)	6	Multi-Pass Protein	Receptor	6-13 x 10^4	Brain, colon, lung, endothelium, spleen, thyroid, thymus	TR: mild-severe/ immediate or delayed HDN: mild-severe
Kidd (JK)	3	Multi-Pass Protein	Transporter	1.4 x 10^4	Kidney	TR: no-severe/ immediate or delayed/ hemolytic HDN: no-moderate
Diego (DI)	22	Multi-Pass Protein	Transporter/ Structure	1 x 10^6	Kidney	TR: no-moderate/ immediate or delayed HDN: no-severe
Gerbich (GE)	11	Single-Pass Protein	Structure	5-13 x 10^4	Erythroblasts, fetal liver, renal endothelium	TR: no-moderate/ immediate or delayed HDN: no
Colton (CO)	4	Multi-Pass Protein	Transporter	8-10 x 10^5	Kidney, liver, gall bladder, eye, capillary endothelium	TR: no-moderate/ immediate or delayed HDN: mild-severe

TR: Transfusion Reaction. HDN: Hemolytic Disease of the Newborn. Modified from: Reid 2012 [41].

1.3.2 HLA Antigens

The human major histocompatibility complex (MHC), also called the human leukocyte antigen (HLA), are highly polymorphic transmembrane glycoproteins ubiquitously found on cells. MHC was first identified due to the powerful immune response elicited after tissue transplant. HLA genes are encoded within the MHC and consist of two major classes. MHC I is expressed on almost all nucleated cells, while MHC II is found primarily on antigen presenting cells (APC) such as dendritic cells (DC), B cells, monocytes and endothelial cells; but can be induced on T-

lymphocytes and granulocytes through activation [52,53]. Neither MHC I or II are present on RBC [52].

The biological function of the MHC is to present antigenic peptides to T-lymphocytes. MHC I and II differ in both the source and the size of antigens that they present. For example, MHC I molecules present peptide fragments approximately 9 amino acids in length from endogenously derived proteins whereas MHC II present slightly larger peptide fragments, generally 11-18 amino acids in length from exogenous sources [52].

Structurally, MHC I proteins consist of one heavy chain α that is non-covalently bound to a β_2 microglobulin. The α chain consists of 3 domains: α1, α2, and α3, with the highest polymorphism (and antigenicity) residing in the peptide binding α1 and α2 regions [54]. MHC II consists of two non-covalently bound α and β chains (**Figure 1.1)**. Both the α and β chains contain two domains, with the highest polymorphism (and antigenicity) located in the peptide binding α1 and β1 domains [54]. Thus, the different allelic forms of MHC are often located in the peptide binding cleft as well as the area that comes in contact with T cell receptors (TCR). This influences the peptide repertoire and contributes to the specificity of MHC receptor contact with T cells.

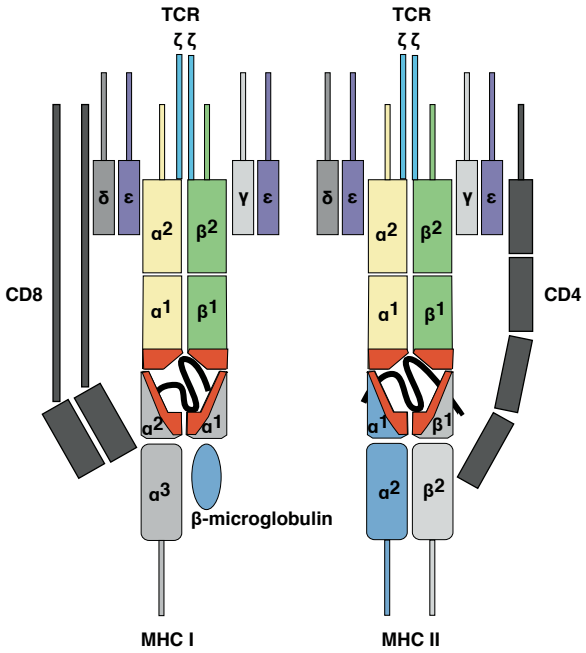

Figure 1.1 Interaction of MHC and TCR. MHC I is comprised of an α chain non-covalently bound to a β_2 microglobulin. MHC II consist of 2 non-covalently bound α and β chains. The TCR is comprised of variable and constant domains (α and β), a short cytoplasmic tail and associated CD3 (γ, δ, ε and ζ chains), which form the TCR complex. In addition, the TCR complex is associated with co-receptors CD4 or CD8. Each variable domain of the TCR contains 3 hypervariable regions (shaded red) that account for the wide antigen repertoire and MHC specificity. Similarly, different allelic forms of MHC are often located in the peptide binding cleft and T cell receptor contact area (shaded red), influencing the peptide repertoire and contributing to the specificity of MHC receptor.

The MHC is more diverse than any other genetic system as a result of the polygenic and polymorphic characteristics of the MHC locus. The MHC is highly polygenic, containing several different MHC class I and II genes that are inherited as a complete set of HLA genes from each parent and are co-dominantly expressed. In addition, the individual MHC genes are highly polymorphic, consisting of high allelic variability that distinguishes individual HLA alleles and confers antigen specificity. For example, over 10,000 HLA alleles have been characterized [55] (**Table 1.2)**. Thus, each person not only inherits multiple genes, but those genes are highly diverse depending on the allelic variants. Similar to RBC blood groups, the frequency and distribution of HLA alleles varies greatly among different ethnic groups and arguments have been made that the variation of MHC in populations may come from interactions with infectious agents [56,57].

Table 1.2 HLA Alleles

HLA Class	Gene	No. of Alleles	HLA Class	Gene	No. of Alleles
Class I Major HLA	A	2884	Class I Minor HLA	E	15
	B	3589		F	22
	C	2375		G	50
Class II Major HLA	DRA	7	Class II Minor HLA	DMA	7
	DRB	1642		DMB	13
	DQ1A	52		DOA	12
	DQ1B	664		DOB	13
	DPA1	38			
	DPB1	422			

Information was retrieved from IMGT/HLA Database [55] September 15, 2014
(www.ebi.ac.uk/ipd/imgt/hla/stats.html)

The antigenic diversity of HLA results in high variability of the antigen binding areas of class I and class II proteins, conferring a large repertoire of antigens capable of being bound and presented to immune cells. Unlike RBC antigens, MHC isoforms can differ by more than 20 amino acids [58], making each variant protein relatively distinct. Although the primary role of HLA molecules is to regulate the immune response, allelic variability plays a central role in both transplantation and transfusion rejection. Indeed, in transplantation and transfusion, host MHC molecules not only present foreign tissue peptides to host immune cells, but also foreign MHC

molecules themselves act as antigens and can provoke the immune response in the recipient, where immune cells recognize MHC receptors as foreign [59]. Thus, given the large variation in MHC molecules, the probability that two individuals share the same MHC repertoire is extremely low.

1.4 Allorecognition

As previously discussed, the antigenicity of human cells often prevents identically matched blood or tissues from being transplanted. When immune cells recognize protein variation within a species as foreign, allorecognition occurs. Allorecognition is a complex event encompassing recognition, adhesion and stimulation by immune cells and components. The subsequent alloresponse to foreign cells can result in rejection, making allorecognition a major obstacle in transfusion and transplantation medicine. Alloresponses encompass elements of both innate and adaptive immunity. Innate immunity refers to the non-specific response, relying on a limited number of receptors and secreted proteins, whereas adaptive immunity uses clonally derived expansion of antigen specific lymphocytes to carry out the immune response. Furthermore, while the following sections are categorized according to cellular and humoral immunity, which contain elements of innate and adaptive immunity, these immune defenses are not mutually exclusive and often overlap in terms of allorecognition of foreign tissues (**Figure 1.2**). The mechanisms of allogeneic tissue rejection will be discussed in subsequent sections focusing on the principles underlying the molecular basis of allorecognition: antigen recognition, cell activation, effector response, and how these events contribute to transfusion and transplantation outcomes.

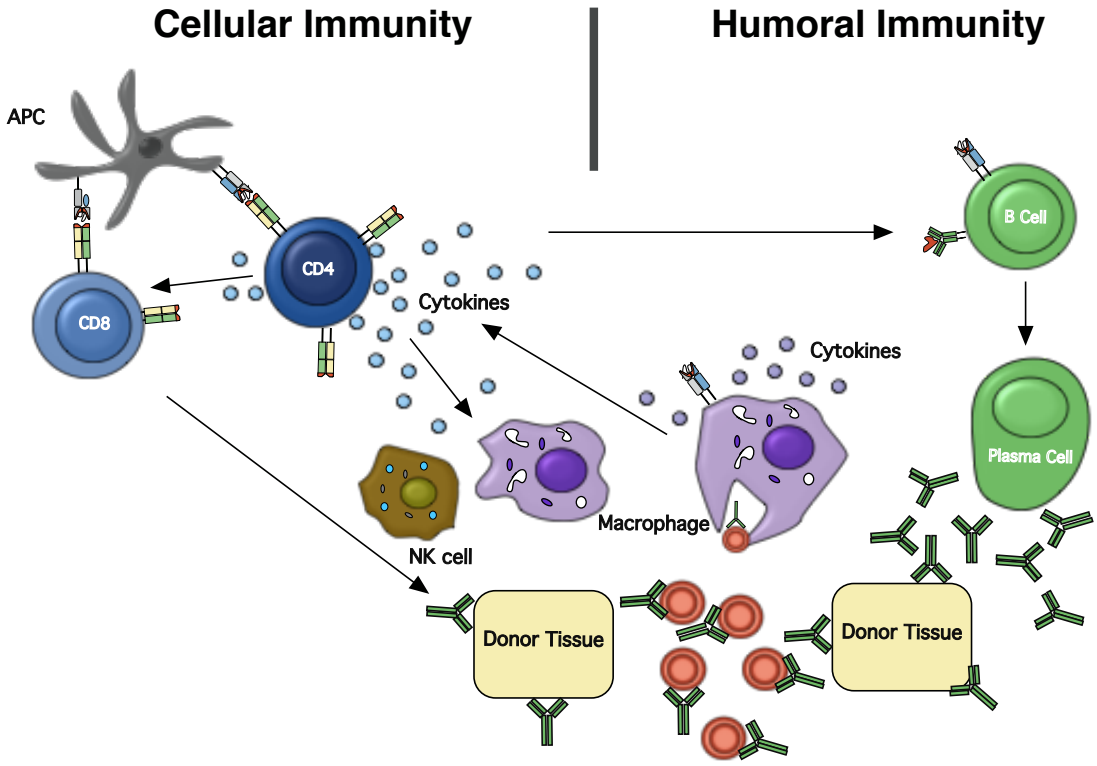

Figure 1.2 The overlap of cellular and humoral immunity. Recognition of foreign donor tissues by antigen presenting cells activates naïve T cells. Activated T cells secrete various proinflammatory cytokines needed for the recruitment and stimulation of inflammatory cells such as macrophages, natural killer (NK) and cytotoxic CD8 cells. These cells can directly kill the donor tissue or phagocytose and present antigen to T cells. Upon activation, macrophages secrete a large amount of IL-12 that helps to maintain T cell responses. Cell contacts by T cells are needed for the maturation of B cells and efficient antibody production. B cells express MHC class II and present antigen to CD4 cells and T cells provide the IL-2 for B and T cell proliferation. Macrophages and NK cells also express Fc receptors and can phagocytose or directly kill donor tissue bound with antibody.

1.4.1 The Development of Cellular Immunity to Allogeneic Cells

Cellular immunity involves the lymphocyte-mediated activation of cells by direct cell-cell interactions and immune mediators such as cytokines. T-lymphocytes play several roles in adaptive immunity including the direct killing of foreign tissues as well as contributing to the effector functions of other cells. For example, T cells assist in the maturation of antibody producing B cells that comprise the humoral arm of the adaptive immune system. Graft rejection is an immunological response facilitated primarily by T cells [60]. This was first evidenced by the failure of T cell deficient mice to reject skin grafts, while the adoptive transfer of T cells could restore this ability [61]. In transplantation and non-leukoreduced transfusions, polymorphic MHC molecules bound with peptides (pMHC) are recognized by T cells, and trigger a response

against either the transplanted tissues (host *vs* graft) or the host tissues (graft *vs* host). In transfusion, RBC antigen recognition also occurs *via* T cell mediated recognition of RBC peptides presented by immune cells in the spleen [58].

Before naïve alloreactive T cells can develop into effector cells that mediate rejection, they must be activated by antigen presenting cells (APC) carrying allogeneic peptides and expressing costimulatory molecules. The presentation of foreign antigens occurs *via* MHC molecules found on the surface of APCs. Several cells from both the adaptive and innate immune systems can present antigens including dendritic cells (DC), macrophages, endothelial cells and B-lymphocytes. DCs, however, are the most efficient at both presenting antigen and activating naïve T-lymphocytes. APCs present foreign antigen or peptide components by phagocytosis; receptor-mediated endocytosis; autophagy; or macropinocytosis, which involves engulfing large amounts of extracellular materials. MHC-bound peptide components obtained intracellularly or extracellularly are displayed on the cell surface by MHC I and MHC II receptors, respectively. Although the mechanisms are not completely understood, *cross presentation* may allow some APCs to process exogenous antigens into the MHC I pathway, while autophagy may allow endogenous peptides to be presented on MHC II molecules. Upon interaction with peptide, activated APCs migrate to the secondary lymphoid tissues, displaying costimulatory molecules along with foreign peptide.

To initiate the adaptive immune response, alloantigens are presented to naïve T cells in the secondary lymphoid organs of the recipient and are recognized by specific host T cell receptors (TCR). The TCR associates with cluster of differentiation 3 (CD3) (γ, δ, ε and ζ chains), forming the TCR complex (**Figure 1.1)**. Each variable domain of the TCR contains 3 hypervariable regions (CDR1-3) that account for the wide antigen repertoire as well as the MHC binding specificity. While there is considerable plasticity in the binding of the TCR with the MHC, CDR1 and CDR2 of the TCR bind to the MHC, while the CDR3 may specifically interact with the

peptide [62]**.** MHC-bound peptide components displayed on the cell surface by MHC I and MHC II bind to CD8 and CD4 T cells, respectively.

There are three mechanisms by which APCs can present alloantigen to naïve T-lymphocytes: direct, indirect and semi-direct allostimulation (**Figure 1.3)**. In direct allostimulation, passenger APCs, either transfused or carried in solid organ transplants, migrate to lymphoid tissues and directly stimulate alloreactive T cells. Indirect allostimulation occurs when the host APC takes up foreign proteins and displays them on self-MHC molecules. Semi-direct allostimulation involves cell contact between host and donor APC that results in the transfer of intact membrane components, including intact donor MHC, which are presented to host T-lymphocytes. Thus, both direct and semi-direct allorecognition relies on the recognition of foreign MHC molecules by CD4 or CD8 T cell receptors, while CD4 cells dominate indirect allorecognition.

While MHC restriction, the ability of the TCR to recognize antigens only when associated with self-MHC, should prevent the TCR from binding to foreign MHC, a large number of T cells (1-10%) directly recognize foreign MHC-peptide complexes [63,64]. Differences in MHC loci are potent triggers for rejection of allografts because many allelic variants of the MHC are found in amino acid sequences on the surface exposed regions that make contact with the TCR [65]. The direct alloresponse to foreign MHC by T cells may be caused by the recognition of polymorphic amino acids in the MHC itself, or by a difference in the conformation of bound peptide that allow MHC restriction to be bypassed. In truth, they may not be mutually exclusive because many alloreactive clones have been shown to recognize both peptide and foreign MHC [65]. Conversely, the indirect alloresponse involves the recognition of processed allo-peptides consisting of major or minor histocompatibility antigens that are presented by self-MHC [66]. Alloantigens shed from the grafts are processed as exogenous antigens and presented with self-MHC class II.

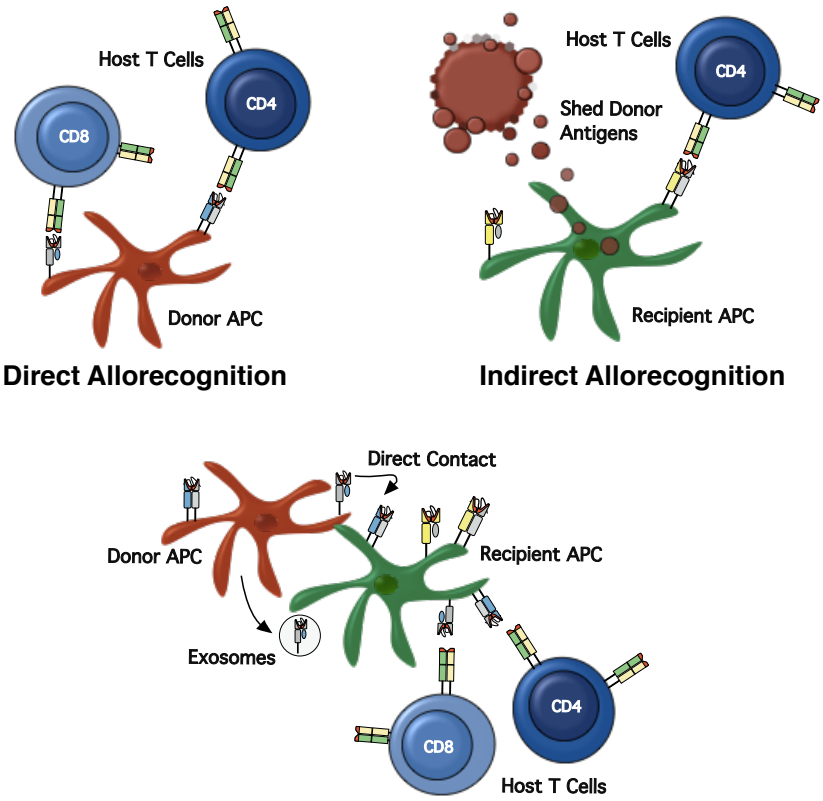

Figure 1.3 Direct, indirect and semi-direct allorecognition. Direct allostimulation occurs when passenger APCs directly stimulate alloreactive T cells. Indirect allostimulation arises when the host APC takes up foreign proteins, processes and displays them on self-MHC molecules. Semi-direct allorecognition involves cell contact between host and donor APC that results in the transfer of intact donor MHC, which are presented to host T-lymphocytes. Modified from Afzali 2007 [59].

Initial cell-cell interactions by various adhesions provide time for T cells to sample the large number of MHC molecules displayed on the surface of APCs. TCR coreceptors CD4 and CD8 bind to non-polymorphic portions of the MHC molecule, providing stability and enhancing signaling [67,68]. In addition, multiple adhesion proteins expressed on T cells (LFA-1/CD2) bind to receptors on the APC providing stability and increasing the interaction time between cells. The redundancy of adhesion proteins found on cell membranes reflects the importance of initial cell-cell interactions, as defects in either LFA-1 or CD2, but not both, were shown to retain normal T cell function and initiate T cell priming [69,70]. This suggests that the remaining adhesion proteins could compensate for the absence of a single adhesion receptor [71].

Priming of T cells to alloantigens occurs in the lymphoid tissues, and interactions between APC and T cells can last from minutes to hours [72]. During this time the APC delivers signals that are required for the naïve T cells to become activated and differentiate into effector cells. In addition to CD4 and CD8 coreceptors, costimulation is essential to the activation,

differentiation, and survival of naïve T cells *via* the propagation and enhancement of various signaling pathways. Costimulation is provided by the APC through several different receptors such as CD80/86 and CD40, which interact with CD28 and CD40L on T cells. Furthermore, other inducible costimulatory ligands and receptors enhance the T cell response following initial activation and promote the upregulation of costimulatory receptor expression. These redundancies support the regulation and control of cell activation. Indeed, costimulatory signals are crucial to activation of naïve T cells, because TCR-pMHC interactions with the absence of costimulatory receptors, or weak costimulation can result in anergy, induction of tolerance, or apoptosis [73-77].

Inhibitory receptors also play a major role in the outcome of T cell-pMHC interactions. Inhibitory receptors, such as CTLA-4 and PD-1 expressed during TCR signaling bind to their respective ligands, CD80/86 and PD-L1/PD-L2 expressed on the APC. These inhibitory receptors are necessary to control the immune response and serve as negative regulators of T cell activation and CD28 costimulation [78]. For example, CTLA-4 deficient mice die from uncontrolled cell proliferation [78,79], and PD-1 deficient mice gradually develop autoimmunity [80], illustrating the importance of immune response regulation. CTLA-4 also plays an important role in the response to alloantigens during transplantation, because blocking CTLA-4 results in accelerated rejection in a murine model [81].

For activation, survival and differentiation of naïve T cells to occur, transmembrane receptors must convert extracellular signals into intracellular biochemical events. The outcome of ligand binding (activation, anergy, death, or tolerance) depends on the type of receptors bound, the strength and duration of signal propagation, as well as the amplification of secondary messengers. Sufficient surface receptor signaling leads to the transduction of three distinct signaling branches important in T cell activation: NFκB, NFAT, and AP-1. The translocation of NFκB, NFAT, and AP-1 to the nucleus results in the transcription of IL2 and other genes important for survival, activation, inflammation, immune regulation and differentiation. IL2 works

in both an autocrine and paracrine fashion to promote cell survival, proliferation, differentiation and enhance signaling pathways. The importance of IL2 during an inflammatory response is illustrated by the increased death of effector cells after the removal of IL2 [82,83].

Several receptors and pathways promote the transcription of genes responsible for cell activation, proliferation, differentiation and survival. Thus, cell activation is not simply a result of turning a pathway on or off, it is the strength of receptor interactions, duration and propagation of multiple signals that determine if cells are activated, become anergic/tolerant or become apoptotic. Indeed, many immunosuppressant drugs decrease signal strength by blocking costimulation, preventing second messenger amplification or by increasing inhibitory coreceptors.

Activation of naïve T cells results in differentiation into various subsets. CD4 cells differentiate into Th1, Th2, Th17 and T-regulatory cells (iTreg), while CD8 cells become cytotoxic T cells. T cell differentiation is determined in large part by the cytokine mediators released from APCs during T cell interaction, as well as by the environmental milieu guided in part by the innate immune response. For example, IFNγ and IL4 favor Th1 and Th2 differentiation, respectively [84,85]. Conversely, TGFβ induces iTreg differentiation, while TGFβ, IL21 and IL6 lead to the development of Th17 cells [86,87]. Effector T cells initiate cellular responses through cell-cell contacts and cytokine release (Th1, Th2, Th17, iTreg), as well as exhibit direct cytotoxic effects (CD8 cells). T cell subsets are categorized based on the cytokine profiles they secrete where certain subsets promote inflammation and rejection (Th1, Th17), while other subsets enhance allograft survival (Th2, Treg). For example, studies using murine models show that concentrations of IFNγ secreted by Th1 may be less permissive to long-term allograft survival than Th2 cytokine environments high in IL4 [88,89]. In addition, iTreg cells can suppress reactive cells by secreting inhibitory cytokines such as IL10 and TGFβ. IL10 has been shown to suppress the production of inflammatory cytokines, and inhibit MHC expression and costimulatory molecules on APCs [90]. TGFβ has been shown to block T cell cytokine

production, and inhibit cell division and effector functions of cytotoxic T cells [91] that cause direct cell tissue damage during acute organ rejection. Tregs have also been shown to delay the onset of rejection in solid organ transplants using a murine model [92], and in graft *versus* host disease (GVHD) in humans [93], indicating that the predominance of alloreactive effector cells or Treg cells may have significant effects on allograft rejection.

Similar to inhibitory receptors discussed previously, various mechanisms are in place to regulate and terminate the effector response. For example, IL1R2 are early response proteins expressed by many cells, including lymphocytes and monocytes, which act as decoy receptors. IL1R2 is upregulated in response to inflammatory cytokines as a way to control the biological effects of IL1 during inflammatory immune responses. In addition, apoptosis plays a role in controlling the immune response and can occur as a result of excessive costimulation (activation induced cell death). Conversely, apoptosis may result from a lack of signals for survival, weak stimulatory signals or from specific death receptors on the surface of cells [76,94]. Apoptotic pathways are controlled by caspases, small proteins critical for cellular integrity, which activate and promote cell death. Apoptosis occurs without eliciting an inflammatory response and may induce either tolerance or non-responsiveness to allografts [76,95]. Interestingly, therapies that involve induction of apoptosis have shown that apoptotic dendritic cells may promote a tolerant or anergic environment favoring allograft survival [96].

Together, initial interactions between naïve T cells and foreign antigens bearing APCs lead to the induction of various pathways involved in activation, differentiation and survival of potentially alloresponsive cells (**Figure 1.4)**. It is the complex interaction of receptors, cytokines and transcription factors that determine the fate of naïve cells. Thus, cellular immunity plays a large part in determining the response to foreign cells and tissues.

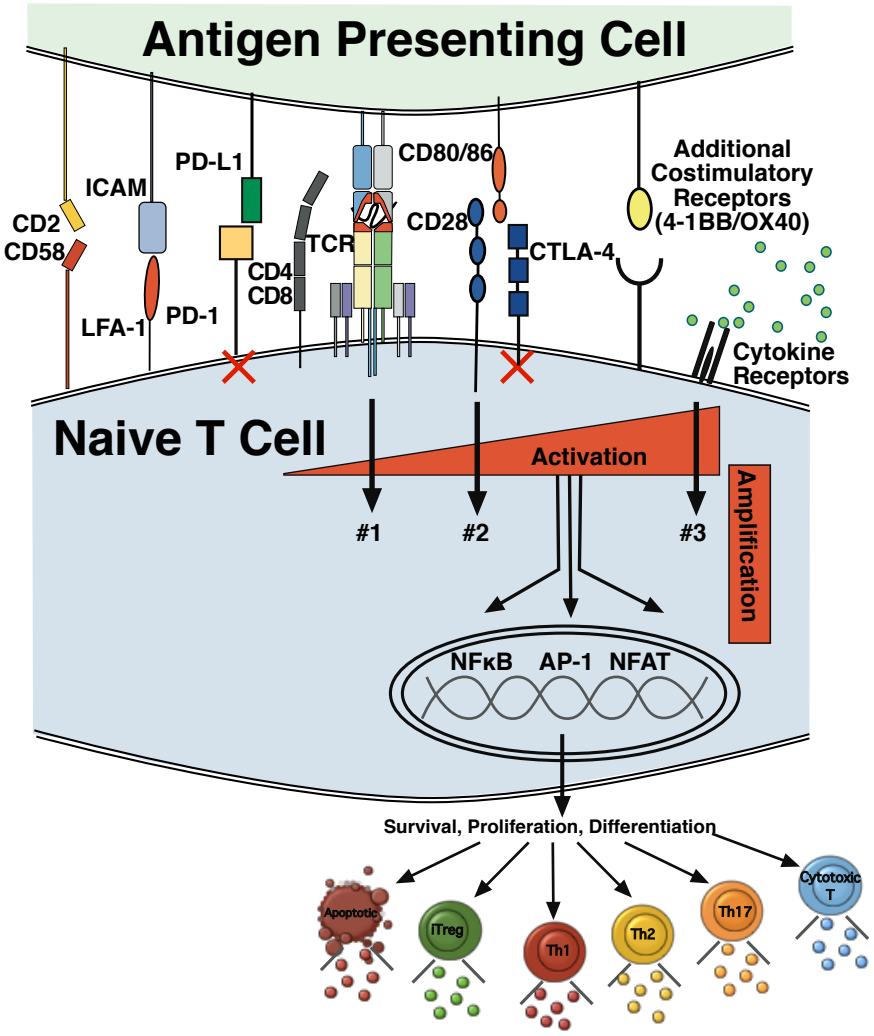

Figure 1.4 Activation of naïve T-lymphocytes. TCR, pMHC, adhesions, coreceptors, costimulatory receptors and cytokines are all involved in promoting the transcription of genes (NFκB, AP-1, NFAT) responsible for cell activation, proliferation, differentiation and survival. Activation is determined by the type and duration of receptor interactions, the signal strength, and the amplification by intracellular signaling proteins. Together, they influence whether cells are activated, become anergic/tolerant or become apoptotic. Activation of naïve T cells results in differentiation into various subsets. CD4 cells differentiate into Th1, Th2, Th17 and T-regulatory cells (iTreg), while CD8 cells become cytotoxic T cells. Cell differentiation is influenced by cytokines from APCs, effector T cells, and innate immune cells that bind to receptors on the surface of naïve T cells.

1.4.2 The Development of Humoral Immunity to Alloantigens

Like T cells, B cells display receptors capable of recognizing a diverse array of antigens. However unlike T cells, B cells recognize natively folded proteins and most often require the help of activated T cells to reach maturity [97,98]. Activated B cells differentiate into plasma cells that secrete antibody.

While B cell responses to alloantigen are often T cell dependent, T cell independent responses may also occur. In T cell dependent responses, the B cell receptor (BCR) recognizes native proteins, which are endocytosed and displayed on MHC II receptors. T helper cells recognize peptide fragments displayed on the B cell MHC and stimulate them *via* surface

receptors and cytokines, resulting in the differentiation of B cells into antibody secreting plasma cells. Conversely, T cell independent responses occur when the BCR binds to repetitive structures, such as bacterial lipopolysaccharides and carbohydrate blood group antigens. This leads to BCR cross-linking and results in direct cell activation and antibody secretion [97].

Antibodies serve two main functions: binding to foreign proteins and recruiting effector cells. The main targets of antibody-mediated rejection are MHC (I and II) and blood group antigens [97]. Antibodies consist of four polypeptide chains (two light chains and two heavy chains) each containing a variable region capable of binding two antigen epitopes and a constant region (Fc) that engages the effector functions of the immune system. The BCR is similar in structure to antibodies, but lacks an exposed constant binding region, and therefore the effector function. Antibodies are bound to antigens *via* reversible non-covalent interactions and the contributions of these forces determine the overall affinity of the antibody to the antigen. Like the TCR, the variable regions of both antibodies and BCR contain hypervariable regions that comprise the antigen-binding site. The contact between the antibody and antigen occur over a broad range, thus determining the antigen specificity, however antibodies only recognize a small portion of the antigen called the epitope.

The primary antibody response occurs after initial recognition of antigen by B cells *via* T cell independent or T cell dependent mechanisms in the secondary lymphoid organs and results in activation of B cells into plasma cells and the secretion of IgM antibody. In the later phase, during T cell dependent responses, somatic hypermutation of the variable region occurs as well as antibody class switching. Somatic hypermutation promotes the selection of antibody with high affinity to antigens. Favorable mutations in the hypervariable region, which increases antibody affinity to antigens, are selected for by interactions with T cells and APC. Antibody class switching results in the expression of different constant regions, which all exhibit different functional properties. The primary antibody response is slow, taking several days to weeks before it may reach a maximum level. However, a subset of activated B cells develop into

memory cells that can be restimulated rapidly, secreting antibodies with high affinity and specificity.

There are 5 classes of antibodies produced: IgD, IgM, IgG(1-4), IgE and IgA (**Table 1.3)**. IgM is the first class produced after an initial antigen exposure in a T cell dependent or independent manner by B cells. Although IgM released after an initial antigen exposure is low affinity because it does not go through affinity maturation, it forms a pentamer in blood and therefore exhibits high avidity to antigens due to multiple binding sites. While IgM is produced during the initial immune response, other classes dominate the later phase. During the later phase, the most common antibody in plasma is IgG. IgG is found in blood, tissues and also can be directly transported across the placenta, resulting in severe reactions for the fetus in alloimmunized mothers.

Table 1.3 Immunoglobulin Classes

	IgG1	IgG2	IgG3	IgG4	IgM	IgA	IgE	IgD
Number of Antigen Binding Sites	2 monomer				10 pentamer	2 or 4 monomer or dimer	2 monomer	2 monomer
Serum Level (mg/ml)	9	3	1	0.5	1.5	3.5	< 0.01	< 0.01
Complement Activation	++	+	+++	-	++++	-	-	-
Binds to Macrophages and Neutrophils	+	-	+	+/-	-	-	-	-
Placental Transfer	+++	+	++	+/-	-	-	-	-

Modified from Murphy 2011 [58].

1.4.3 The Effects and Outcomes of Allorecognition

Allorecognition results in acute or chronic destruction of allogeneic cells and tissues. While the immune recognition of blood group and MHC antigens differ, commonalities exist in the immunological responses to allogeneic mismatched RBC and other transplanted tissues (**Figure 1.5**). Moreover, the absolute contributions of the different allorecognition pathways in rejection are not known, however direct allostimulation is linked to acute rejections, whereas

indirect allostimulation may contribute more to chronic rejection [99]. Since passenger lymphocytes are the main mediators of the direct pathway, the response is vigorous early in transplantation and diminishes with their death and removal [60,99]. The indirect pathway plays a more dominant role in chronic rejection as inhibition of acute rejection by depleting passenger lymphocytes delays, but does not prevent development of chronic rejection [100-103]. In addition, there remains a continuous influx of processed donor antigen *via* the indirect pathway, which continues for the life of the transfused cells or transplanted tissues. The indirect pathway is also thought to be important for development of antibody responses and the production of alloantibodies [97,104]. The relative contribution of the semi-direct pathway to acute and chronic rejection requires further elucidation.

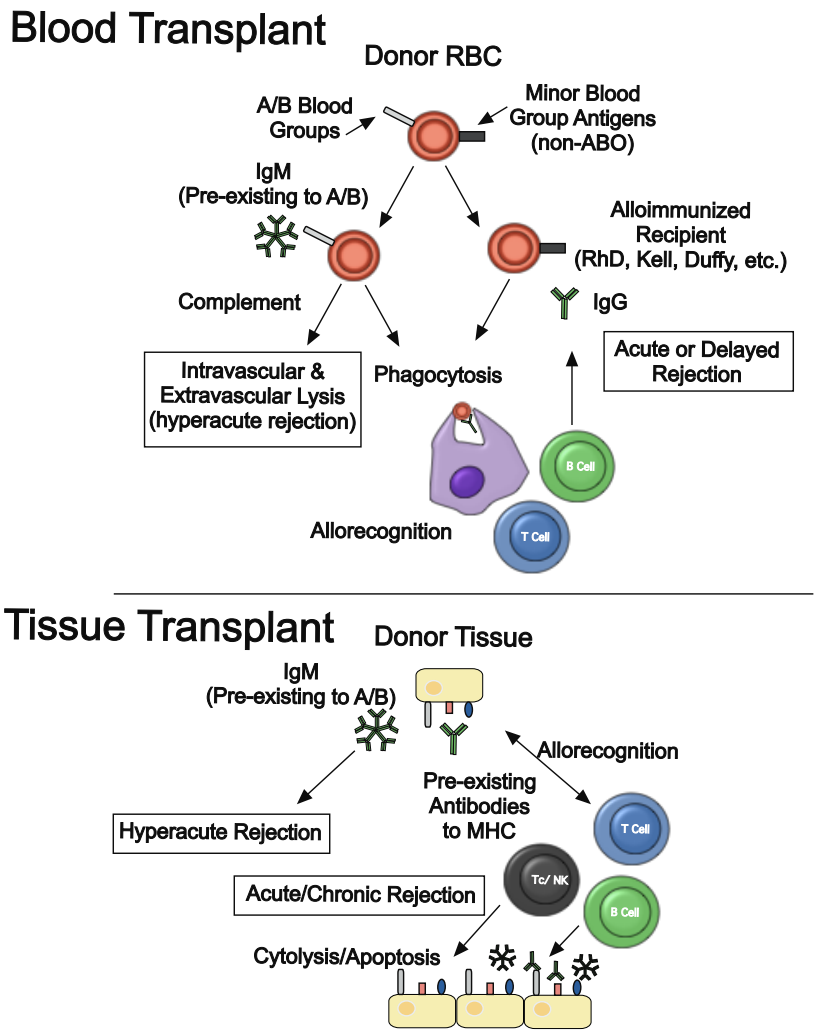

Figure 1.5 Immune responses to blood and tissue transplants utilize similar mechanisms. The consequences of transfusion or transplantation of mismatched blood or tissues includes both cellular and humoral responses that may result in hyperacute, acute or chronic rejection of foreign cells and tissues. Tc- cytotoxic T cell; NK- natural killer cells. Modified from Scott and Chen 2001 [105].

The cellular events that contribute to acute and chronic rejection include alloreactive cytotoxic T cells and natural killer cells that directly recognize alloantigens and release enzymes that destroy tissues or trigger apoptosis. T cell activation also leads to the secretion of cytokines that recruit various inflammatory cells, such as macrophages, which are involved in both acute and chronic tissue damage [106-108]. These inflammatory cells further promote tissue destruction by secreting large amounts of proinflammatory cytokines.

Destruction of allogeneic tissues bound with antibodies contributes to hyperacute, acute and delayed rejection *via* two pathways: complement mediated lysis or destruction by phagocytic mononuclear cells. The immune response to cells or tissues bound by antibodies depends on various factors including genetic host factors, the amount of incompatible tissue, the nature of the antigen (size and number of antigen sites) and the antibody class.

Complement activation *via* binding of IgM antibodies to ABO incompatible tissues is the major cause of hyperacute transfusion and transplantation rejection. ABO antigens are densely expressed on the cell surface and can be directly bound by preformed antibodies in antigen negative recipients, causing cell lysis and the release of inflammatory mediators. This occurs by binding of complement component C1q to the Fc region of IgM, resulting in activation of the classical complement pathway. While IgM and some types of IgG (subtypes 1-3) are capable of activating complement, to achieve the binding necessary for complement cascade activation multiple molecules of IgG would need to be bound within 30-40nm of each other [58]. Since IgM is a pentamer and multiple arms bind simultaneously, IgM is a more efficient activator of complement than IgG. Bound C1q results in the recruitment of various complement components and the formation of a membrane attack complex (transmembrane channel), resulting in cell lysis and the release of inflammatory molecules. Although these reactions rarely occur because of cross matching, the transfusion or transplantation of mismatched ABO tissues results in hyperacute hemolytic transfusion or graft rejection characterized by immediate intravascular red

cell lysis, vasodilation, hypotension, contraction of smooth muscle, thrombosis and organ dysfunction. Duffy and Kidd antigens can also activate complement [109-111].

Allogeneic donor cells bound typically with IgG (IgA and IgE can also bind) initiate phagocytosis by interaction with Fc receptors on leukocytes. This mechanism is indicated in both acute and delayed extravascular hemolysis reactions to blood group antigens, and contributes to a lesser extent during acute and chronic rejection of transplanted tissues [111,112]. Cells bound by IgG antibodies typically triggers their destruction by macrophages, neutrophils, or natural killer cells through phagocytosis or granule release.

The severity and type of non-ABO hemolytic reactions varies by blood antigen mismatch, the number of mismatched transfusions, the amount of antibody present in the plasma, whether the antigen initiates a primary or secondary response, and antibody class. For example, alloimmunization of RhD negative individuals occurs through the transfusion of RhD positive blood or pregnancy with a RhD positive fetus. Subsequent exposure of RhD positive blood through transfusion or pregnancy may result in severe, immediate, or delayed hemolytic reactions, including hemolytic disease of the fetus. In addition, many other non-ABO/RhD antigens are of clinical significance, such as Kell, Duffy, Kidd, Diego, and MNS, which result in mild to severe hemolytic transfusion reactions, accelerated clearance of RBC, as well as hemolytic disease of the fetus or newborn. Furthermore, patients receiving multiple transfusions to treat hematopathologies often become alloimmunized to several antigens leading to early RBC clearance, thereby decreasing the therapeutic efficacy of transfusion.

1.5 Current Treatment for Transfusion and Transplantation Rejection

The most effective strategy for preventing allorecognition is blood and tissue matching. Blood is routinely tested for ABO/RhD compatibility and, in addition to ABO matching, HLA antigens of both recipient and donor are determined prior to transplantation. Donor and recipients are generally only typed for HLA-A, B and DR antigens due to the immunogenicity of

these alleles. Indeed, incompatibility of these antigens results in a number of *taboo* allele combination pairings that contribute to the robust rejection of allografts [65,113]. However, preliminary tissue-matching protocols are often insufficient for chronically transfused patients, which may have multiple non-ABO alloantigens, as well as individuals who have increased risk of developing reactions due to previous transplants. Extensive clinical tissue typing can be performed in special situations for alloimmunized patients, although, cyclic fluctuations and intermittent antibody titers may result in antibodies not being detected at the time of testing [44,114,115]. Moreover, extensive testing comes at both an expense to the blood and tissue supply as well as economic cost. For example, the limited storage time of organs restricts extensive testing. The storage time of solid organs is generally less than 12 hours, in contrast to RBC units that can be stored for up to 42 days. Furthermore, even with extensive typing of RBC and HLA antigens, finding sufficient supply of tissues or RBC units would become extremely difficult. The extensive testing of blood and tissues would also increase costs due to both testing and the increased expense to procure matched tissues and rare RBC units [116].

Leukoreduction of both tissues and blood components is another method utilized to reduce the alloresponse to HLA antigens. While several reports show promising decreases in acute alloresponses and decreased non-hemolytic febrile reactions, leukocyte reduction may be detrimental in certain situations. For example, leukoreduced hematopoietic stem cell transplantation, used as a treatment for multiple myeloma or leukemia, decreases graft *versus* host disease (GVHD), however, it may also decrease graft survival and increase relapse of disease by inhibiting graft *versus* leukemic effects [117].

While tissue matching, blood typing, and leukoreduction may decrease alloresponses, once the process of allorecognition occurs it becomes extremely difficult to control. Therefore, effective means of minimizing the immune response is achieved through the global and non-specific suppression of the immune system using immunosuppressive agents. Indeed,

immunosuppression is an essential component of transplantation, facilitating transplants across MHC barriers.

Conventional immunosuppressants are divided into several categories: anti-inflammatory drugs, cytotoxic agents, as well as drugs utilized for the targeted suppression of cell surface molecules, intracellular signaling pathways and the effector functions of cells. Many immunosuppressants are used in combination and exhibit broad inhibition, suppressing helpful as well as harmful responses, resulting in severe side effects such as cancer, infection as well as direct damage to allografts due to drug toxicity.

Anti-inflammatory corticosteroids (dexamethasone, prednisolone, prednisone) bind to DNA and interact with several transcription factors including NFκB. These drugs exert multiple and broad effects such as decreasing proinflammatory gene (IL1β, IL2, IL6, and TNFα) expression, while increasing anti-inflammatory gene expression [118]. Corticosteroids target the proinflammatory effects of monocytes, macrophages, and CD4 T cells. However, a high concentration of the drug is often necessary for therapeutic effects, resulting in toxicity to grafts and severe side effects for patients including atherosclerosis, ulcers, hypertension, and bone disease [119].

Cytotoxic drugs (azathioprine, mycophenolate mofetil, cyclophosphamide) are mitotic inhibitors that suppress cell division of continually dividing cells such as lymphocytes. In addition, azathioprine has been shown to interact with CD28, causing apoptosis of potentially reactive lymphocytes [120]. However, these drugs are toxic for all rapidly dividing cells such as skin, gut lining and bone marrow. Side effects include anemia, leukopenia, thrombocytopenia, and increased risk of infection [121].

Drugs that impede T cell signaling (tacrolimus, cyclosporine A, rapamycin, everolimus) are derived from bacteria and soil fungi. These drugs bind to intracellular proteins and interfere with signaling. Both cyclosporine and tacrolimus reduce activation of NFAT signaling, resulting in decreased IL2 production and cell proliferation [122]. Rapamycin and everolimus inhibit the

mTOR pathway, which regulates cell growth, differentiation, proliferation, and cell survival, resulting in decreased proliferation and IL2 secretion [123]. Several studies show that rapamycin increases functional Treg cells both *in vitro* and *vivo* [124]. Though many drugs that inhibit signaling show severe toxicity to organs such as liver, lung and kidney as well as induction of diabetes and hypertension [121,124].

Targeted suppression of surface markers involves the use of polyclonal or monoclonal antibodies that block receptors or act as receptor decoys to prevent activation. Monoclonal antibodies to CD3, CD25, CD28, and CD40 have been developed and several have demonstrated significant and targeted immunosuppressive effects. However, mAb such as OKT-3 (a mouse monoclonal anti-CD3) and depleting antibodies such as ATG may result in the induction of humoral responses and inflammatory cytokine release due to the presence of xenogeneic components and initial activation and lysis of T cells [121]. CTLA4-Ig (belatacept) has also been developed to prevent CD28 interaction with CD80/86. CTLA4-Ig acts as a decoy receptor and results in decreased proliferation and activation of lymphocytes. However, CD28 costimulatory blockade, while effective in rodent models were not sufficient in primate models [125-127] and several CD28 specific mAbs also demonstrated unwanted agonist side effects [128]. In addition, blocking CD80/86 prevents CTLA-4 ligation on T cells, negating inhibitory signaling. While targeted suppression of individual surface markers has been shown to delay rejection, single drug therapy has less effect on long-term graft survival. Furthermore, the blockade of any single receptor may be inadequate to prevent allorecognition and rejection due to the redundant nature of costimulation receptors.

All current immunosuppressant drugs suffer from severe side effects. While these drugs have proven to significantly decrease acute rejection, they are less effective in preventing chronic rejection leading to long-term complications due to toxicity and poor long-term outcomes. Therefore, novel, non-toxic methods to prevent allorecognition or modulate alloresponses would be beneficial. Indeed, once an alloresponse occurs, methods to prevent

effector cell function must rely on broad immunosuppression regimens. An ideal approach in transfusion and transplantation medicine would be to prevent allorecognition and induce tolerance; methods that would both decrease the need for life-long immunosuppressive drugs and increase the long-term outcomes of allografts.

1.6 Immunocamouflage of Allogeneic Cells

1.6.1 History of PEGylation

Bioengineering of donor tissues by the covalent attachment of polyethylene glycol (PEG) to proteins (PEGylation) could provide a novel means to attenuate allorecognition. Davis and Aubuchowski first described PEGylation in regards to the modification of catalase and albumin to overcome the instability, degradation and potential immunogenicity of these therapeutic proteins [129,130]. PEG-modified proteins were shown to have decreased antigenicity and prolonged circulation half-life, while retaining their activity in rodent models. This led to the first FDA approved PEGylated product PEG-adenosine deaminase (Adagen®) [131] that came to market in 1990, followed by a number of other PEGylated proteins. Thus, PEGylation has been a successful approach to limit the immunological barriers of drug therapies involving proteins, enzymes, and other small molecules. The success of PEGylation comes from the ability of PEG to confer biological advantages to molecules to which it is attached. PEGylation results in improved therapeutic effects and circulation time due to increased solubility, decreased antigenicity (exclusion of antibodies, cells and proteolytic enzymes) and increased molecular size [132].

PEGylation has expanded and now encompasses a vast array of PEGylated targets. For example, there are a number of PEG-conjugated polypeptides, oligodeoxynucleotides, small molecules, hydrogels, and liposomes that have been developed [133,134]. More recently, the PEGylation of intact cells has been investigated. PEGylation of allogeneic blood cells, leukocytes, and pancreatic islets show decreased antigenicity using both *in vitro* and *in vivo*

models [135-139]. Furthermore, PEGylation of viruses or their target cells inhibits viral infection rates *in vitro* [140,141].

1.6.2 Polyethylene Glycol and Polymer Alternatives

PEG is a non-toxic FDA approved compound that is currently the gold standard for polymer-based therapeutics. However, several other polymers are being investigated as alternatives to PEG. For example, polyglycerols (PG) have been used as conjugates for liposomes [142], hydrogels [143,144] as well as for the camouflage of intact cells (RBC) [145,146]. PG can be linear as well as hyperbranched (HPG) in structure and shows promising potential for exclusion of immune components and cells [147]. Polyoxazolines (POZ) were first discovered in the 1960s and used as an additive in the food and cosmetic industry. More recently, a wider range of potential uses has built up around this class of polymers, including biomedical applications [149]. Indeed, POZ exhibits several attributes that make it an attractive alternative to current polymers such as decreased viscosity and degradation potential [149,150].

In addition, several other alternatives such as polyaminoacids and vinyl polymers are also currently under investigation [151]. However, two polymer species will be the focus of this thesis: polyethylene glycol (PEG) and polyoxazoline (POZ).

1.6.3 Chemistry of PEGylation

PEG is derived from the polymerization of ethylene oxide units and can be a linear or branched polyether terminated with a hydroxyl group. Due to the reactivity of the hydroxyl moiety, a methoxy is often added as a cap (mPEG) (**Figure 1.6a**). The size of the polymer chain is determined by the number of repetitive ethylene units and is commercially available in 2, 5, 10, 20, and 30 kDa sizes.

POZ is derived from the ring opening polymerization of 2-oxazoline units [150] and is slightly branched in nature. The number of 2-oxazoline units determines the size of the POZ

polymer and the type of side chain determines the length of the branch (*i.e.,* methyl, ethyl or propyl). For this thesis, 20 and 30 kDa polyethyloxazoline (PEOZ) was utilized (**Figure 1.6b**).

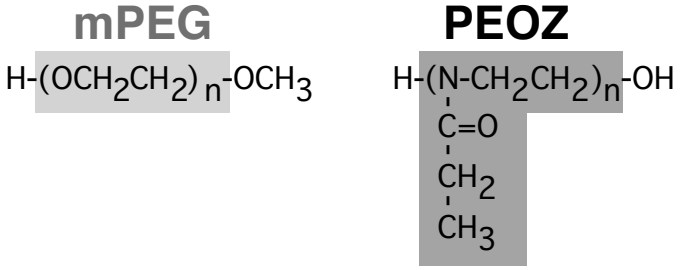

Figure 1.6 The structures of mPEG and PEOZ. The shaded areas denote the repeating structures of mPEG and PEOZ. Modified from Kyluik-Price 2014 [148].

In order to couple polymer chains to a molecule, a functional linker is added to produce an activated mPEG or POZ. The linker is chosen based on the type of functional group targeted for modification. Many different linkers are available for specific attachment to lysine, cysteine or oxidized carbohydrates [152]. In general, lysine and N-terminal amino group targets are commonly used because of the ubiquitous nature of lysine in proteins. Although these activated linkers could theoretically bind to any charged amino group, studies show that lysine residues are the primary targets [153,154]. Indeed, lysine is the most prevalent amino acid in proteins and contributes to approximately 10% of the overall amino acid sequence [152].

Amine modification takes advantage of the different pKa of alpha (9.0) or epsilon (10.5) amino lysine residues (**Figure 1.7a**) and the attachment of polymers is optimal when lysine is in a deprotonated form (at high pH). However, to balance the high pKa with the physiological conditions required for biologics, polymer modification is done in an aqueous solution at a lower pH (8.0). At this pH, most lysine residues are in a protonated form (1+) with a small amount as deprotonated anions (1-) in a ratio of approximately 99:1 [155] (**Figure 1.7b**). As polymers become covalently attached to the deprotonated anion, there is a shift in equilibrium that restores the cation:anion ratio, and thereby provides available anion binding sites for subsequent polymer attachment.

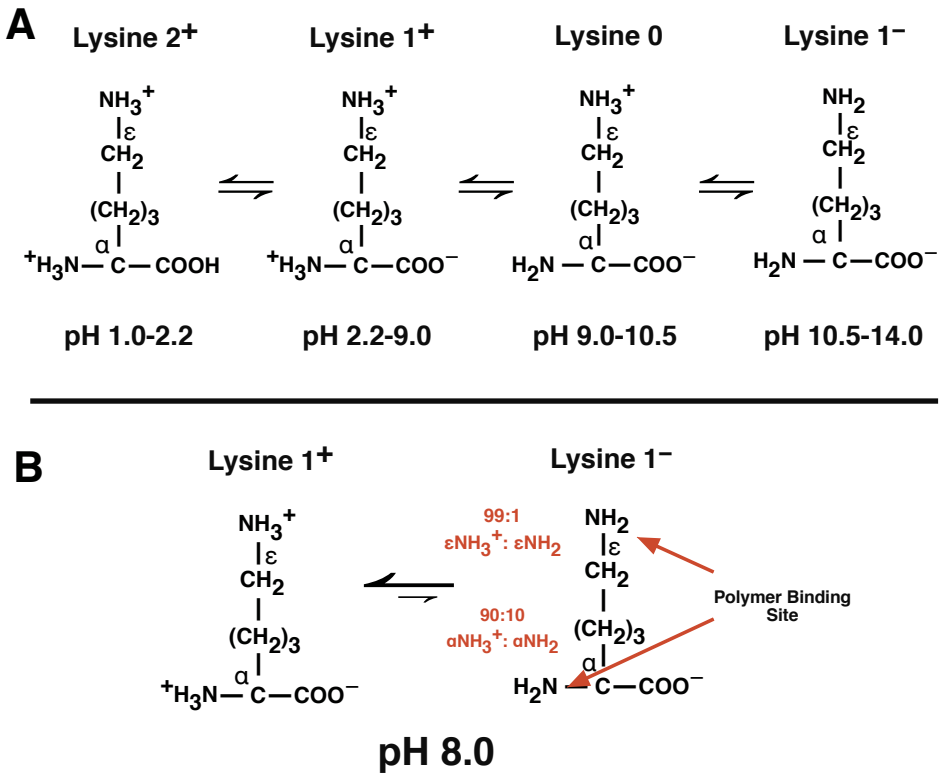

Figure 1.7 Ionization states of lysine. (A) Lysine possesses predominant ionization states depending on the pH. Three ionizable groups (COOH, NH3α, NH3ε) can become deprotonated, resulting in four charged states of lysine. (B) The covalent attachment of polymers takes place at a pH of 8.0, when the majority of lysine is in the 1+ ionization state. However, a small amount of the negatively charged form is capable of reacting with the polymer. This negatively charged population is not depleted upon polymer grafting due to a shift in equilibrium (Le Chatelier's Principle) maintaining the constant concentration. Modified from Nelson and Cox 2013 [155].

Several linker chemistries that target lysine residues have been developed including succinimidyl valerate (SVA) and succinimidyl propionate (SPA), the two linker chemistries used in this thesis. The carbonyl groups of the linkers are attacked by the nucleophilic nitrogen atoms of the primary amines, resulting in formation of a covalent bond and release of the free linker group- N-hydroxy succinimide (NHS) (**Figure 1.8)**. Since polymer attachment occurs in aqueous solutions, water molecules compete with nitrogen atoms, resulting in hydrolysis of the linker over time, preventing covalent polymer attachment. The hydrolysis half-life of the two linkers differ, with SVA and SPA being 33.6 and 16.5 minutes (25°C, pH 8.0) respectively.

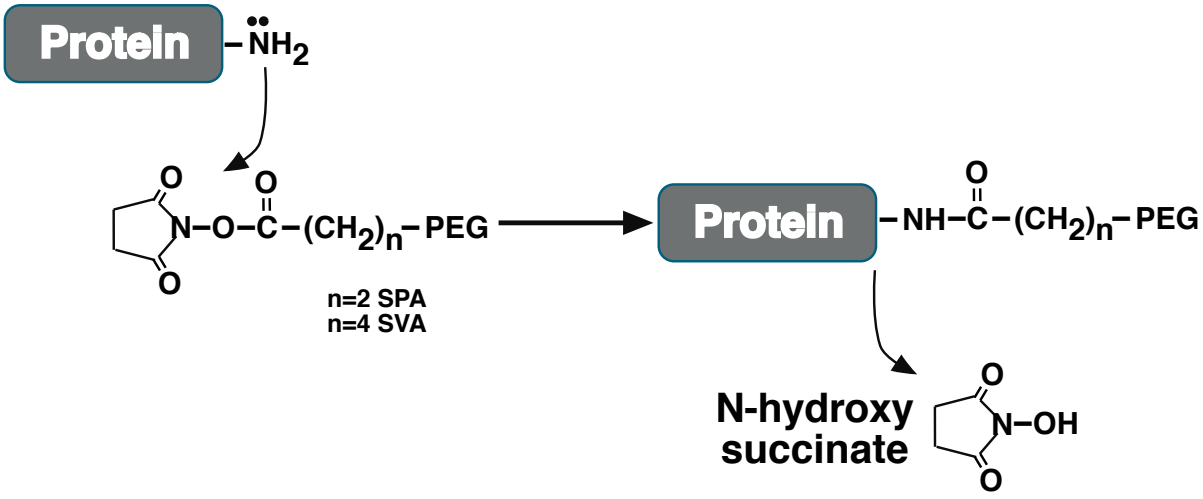

Figure 1.8 The covalent attachment of polymers to proteins. A nucleophilic attack by the primary amine on a protein results a substitution reaction, the release of N-hydroxy succinate (free linker group) and the formation of a covalent bond between the protein and the polymer. Modified from Le and Scott 2010 [156].

1.6.4 Polymer Characteristics: Physical Properties, Metabolism, Toxicity and Immunogenicity

The large exclusion volumes characteristic of biocompatible polymers are due to their ability to bind water and chain flexibility. mPEG polymers are very hygroscopic, capable of binding 2-3 water molecules per ethylene unit [152]. POZ shows comparable water binding capabilities, although some studies suggest that mPEG may have a slightly larger hydrodynamic volume compared to POZ, indicating that POZ may be slightly less hydrated [150]. However, both polymers exhibit volumes 3-5 times their molecular weights [134,152,157,158]. Both mPEG and POZ exhibit high flexibility, with mPEG exhibiting free rotation every 4-5 ethoxy units [159]. Although both polymers are very flexible, the slightly branched nature of POZ may decrease its chain flexibility [160,161], although no specific comparison study has been done.

The Flory radius (R_F) defines the limits of polymer-mediated surface coverage (**Figure 1.9a**). Both the number and the length of monomer chains affect the R_F. Therefore, the R_F increases with polymer length. For example, the 2, 5, and 20 kDa polymers exhibit radii of 3.4, 6.0 and 13.7 nm, respectively [162]. Polymer chains exhibit different conformations when

covalently attached to biological or synthetic surfaces, which is determined by both R_F and grafting concentration [162]. Low grafting concentrations, in which the distances between two polymer-anchoring points is larger than the Flory radius, preventing interaction of the individual chains, leads to a mushroom conformation (**Figure 1.9b**). Conversely, if the attached polymers are grafted at high concentrations, where there are short distances between the anchor points, associations between polymer chains results in a random coil or extended chain formation (**Figure 1.9b**). In addition, the conformations formed when polymers are attached to cell surfaces are also affected by the protein distribution on the surface of the cell and the topography. Thus, it is likely that at biologically relevant grafting concentrations, the majority of polymers assume a mushroom conformation, although extended conformations may occur in protein dense regions such as protein complexes found on cell surfaces.

The large hydrodynamic volume and polymer flexibility allows surface attached polymers to occupy large volumes on the cell surface, leading to the exclusion of biological components such as cells and macromolecules. This protects both the polymer bound protein (direct camouflage) as well as proteins within the Flory radius (indirect camouflage) from immune components (**Figure 1.9c**). In addition to steric camouflage, the hydration sphere created by the hygroscopic nature of polymers results in charge camouflage, burying the charges beneath the neutral PEG layer and hindering ligand-receptor interactions [156].

The biodistribution and metabolism of PEG and POZ are well documented, showing that both polymers are primarily excreted through the urine. Intravenous administration of POZ in mice showed that the polymer was excreted *via* the kidneys without significant accumulation in organs, although very high molecular weight polymers (45 kDa and 120 kDa) were found in skin and muscle [163]. However, a subsequent study by Gaertner *et al* [164] found no accumulation using more biologically relevant polymer lengths (15 and 29 kDa). Similarly, studies using PEG have shown that polymers ≤ 30 kDa are excreted through passive glomerular filtration, while

large molecular weight polymers are retained for longer time periods in the body and are excreted *via* both the kidney and hepatic system [165,166].

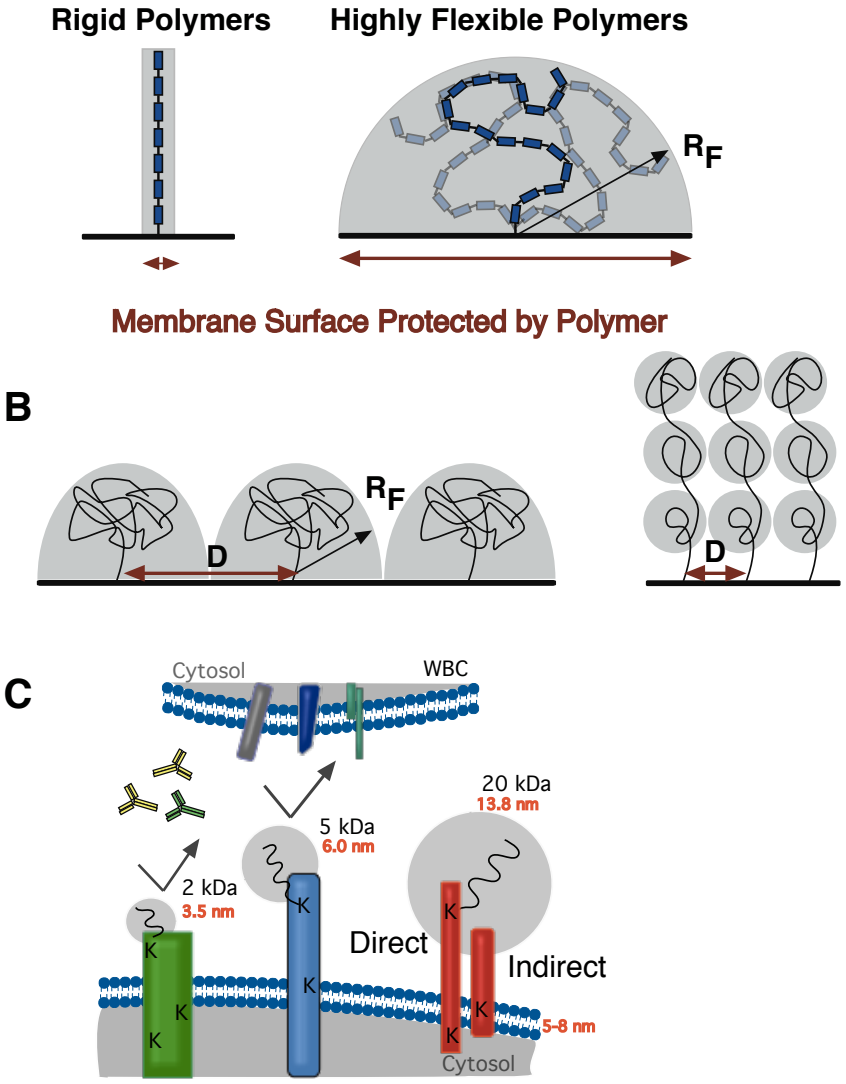

Figure 1.9 Physical properties of polymer mediated camouflage. (A) The Flory radius (R_F) defines the limits of polymer-mediated surface coverage. Rigid polymers have a small R_F whereas highly flexible mPEG and POZ polymers exhibit extended coverage of the surfaces they modify. Modified from Chen 2006 [167]. (B) R_F and grafting concentration dictates the conformations of covalently attached polymer chains. Distances (denoted by D) larger than the Flory radius (low concentrations) between attachment points, leads to mushroom conformations. High concentrations with short distances between anchor points, results in extended chain formations. Modified from de Gennes 1980 [162]. (C) Camouflage of cell surfaces leads to the exclusion of cells and immune components (immunocamouflage) that is dependent on polymer grafting concentration and size. Both direct and indirect camouflage may occur due to the complex surface topography of cells. K= lysine residue.

While toxicity has been studied more extensively for PEG than POZ, both are FDA approved compounds found in food and beauty products. However, PEG is utilized much more

frequently than POZ. Both acute and long-term toxicological studies of PEG indicated safety across all routes of administration and only showed signs of toxicity at extremely high parenteral doses, with the target organ being the kidney (which would have the largest concentrations) [168]. According to the World Health Organization, an accepted dose of PEG is very high at 10 mg/kg [165]. Similarly, toxicity studies using POZ showed that single or repeated injections of 10 kDa at 0.5, 1, and 2 g/kg in rodents demonstrated no adverse effects or pathological evidence in organs or tissues [150]. Furthermore, these polymers were shown to be neither carcinogenic nor mutagenic [168,169].

Recent publications suggesting pathological changes and the appearance of vacuoles in cells, which occurred after multiple high doses of PEG, resulted in no functional deficit and resolved over time [165]. However, toxicity may be a function of molecular weight. For example, the metabolism of alcohol groups *via* alcohol dehydrogenase to toxic metabolites has been found in urine with a greater frequency (25%) using very small molecular weight PEG polymers (0.4 kDa) compared to larger molecular weight polymers (6 kDa) found in only 4% of patient's urine [170,171].

Although clinically proven as a low toxic and low immunogenic polymer, recent observations of anti-PEG antibodies have appeared in the literature. Observations of antibodies against the PEG moiety were detected in patients treated with allergens [172], PEG-uricase [173], PEG-asparaginase [174] and liposomes [175]. Although these anti-PEG responses have been reported in patients treated with PEG-therapies, they have resulted in extremely low titers of IgM and IgG (PEG-uricase) [173,176] or had conflicting results regarding the influence of antibodies for the efficacy of treatment (PEG-interferon) [177,178]. Also, a single study suggested that anti-PEG antibodies were identified in 25% of healthy blood donors who were not previously given treatments with PEGylated drugs [179]. This study is often compared to studies from 1984 where 0.2% of healthy donors had detectable anti-PEG antibodies [172], and is cited as evidence of an increased incidence in the population. However, these results are in

sharp contrast to a recent report in which only 4% of healthy donors were found antibody positive [180]. Subsequent studies have been done to induce anti-PEG antibodies in animals, but have led to conflicting results. For example, in all cases a PEG conjugated product was needed as PEG alone did not induce a response, while other times a strong adjuvant was necessary [181,182]. Furthermore, in the context of mPEG modified RBC, tertiary or hyper-transfused mice given mPEG modified RBC exhibited normal survival and circulation time, indicating a lack of antibody response [183]. Indeed, there are few reports in which antibodies to PEG resulted in adverse immunological consequences in over 30 years of clinical use, indicating that the immunogenicity of PEG remains to be established.

1.6.5 PEGylated Proteins, PEGylated Liposomes and Cell Encapsulation

Since initial PEGylation studies using catalase and albumin resulted in reduced immunogenicity and prolonged half-life, protein PEGylation has brought into market several conjugates with great therapeutic performance. The first FDA approved PEG protein was PEGylated adenosine deaminase (Adagen®) used for the treatment of severe combined immunodeficiency syndrome (SCID) [131], followed soon by a PEGylated asparaginase for the treatment of acute lymphoblastic anemia [184]. Since then, several different PEGylated proteins have been FDA approved including PEG-INFα as a treatment for hepatitis, PEG-G-CSF for treatment of neutropenia, PEG-epoetin-beta for treatment of anemia, and more recently PEG-uricase for treatment of gout [185]. Thus, PEGylation technology has proven efficacy for protein modification, improving the pharmacokinetic properties of protein and enzyme based therapies, resulting in a multi-billion dollar business.

PEGylation of liposomes and other drug carriers has also proven efficacious for the targeted delivery of therapeutics. PEGylated liposomes decrease immune recognition, allowing for longer circulation time and greater drug efficacy [186,187]. Like PEGylated proteins, several

FDA approved liposomes are on the market for the treatment of various conditions such as infections and cancer and are also used in vaccines.

The ability of polymers to protect tissues from immune recognition has also been explored *via* hydrogel encapsulation of intact cells [144,188]. Encapsulation is a means to facilitate the transplantation of cells, while providing a protected environment from the immune response. Bio-encapsulation has promising implications for many diseases, including diabetes, and several studies have used hydrogels containing insulin producing beta cells. However, problems may occur due to the physical thickness of encapsulation, hindering efficient oxygen and molecular exchange between cells and their environments, including nutrients and regulatory factors needed for survival [188,189].

1.6.6 Direct PEGylation of Intact Cells: Red Blood Cells, Leukocytes, Viruses and Islets

The direct PEGylation of intact allogeneic cells decreases immunogenicity by acting as a molecular sieve, effectively repelling large molecules such as immune cells and components while allowing the diffusion of essential small molecules such as oxygen and glucose. The direct PEGylation of RBC has demonstrated both normal cell function and structure while exhibiting decreased immunogenicity both *in vitro* and *in vivo*. For example, mPEG-RBC decreased agglutination by pre-formed antibodies and prevented phagocytosis of foreign RBC, demonstrating that mPEG attenuates the antigenic recognition of RBC surface proteins [135]. Furthermore, single, repeated or hyper-transfusion of mice with mPEG-RBC demonstrated no toxicity and mice exhibited normal survival (**Figure 1.10)** [135,136]. Even xenogeneic transfusions of mPEG-modified sheep RBC into mice demonstrated significantly increased survival compared to the unmodified control [135]. Additional functional RBC studies were performed *in vitro* showing that at moderate grafting concentrations (≤ 2.4 mM) RBC exhibited normal morphology, osmotic fragility, anion and cation transport, and decreased surface charge

[136]. Steric and charge camouflage was further demonstrated by decreased protein absorption on mPEG modified latex beads (biophysical model) showing that both hydrodynamic surface charge camouflage and steric prevention of surface macromolecule interactions were polymer and target size dependent [156].

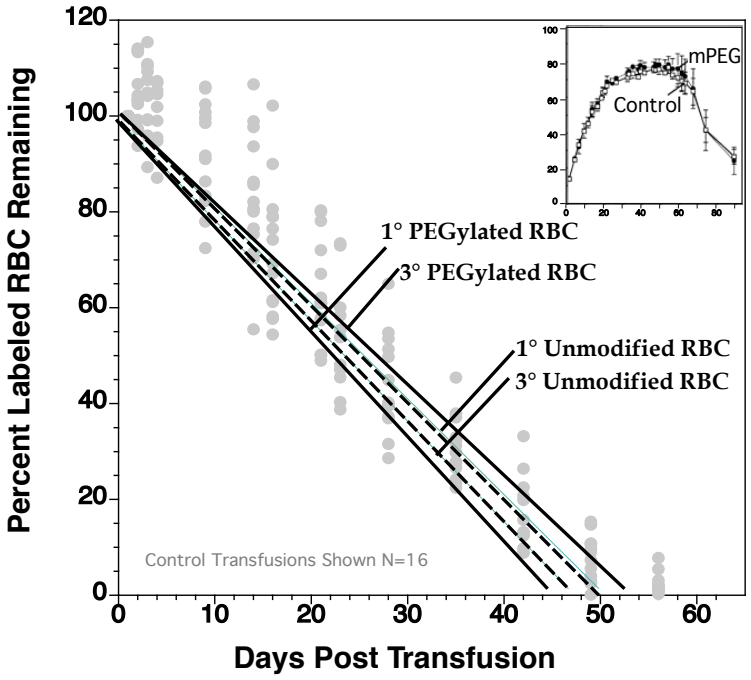

Figure 1.10 *in vivo* survival of mPEG modified RBC. Autologous murine transfusions have normal *in vivo* survival, demonstrating the non-toxic and non-immunogenic nature of mPEG polymers. The primary and tertiary transfusions of control-RBC (dashed lines) and 2.0 mM mPEG-RBC (solid lines) show normal *in vivo* survival. Hypertransfused mice (insert) with mPEG- and control-RBC emphasize the *in vivo* normality of modified RBC. Mice received 33 transfusions of control or mPEG-modified RBC. Modified from Scott 1998 [183].

The successful work with mPEG-RBC initiated work with PEGylated leukocytes as a means of preventing transfusion associated graft *versus* host disease (TA-GVHD). Studies demonstrated inhibition of allorecognition between two disparate leukocyte populations *in vitro*, as reflected by a polymer dose dependent decrease of cell proliferation, and *in vivo* as shown by a decrease in GVHD associated morbidity and mortality in mice [138]. Studies also showed that mPEG modified leukocytes displayed normal morphology and viability as well as inhibition of antibody binding [137,138]. More recently, PEGylation of allogeneic lymphocytes has been shown to induce a tolerant state, *in vitro* and *in vivo*, resulting in decreased inflammatory cytokines and cells as well as increased Treg cells (**Figure 1.11)**. Importantly, these effects were long-lived [190].

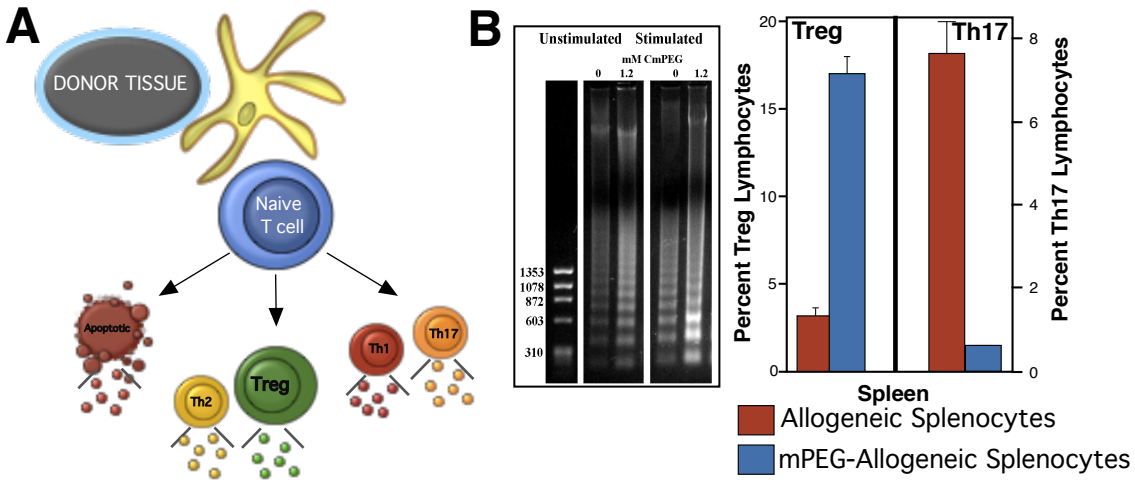

Figure 1.11 Induction of immunotolerance by mPEG modification of allogeneic cells. (A) Schematic showing altered T cell differentiation. PEGylation of donor leukocytes leads to altered cell differentiation, resulting in increased suppressive cells (Treg and apoptotic cells) and decreased inflammatory cells. The size of the cell denotes the increase or decrease of the population. (B) Previous studies indicate enhanced DNA laddering (indicative of apoptosis) of polymer-modified cells compared to control. In addition, mice injected with mPEG-modified splenocytes show elevated levels of Treg cells and decreased levels of inflammatory Th17 cells compared to the control. Shown are the results from analysis of cell types in the spleen, 5 days post transfusion. Similar results were found from the examination of the lymph nodes and blood. These effects were long-lived, showing similar results 30 days post transfusion. Modified from Chen 2003 [138], Wang 2011 [190].

The receptor-mediated interactions between allogeneic cells and immune components are somewhat analogous to receptor interactions between viruses and host cells. Therefore, PEGylation was also investigated on viruses and their target cells as a means of broad-spectrum prophylaxis against viral infection. Several studies demonstrated that both direct PEGylation of virus (both enveloped and non-enveloped) and target cells resulted in effective attenuation of viral infection [140,141,191]. Furthermore, the direct PEGylation of a wide variety of viruses has shown that both receptor-mediated and fusion entry can be prevented. The size of the PEGylated target determined the efficacy of immunocamouflage and the prevention of virus infection, with the smaller polymers showing increased efficacy for virus camouflage and the larger polymers showing increased efficacy for cell camouflage [140,141].

Applications of cell PEGylation have also been explored in pancreatic islet cells, showing that PEGylation of islets could provide immunological protection of renal subcapsular allotransplanted islets, while maintaining normoglycemia, cell viability, and the functional

capacity of islets [105,139,192,193]. Furthermore, PEGylated islets demonstrate benefits to early transplant periods and long-term outcomes when combined with immunosuppressants, remaining functional for more than one year *in vivo* [192]. Thus, the ability of PEG to prevent interactions between immune components and cells, while maintaining cell viability, generates exciting possibilities for the PEGylation of allogeneic cells and tissues in transplantation and transfusion medicine.

1.7 Hypothesis and Specific Aims

Allorecognition initiates the adverse events associated with RBC alloimmunization and tissue rejection. Current clinical approaches utilize tissue matching (HLA and blood typing) as well as immunosuppressive agents in an effort to attenuate allorecognition and control the alloresponse. However, these practices lead to both inventory and drug toxicity issues for patients.

Approved PEGylated proteins have been widely used for drug delivery to enhance bioavailability and decrease immune responses. More recently, the direct PEGylation of intact cells (e.g., RBC, WBC) and tissues (e.g., pancreatic islets) have been examined. These studies demonstrated efficient camouflage of cell antigens and decreased allogeneic response, with no substantial effects on cell survival. This suggests that PEGylated cells and tissues may have significant utility in transfusion and transplantation research, where prevention of allorecognition is critical. Therefore PEGylation, unlike current immunosuppressive drugs, is a novel approach that could prevent initial allorecognition events by the global camouflage of allogeneic cells. Although, many aspects of immunocamouflage are well understood, the efficacy of alternative polymers and the effect of grafted polymer on leukocyte signaling cascades have not been fully explored.

While mPEG is the dominant polymer used in today's clinical products, a search for alternative polymers with improved properties would be beneficial to expand the repertoire of

polymers for therapeutic use. Polyethyloxazoline (PEOZ) exhibits several attributes that make it an attractive alternative to traditional mPEG for the immunocamouflage of cells and tissues. Therefore, the first part of this thesis compared PEOZ to mPEG in order to assess the utility of PEOZ for immunocamouflage of intact cells. Furthermore, our studies to date have not fully defined the underlying molecular events (altered cell-cell interactions and intracellular signaling cascades) leading to the reduced allogeneic response observed during PEGylated allogeneic leukocyte studies. Maximizing immunocamouflage efficacy and understanding the mechanism of the induced immune quiescent state, following the polymer modification of cells, is important for producing improved and/or novel cellular blood products.

Our hypothesis is that **allorecognition (e.g., blood group antigens or MHC) can be prevented by the covalent membrane grafting of non-immunogenic polymers. Moreover, it is anticipated that the efficacy of immunocamouflage will be a function of both polymer species and polymer size. For leukocytes, it is further proposed that the grafted polymer affects both cell-cell interactions and intracellular signaling cascades.** To test this hypothesis, as illustrated in **Figure 1.12,** the specific aims were to assess:

1. The comparative utility and differential effects of grafted PEOZ and mPEG on blood cells. PEOZ was compared to mPEG in terms of grafting efficiency, structural and functional consequences of polymer attachment, and comparative immunocamouflage of RBC and WBC *in vitro*.

2. The effect of grafted polymer on surface marker (CD) immunocamouflage and cell-cell interaction. The surface immunocamouflage of various lymphocyte receptors involved in adhesion and activation events were investigated. Moreover, the inhibition of allorecognition was examined by assessing lymphocyte-APC conjugation events during allogeneic challenge using mPEG-modified lymphocytes. The effect of surface protein immunocamouflage and inhibition of cell interactions was explored in relation to the proliferative capacity of mPEG-modified cells during allogeneic and mitogen challenge.

3. The consequence of grafted mPEG on intracellular signaling cascades. Activation and cell death pathways were evaluated to determine their involvement in the decreased proliferative response seen in modified cells during allogeneic challenge. To test this, alterations to mRNA and protein expression involved in allorecognition and cell activation pathways (NFκB) as well as changes in early and late apoptotic events were assessed.

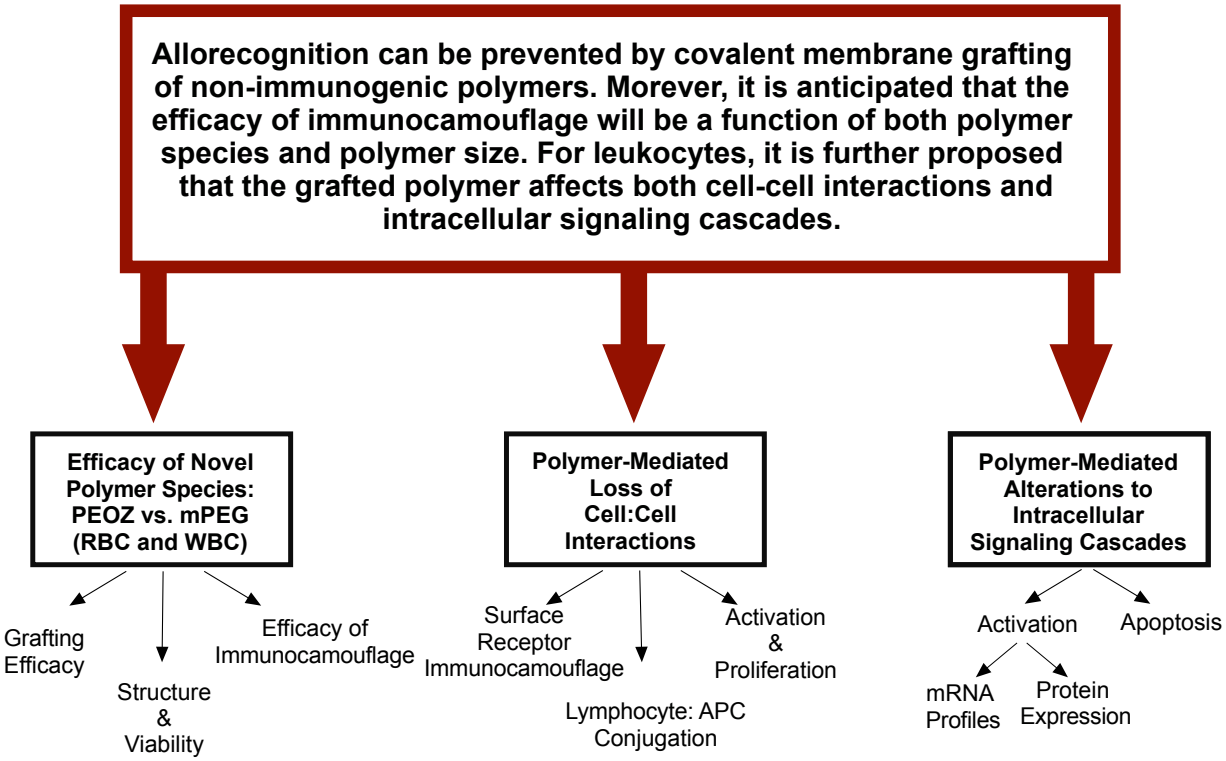

Figure 1.12 Outline of project. To expand the repertoire of polymers for potential therapeutic use in transplantation and transfusion medicine, a novel polymer (PEOZ) was investigated. PEOZ was compared to mPEG in terms of grafting efficacy, structural and functional assays and comparative immunocamouflage of RBC and WBC. To clarify the cellular mechanism of immunocamouflage imparted by polymer grafting, important for the development of novel immunocamouflage therapeutics, both alterations to cell-cell interactions as well as changes to intracellular activation and apoptosis pathways during allogeneic challenge (mixed lymphocyte reaction) were investigated.

2 CHAPTER 2: Methods and Materials

2.1 Polymer Species

Succinimidyl valerate activated mPEG (mPEG; 5, 20 and 30 kDa) was purchased from Laysan Bio Incorporated (Arab, AL, USA). N-hydoxysuccinimidyl ester of polyethyloxazoline propionic acid (PEOZ; 20 and 30 kDa) was obtained from Serina Therapeutics Incorporated (Huntsville, AL, USA). The structures and characteristics of mPEG and PEOZ are shown in **Figure 2.1**.

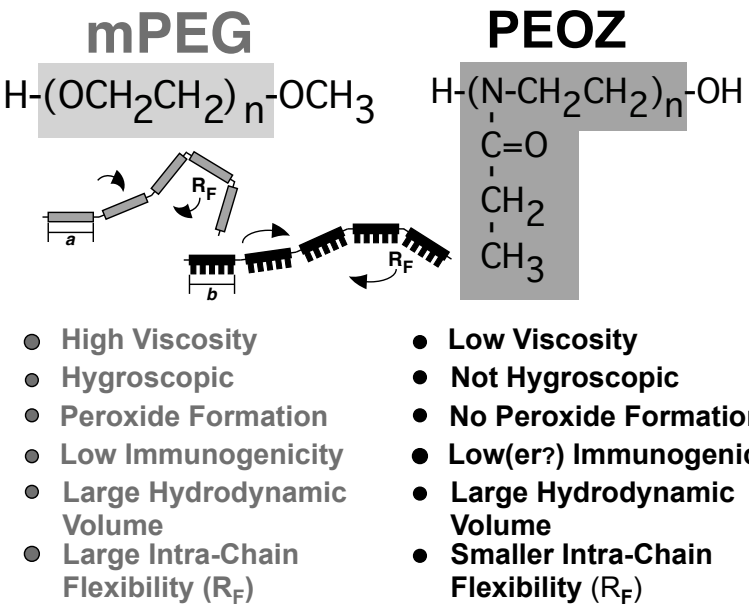

Figure 2.1 Structure and characteristics of mPEG and PEOZ. The shaded areas denote the repeating structures of mPEG and PEOZ. The (*a*) and (*b*) notations show the independent rotational segments of mPEG and PEOZ (respectively) governing intra-chain mobility. The relative intra-chain mobility of the polymers, coupled with polymer size (e.g., 2 *versus* 20 kDa), underlies the radius of gyration of the grafted polymer. The relative radii of gyration for mPEG and PEOZ are indicated by the arrows, denoting the Flory radii (R_F) of the polymers. As illustrated, the side-branches of PEOZ may decrease intra-chain mobility. From Kyluik-Price 2014 [148].

2.2 Cell Models

2.2.1 Red Blood Cell (RBC) and Peripheral Blood Mononuclear Cell (PBMC) Extraction and Isolation

Whole blood was collected from donors, following informed consent, into tubes containing sodium heparin. For packed red blood cell (pRBC) collection, whole blood was washed 3x in phosphate buffered saline (PBS) and centrifuged for 5 minutes at 1000 x g.

Peripheral blood mononuclear cells (PBMC) were isolated using Histopaque-1077 (Sigma-Aldrich, St. Louis, MO, USA) according to manufacturer's protocol.

2.2.2 Generation of Monocyte Derived Dendritic Cells (moDC)

Freshly prepared PBMC were seeded in 6-well plates (Becton Dickinson, Franklin Lakes, NJ, USA) at 5 x 10^6 cells/ml in AIM V medium (Invitrogen, Grand Island, NY, USA). PBMC were incubated at 37°C, 5% CO_2, and 95% humidity for 3 hours to allow cells to adhere. After 3 hours, non-adherent cells were removed by washing the plate twice with pre-warmed AIM V medium. The remaining monocyte rich adherent cells were incubated in AIM V medium supplemented with IL-4 (100 ng/ml) and GM-CSF (50 ng/ml) (R&D Systems, Minneapolis, MN, USA). IL-4 and GM-CSF was added again on day 3. On day 6, cells were removed with cell scrapers, washed twice, centrifuged at 400 x g and suspended at 5 x 10^5 cells/ml in AIM V medium. Cells were supplemented again with IL-4, GM-CSF and maturation/activating cytokines TNF-α (5 ng/ml), IL-1β (5 ng/ml), IL-6 (150 ng/ml) (R&D systems Inc., Minneapolis, MN, USA) and prostaglandin E2 (1 µg/ml) (Sigma-Aldrich, St. Louis, MO, USA). Mature monocyte derived dendritic cells (moDC) were harvested on day 7 and assessed by flow cytometry for maturation markers CD80 and CD86 (BD Biosciences, San Jose, CA, USA) prior to downstream assays (**Figure 2.2)**. Briefly, 4 µl of antibody was added to 5 x 10^5 cells total in flow tubes and incubated for 30 minutes in the dark. Cells were washed twice in PBS+0.2% bovine serum albumin (BSA), centrifuged for 5 minutes at 300 x g and suspended in 500 µl PBS+0.2% BSA prior to flow cytometry. Data acquisition and analysis was performed using Cell Quest Software. A minimum of 20,000 events was collected per sample.

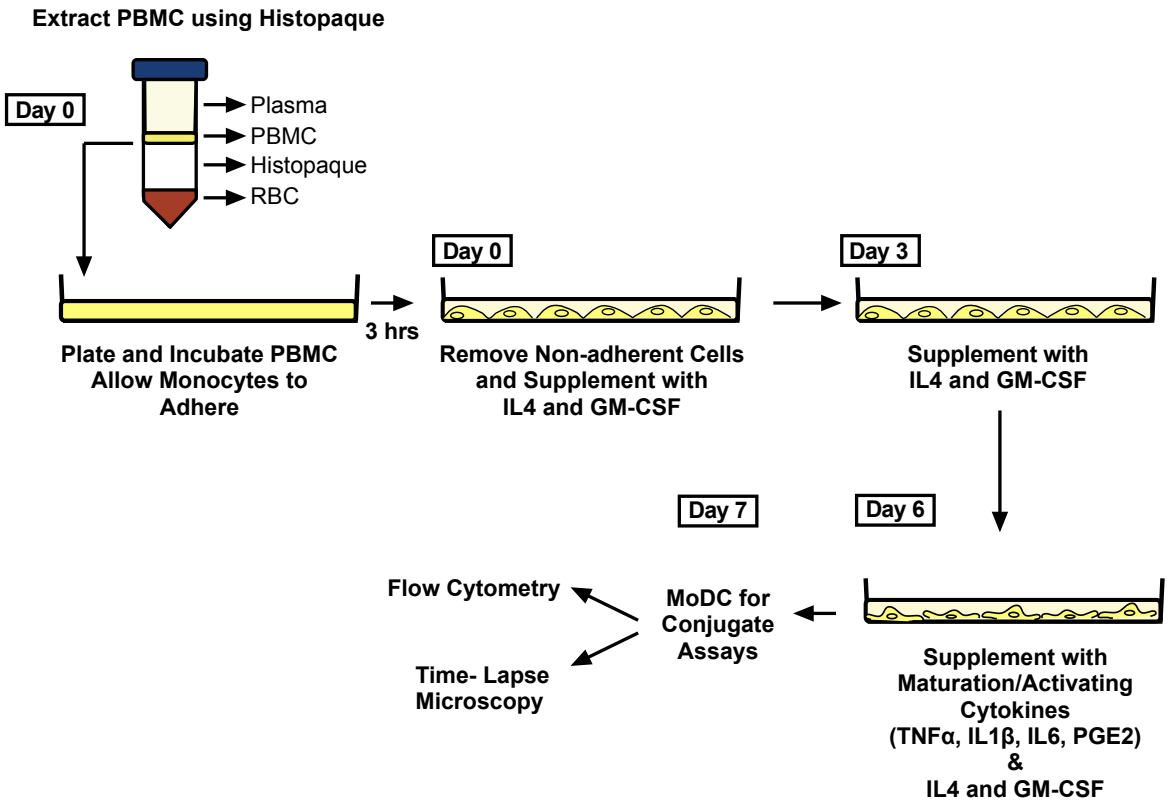

Figure 2.2 Generation of monocyte derived dendritic cells (MoDC). Freshly isolated human PBMC were plated in 6-well culture plates and incubated at 37°C, 5% CO_2, and 95% humidity for 3 hours to allow cells to adhere. On day 0 and 3, cells were supplemented with IL4 and GM-CSF. Cells were harvested from the plate on day 6, washed and plated with maturation/activating cytokines for 24 hours before being harvested for downstream assays.

2.3 Polymer Modification of Cells

Isolated RBC and PBMC were suspended to 12% hematocrit (5 g%Hb) and 4 x 10^6 cells/ml, respectively in mPEG buffer (50 mM K_2HPO_4, 105 mM NaCl, pH 8.0) with desired amount of mPEG (2, 5, 20, 30 kDa) or PEOZ (20, 30 kDa) to reach appropriate grafting concentrations (0-4 mM). Cell suspensions (RBC or leukocytes) were mixed by gentle inversion and the reaction was performed for 1 hour at room temperature. RBC or leukocytes were washed 3x with PBS or RPMI-1640 supplemented with 25 mM HEPES and 0.01% human albumin (Invitrogen, Carlsbad, CA, USA), respectively. Leukocytes were stained with trypan blue (Invitrogen, Grand Island, NY, USA) and enumerated using a hemocytometer.

2.4 Two-Phase RBC Partitioning

To quantify the efficiency of polymer grafting, aqueous two-phase partitioning studies of control, mPEG, or PEOZ-modified human RBC (2, 5, 20 and 30 kDa mPEG or 20 and 30 kDa PEOZ; 0-5 mM) were performed as previously described [194-196]. In this system, polymer-modified RBC partition to the upper PEG layer, whereas unmodified or poorly modified cells partition to the lower Dextran layer or remain at the phase-interface. The two-phase system consisted of 5% ww Dextran, 4% ww PEG8000, 0.15 mol/L NaCl and 6.84 mmol/L $NaHPO_4$. A 10 µl aliquot of the control RBC, mPEG-RBC, or PEOZ-RBC suspension (5% Hb) was added to 0.5 ml of the PEG rich phase, mixed and overlaid on the Dextran rich phase (0.5 ml). The RBC-phase solution was mixed thoroughly by inversion and phases were allowed to separate at room temperature for 20 minutes. A 250 µl aliquot was removed from the upper phase and washed 3x in PBS. Hemoglobin was assessed by Drabkin's assay [197]. For Drabkin's assay, the hemoglobin concentration is determined by a colourmetric cyanmethemoglobin method using Drabkin's Reagent (Sigma Aldrich, St. Louis, MO, USA). Total hemoglobin is converted to a cyano derivative and the absorbance is determined at 540 nm. The following equation was used to calculate the concentration of total hemoglobin in the samples.

$$[Hb] = \frac{OD_{540} \times (\text{final volume}/\text{sample volume})}{6.8 \text{ (extinction coefficient)}}$$

The percent recovery was determined by dividing the initial hemoglobin concentration by the recovered hemoglobin concentration in the upper phase.

2.5 Morphological Analysis of Polymer Modified Cells

For morphology studies, freshly derivatized RBC or PBMC (5, 20 and 30 kDa mPEG or 20 and 30 kDa PEOZ; 0-4 mM) were fixed in 4% methanol free formaldehyde and assessed using Zeiss Axioplan 2 (Micro-Optik, Deursen, Netherlands) or Olympus CK40 microscope (Olympus America Inc., Melville NY, USA) fitted with Q-imaging camera (QICAMFAST, Qimaging Corporation, Surrey, BC, Canada). Transmitted light images were taken at 1000x

magnification with Northern Eclipse software or at 200x and 400x magnification with Q-capture imaging software (v.2.8.1).

2.6 Osmotic Fragility and Hemolysis

The structural stability of mPEG and PEOZ-modified RBC, relative to unmodified cells, was examined *via* osmotic fragility studies as previously described [135,136]. After polymer modification, RBC were processed immediately (T=0) or incubated in PBS at 37°C water bath for 24, 48, and 68 hours. Samples were suspended to 10% hematocrit and 100 µl of unmodified (0 mM) or polymer modified RBC (20 and 30 kDa mPEG or PEOZ; 0-2 mM) was added into tubes containing 1 ml of various saline concentrations (0-0.9%) and mixed by inversion. Total and supernatant hemoglobin concentrations were measured at the indicated timepoints by Drabkin's assay to determine percent lysis.

2.7 Surface Marker Analysis

2.7.1 Red Blood Cell Antigens

The immunocamouflage of RBC RhD and Kell (k) blood group antigens was determined *via* flow cytometry (FACSCalibur flow cytometer; BD Biosciences, San Jose, CA, USA) following cell derivatization (5, 20 and 30 kDa mPEG or 20 and 30 kDa PEOZ; 0-4 mM). For measuring the comparative efficacy of mPEG and PEOZ on the immunocamouflage of the RhD and Kell blood group antigens, a 3% hematocrit solution was placed into flow tubes with primary antibody anti-k (Immucor Inc., Norcross, GA, USA) and/or anti-RhD (Novaclone anti-D, Dominion Biologicals Ltd., Dartmouth, NS, Canada). The mixture was incubated for 30 minutes with gentle rocking at 37°C. Cells were washed 3x with PBS and incubated with FITC conjugated secondary antibody anti-IgG (Abdserotec, Oxford, UK) for 1 hour, as previously described [195,198]. Control samples for background signal as well as non-specific antibody binding consisted of unstained RBC or RBC incubated with primary or secondary antibody only. Cells

were washed 3x with PBS and suspended in 0.5 ml of 1% methanol free formaldehyde prior to flow cytometry. Analysis of the efficacy of immunocamouflage was analyzed based on total mean cell fluorescence (MCF) and percent positive cell values (PPC). Data acquisition and analysis was performed using Cell Quest Software (BD Biosciences, San Jose, CA, USA). For all studies a minimum of 20,000 events per sample was collected.

2.7.2 Cluster of Differentiation (CD) Markers

Freshly isolated control or polymer modified PBMC (5, 20 and 30 kDa mPEG or 20 and 30 kDa PEOZ; 0-4 mM) was assessed for immunocamouflage by the exclusion of fluorescently labeled antibodies to leukocyte cluster of differentiation (CD) markers: CD3, CD4, CD11a, CD25, CD28, CD62L and CD71. Surface marker analysis was done *via* flow cytometry following cell derivatization. PBMC cell suspensions (1×10^6 cells) were placed into flow tubes with anti-CD3 PerCP, anti-CD4 PE, anti-CD11a FITC, anti-CD25 PE, anti-CD28 FITC, anti-CD62L PE or anti-CD71 FITC according to manufacturer's instructions (BD Biosciences, San Jose, CA, USA) and incubated for 1 hour on ice. Unstained cells and isotype control antibodies were utilized for each fluorophore to determine the degree of non-specific binding and background fluorescence. PBMC were washed 3x (PBS, 1% bovine serum albumin, 0.1% NaN_3) and suspended in 0.5 ml wash buffer before being analyzed by flow cytometry. Analysis of the efficacy of immunocamouflage was performed as described previously for RBC surface antigens.

2.8 Monocyte Monolayer Assay (MMA)

The monocyte monolayer assay (MMA) was used to measure the effect of mPEG and PEOZ on immune recognition (**Figure 2.3)**. The MMA measures FcγR-mediated phagocytosis *in vitro* using adherence-purified allogeneic monocytes isolated from PBMC [199-202]. To prepare the monocyte monolayer, isolated PBMC were suspended in AIM V medium, aliquoted onto tissue cultures slides, and incubated for 1 hour in a humidified 5% CO_2, incubator at 37°C. Non-adherent cells were removed by washing. RhD+ or RhD- RBC were incubated with RBC-

matched serum (negative control) or opsonized using a commercial anti-RhD antibody (Rho(D) Immune Globulin (Human) RhoGAM Ultra-Filtered PLUS, Ortho Clinical Diagnostics, Markham, ON, Canada), washed and overlaid on the monocyte monolayer in humidified, 5% CO_2, incubator at 37°C for 1 hour. Excess media from red cell suspensions were aspirated from each slide. Slide chambers were removed and slides were stained with Wright-Giemsa stain. The number of phagocytized control or modified RBC (20 and 30 kDa mPEG or PEOZ; 2.0 mM) was enumerated per 100 monocytes (Monocyte Index; MI). Positive (*i.e.*, anti-D opsonized unmodified RhD+ RBC) control values typically yield an MI of between 60 and 100. Using the MMA, MI values of ≤ 5-6 indicate that the donor cells can be transfused with minimal risk of an acute hemolytic reaction (though the MMA is less predictive of long-term circulation of donor RBC). Within the transfusion medicine community, the MMA is considered to be the best assay currently available for correlation of the *in vitro* evaluation of FcγR-mediated phagocytosis of antibody-coated human red cells with *in vivo* clinical relevance [203,204].

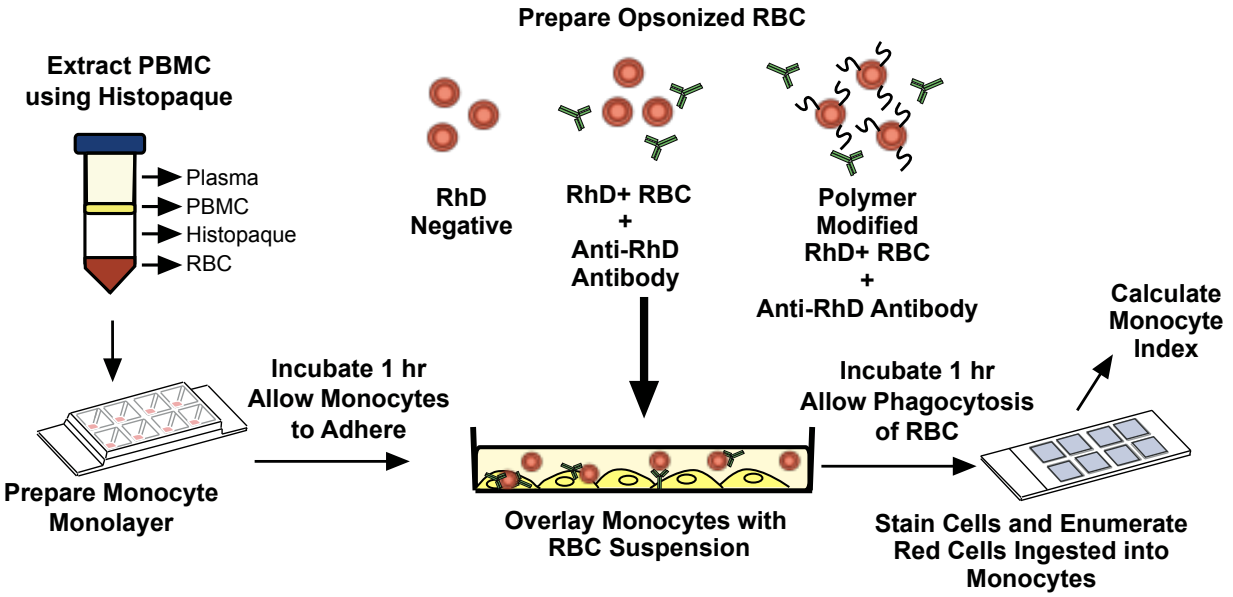

Figure 2.3 Monocyte monolayer assay. A monocyte monolayer was prepared by incubating PBMC on culture slides for 1 hour at 37°C, 5% CO_2, and 95% humidity to allow monolayer to adhere. Control or opsonized RBC (unmodified or modified) was overlaid on the monolayer and cells were incubated for 1 hour to allow phagocytosis of RBC. Monocytes were washed, slide chambers were removed and cells were stained. Monocyte engulfment index was calculated by counting the number of RBC ingested per 100 monocytes.

2.9 Two-Way Mixed Lymphocyte Reaction (MLR)

The mixed lymphocyte reaction is an *in vitro* assay used to assess HLA disparity between individuals. When two disparate PBMC populations are co-cultured, both populations are capable of acting as stimulator and responder cells, resulting in activation and cell proliferation (two-way MLR). To assess the effects of polymer modification of leukocytes during allorecognition, one disparate PBMC population (or both where indicated) was modified with polymer (20 and 30 kDa mPEG or PEOZ; 0-2 mM) as described previously. An equal number of cells from two disparate PBMC populations were suspended in AIM V medium to a final concentration of 2 x 10^6 cells/ml using 24 or 48 well tissue culture plates (Becton Dickinson, Franklin Lakes, NJ, USA). Negative and positive control wells consisted of PBMC alone from each PBMC donor ('resting PBMC') as well as mitogen (phytohaemagglutinin; PHA) stimulated unmodified PBMC from each PBMC donor (2 µg/ml), respectively. The resting PBMC control wells were used to assess any background cell activation during PBMC isolation, whereas mitogen stimulation was used to examine the proliferative capacity of control PBMC preparations. Wells containing MLR and PBMC controls were incubated in a humidified, 5% CO_2 incubator at 37°C. Cells were harvested for downstream assays at various timepoints as indicated. For proliferation and conjugation assays, cells were stained with amine reactive fluorescent probes prior to cell modification with polymer (see section 2.10 and 2.12 for details).

2.10 CFSE Proliferation Assay

The proliferative response of PBMC was used to assess the effects of cell modification on allorecognition (MLR) as well as the response to mitogen challenge (PHA) (**Figure 2.4)**. MLR was used to evaluate the efficacy of polymers to prevent allorecognition, whereas PHA was utilized to assess the polymer-mediated exclusion of small stimulatory molecules. PBMC proliferation was evaluated using a dye-dilution assay. Freshly isolated human PBMCs from two disparate donors were counted and stained with carboxyfluorescein diacetate succinimidylester

(CFSE; Cell Trace- Molecular Probes, Invitrogen, Carlsbad, CA, USA). Following CFSE staining, PBMC from one donor population was derivatized with mPEG or PEOZ (20 or 30 kDa) using 0-2 mM grafting concentrations. PBMC from one donor (PHA) or both donors (MLR) were suspended in AIM V medium to a final concentration of 2 x 10^6 cells/ml. For mitogen stimulation, PHA was added at 2 µg/ml. Cells were incubated in a humidified 5% CO_2 incubator at 37°C. Proliferation of the CD3+CD4+ population was assessed on days 7, 10 and 14 for MLR and day 5 for PHA stimulation by flow cytometry, which measured the progressive halving of CFSE fluorescence following cell division. The CD3+CD4+ population was determined using anti-CD3 PE and anti-CD4 APC antibodies (BD biosciences, San Jose, CA, USA) following a 1-hour incubation at room temperature in the dark according to manufacturer's instructions. Data acquisition and analysis was performed using Cell Quest Software as previously described.

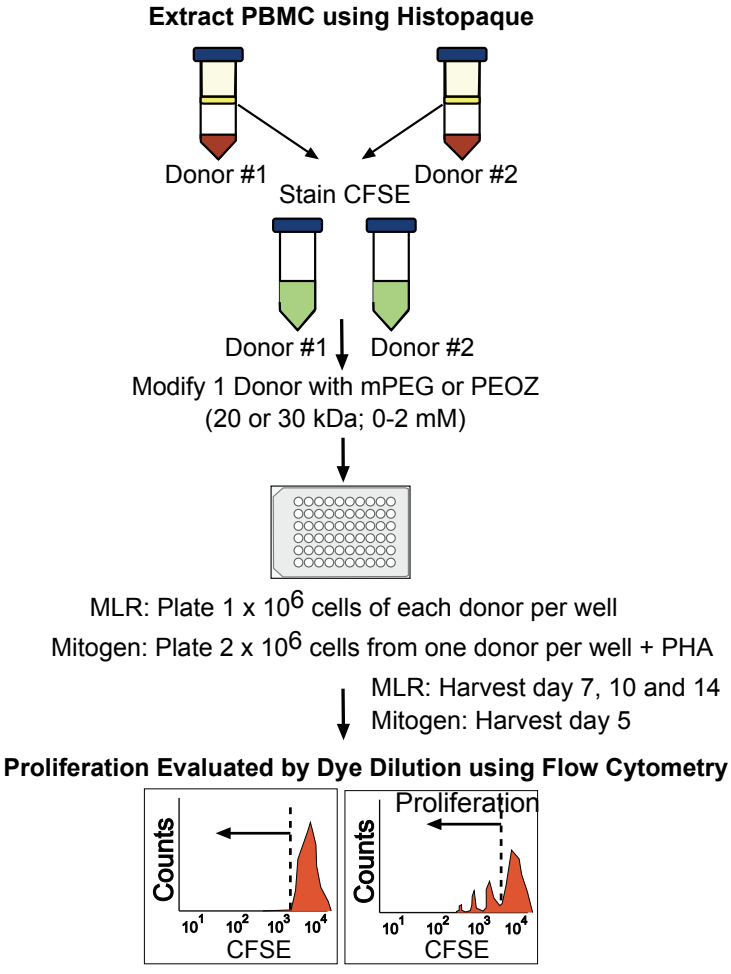

Figure 2.4 Cell proliferation assay using CFSE. The proliferative response of PBMC was used to assess the effects of leukocyte modification on allorecognition (MLR) as well as response to mitogen challenge (PHA). Freshly isolated human PBMCs were counted and stained with carboxyfluorescein diacetate succinimidylester (CFSE). Following CFSE staining, one donor population was derivatized with mPEG or PEOZ (20 or 30 kDa) at 0-2 mM grafting concentrations. PBMC from one donor (PHA) or both donors (MLR) were suspended to a final concentration of 2 x 10^6 cells/ml. For mitogen stimulation, PHA was added at 2 µg/ml. Cells were incubated in a humidified 5% CO_2 incubator at 37°C. Proliferation was assessed by flow cytometry, which measured the progressive halving of CFSE fluorescence following cell division. Proliferation was examined on days 7, 10 and 14 for MLR and day 5 for PHA stimulation.

2.11 Time-Lapse Microscopy

Matured moDC were co-cultured with control or PEGylated allogeneic human PBMC (20 kDa mPEG; 2.0 mM) to examine the effect of PEGylation on direct allorecognition of foreign antigen. Co-cultures of moDC and control or mPEG-PBMC were suspended in RPMI supplemented with 25 mM HEPES and 0.01% human albumin, in a ratio of 1:5 (moDC: PBMC), and seeded on chambered cover glass (Becton Dickinson, Franklin Lakes, NJ, USA) at a cell concentration of 5 $x10^5$ cells/ml in a 37°C heated humidity chamber. Images were taken at 200x magnification every 20 seconds for 90 minutes using a Nikon Eclipse Ti microscope mounted with a camera (Digital sight DS-U3) and analyzed using NIS-elements software. Cell trajectories were obtained by tracking the location of moDC in unmodified and modified co-cultures every 20 seconds over a time course of 90 minutes using NIS-elements software.

2.12 Cell Conjugate Assay

To quantify the effects of mPEG modification on cell conjugation events, matured moDC were co-cultured with PEGylated allogeneic human PBMC, syngenic, or unmodified allogeneic control PBMC. The number of conjugates formed after 20 minutes was assessed by flow cytometry. Enumeration of cell conjugation events was modified from Grebe *et al* [205]. Briefly, PBMC and moDC were stained with amine reactive fluorescent probes at a final concentration of 0.5 μM CFSE and 2.5 μM Far Red DDAO (CellTrace, Molecular Probes) per 2 x 10^6 cells, respectively. Cells were washed 3x in excess RPMI to remove any unincorporated stain. Following CFSE staining, PBMC were derivatized with mPEG (2 or 20 kDa) at 0-2 mM grafting concentrations. MoDC and human PBMC co-cultures were suspended in AIM V medium in a ratio of 1:10 (moDC: PBMC) for a final concentration of 1 x 10^7 cells/ml. Co-cultures were centrifuged for 30 seconds at 200 x g and incubated at 37°C, 5% CO2, and 95% humidity for 20 minutes to allow conjugation of cells. After 20 minutes, cells were fixed by addition of 0.5 ml of 2% methanol free formaldehyde and incubated at room temperature for 15 minutes before being

evaluated by flow cytometry. The double-staining population (CFSE+Far Red-DDAO+) was examined to determine the percentage of cell conjugation using flow cytometry as previously described.

2.13 Real-Time PCR (qPCR)

To assess the effects of polymer modification of cells on T cell activation pathways during allogeneic recognition, real-time PCR was performed using the human NFκB signaling targets RT^2 Profiler PCR arrays (Qiagen, Limberg, Netherlands). NFκB is an important transcription factor for the activation of cells during an alloresponse, including the regulation of IL2 production. This array provides a profile of the expression of 84 genes that are responsive to NFκB signal transduction, including genes involved in inflammation, immune response, differentiation and apoptosis (**Table 2.1)** as well as appropriate housekeeping genes and controls for data normalization. Results can be used to assess activation or inhibition of NFκB signaling. To examine the effects of mPEG-PBMC modification on NFκB signaling during a MLR, the mRNA expression of NFκB target genes was examined in control and mPEG modified MLR (20 kDa; 2.0 mM) at 2, 6 and 24 hours. Cells were harvested, washed 2x in cold PBS and centrifuged at 400 x g, 4°C for 10 minutes and then placed on ice. Total mRNA was extracted using *Mir*Vana Paris Kit (Ambion Life Technologies, Carlsbad, CA, USA) according to manufacturer's instructions. The concentration of RNA eluent was determined by nanodrop and samples were stored at -80°C until further use. cDNA synthesis and genomic DNA elimination from total RNA preparation was done using RT^2 First Strand kit, according to manufacturer's protocol, using Eppendorf Mastercycler gradient (Hamburg, Germany). cDNA samples were processed immediately or stored at -20°C for further use. Real-time PCR was performed using Applied Biosystems StepOnePlus (Life Technologies, Carlsbad, CA, USA) with Human NFκB Signaling Targets RT^2 PCR array and RT^2 SYBR Green Mastermix (Qiagen, Limberg, Netherlands) according to manufacturer's protocols. Threshold, baseline and CT values were

calculated using StepOnePlus software (v.2.1). Analysis of PCR results was performed using Qiagen GeneGlobe data analysis.

Table 2.1 NFκB Profiler Array Kit: Functional Gene Groupings for Gene Targets in Array Plate

Functional Gene Groupings	Genes
Cytokines & Chemokines	CCL11, CCL2, CCL22, CCL5, CSF1, CSF2, CSF3, CXCL1, CXCL10, CXCL2, CXCL9, FASLG, IFNB1, IFNG, IL12B, IL15, IL1A, IL1B, IL1RN, IL2, IL4, IL6, IL8, LTA, LTB, TNF, TNFSF10
Inflammation	AGT, AKT1, C3, CCL2 CCL5, CCL11, CCL22, CCR5, CD40, CFB, CXCL1, CXCL2, CXCL9, CXCL10, F3, F8, IL1A, IL1B, IL1RN, IL2, IL2RA, IL6, IL8, IL15, INS, MYD88, PTGS2, SELE, SELP, STAT3, STAT5B, TNF, TNFRSF1B
Apoptosis	AGT, BIRC2, EGFR, FASLG, GADD45B, IFNB1, IFNG, IL2RA, IL4, IL12B, INS, LTA, MAP2K6, MMP9, NQO1, NR4A2, PTGS2, STAT1, TNFRSF1B, TNFSF10, TP53, TRAF2
Anti-Apoptosis	ADM, AKT1, BCL2A1, BCL2L1, BIRC3, CCL2, CDKN1A, CSF2, F3, FAS, IL1A, IL1B, IL2, IL6, MYD88, NFKBIA, SOD2, STAT5B, TNF, XIAP
Immune Response	C3, CCL2, CD40, CD80, CD83, CFB, FAS, FASLG, ICAM1, IFNB1, IFNG, IL1B, IL1R2, IL2, IL4, IL6, IL8, IL12B, INS, LTA, LTB, MYD88, NFKBIA, STAT5B, TNF, TNFSF10, TRAF2
Type I Interferon Responsive Genes	ADM, CCL2, CCL5, CD69, CD80, CDKN1A, CFB, CXCL9, CXCL10, IL15, IL1RN, IRF1, MYD88, NCOA3, STAT1, TNFSF10
Development and Differentiation	Lymphoid: CD80, CD83, IL2, IL2RA, IL4, IL12B, IL15, IRF1, STAT5B, TP53, VCAM1 Myeloid: CCL5, CSF1, CSF2, CSF2RB, CSF3, IL4, MMP9, NFKBIA, STAT5B, TNF Nervous System: AGT, ALD3A2, CXCL1, EGFR, EGR2, IFNG, NR4A2, SNAP25, SOD2, STAT3, TP53
Stress Response	ADM, AKT1, BCL2L1, BIRC2, CCND1, CDKN1A, GADD45B, IFNG, IL1A, IL1B, MAP2K6, NQO1, PDGFB, PLAU, SOD2, TNF, TP53, XIAP
NFκB Pathway	BIRC2, CD40, EGR2, FASLG, IL1B, IRF1, MYD88, MYC, NFKB1, NFKB2, NFKB1A, NR4A2, REL, RELA, RELB, STAT1, STAT3, STAT5B, TNF, TNFSF10, TP53

2.14 Preparation of Protein Lysates

As previously discussed, an important pathway for the activation of naïve T cells during allorecognition is NFκB. To assess the mRNA targets differentially regulated in the PCR array between control and mPEG MLR, the protein expression of IL2Rα, IL2Rβ, and IL1R2 was examined on day 4 and 7 of an MLR by western blot. Since IL1R2 can be secreted as well as membrane bound, both cell culture supernatants and cells were harvested on day 4 and 7. Cells

were washed 2x in ice cold PBS and lysed with RIPA buffer (150 mM NaCl, 1% Triton X-100, 0.5% sodium deoxycholate, 0.1% sodium dodecyl sulphate, 50 mM Tris pH 8.0 and 1x Halt™ protease and phosphatase inhibitor cocktail) on ice for 30 minutes with regular mixing. The lysate was centrifuged at 14,000 x g, 4°C for 30 minutes. The supernatant (total cell extract) was removed and frozen at -80°C. Protein concentrations of all lysates were determined by the BCA protein assay (Thermo Scientific Pierce, Waltham, MA, USA) according to manufacturer's instructions.

2.15 SDS-PAGE and Western Blot

Control and experimental lysates (20 µg) as well as molecular weight standards (Dual Color precision plus protein standards Bio-Rad Laboratories, Hercules, CA, USA) were separated on 10% sodium dodecyl sulfate-polyacrylamide (SDS-PAGE) gels and transferred for 60 minutes onto Immun-Blot PVDF membranes (Bio-Rad Laboratories, Hercules, CA, USA). IL1R2 from cell culture supernatant was concentrated using protein A/G PLUS-agarose immunoprecipitation reagent (Santa Cruz Biotechnology, Dallas TX, USA) according to manufacturer's instruction, prior to SDS-PAGE analysis. Membranes were blocked overnight in 5% non-fat milk at 4°C with rocking, washed 3 x in tris buffered saline with tween (TBST) and probed with primary antibodies against IL1R2 (R&D Systems, Minneapolis, MN, USA) and IL2α (ab61777), IL2β (ab137699) and anti-beta actin (ab88229) used as a loading control (Abcam, Cambridge, MA, USA). Membranes were washed 3 x in TBST, followed by labeling with Licor IRDye® secondary antibodies (Licor, Lincoln, NE, USA) for 1 hour. Protein band signals were assessed using Licor Odyssey and intensities were analyzed by densitometry and normalized to actin loading control using Odyssey software v3.0.

2.16 Cell Viability and Apoptosis

Cell viability studies were done to assess the effect of polymer species and polymer grafting concentration on the viability of resting PBMC and PBMC during a MLR (**Figure 2.5).** To compare the effect of polymer species during polymer modification of PBMC, cell viability of control, mPEG- and PEOZ-modified PBMC (20 or 30 kDa; 0-4 mM grafting concentrations) were examined using 7-amino-actinomycin D (7AAD; BD biosciences, San Jose, CA, USA) immediately after cell modification. 7AAD are fluorescent nucleic dyes that are excluded from viable cells but are able to permeate non-viable cells due to increased membrane permeability. Cells were stained with 7AAD to a final concentration of 0.05 mg/ml and incubated at room temperature for 10 minutes prior to flow cytometric analysis as previously described. Heat-killed PBMC were used as positive control cells.

Previous studies have suggested that polymer modified cells undergo increased apoptosis during an MLR as a result of weak stimulation events during allorecognition. Therefore, flow cytometry was used to assess early and late apoptotic events in mPEG-modified PBMC (20 kDa; 0-2 mM) and during allogeneic (MLR) challenge over 72 hours (**Figure 2.5)**. To evaluate early apoptotic events, caspase activation was examined. Caspases are cysteine proteases that play a role in the cleavage of protein substrates during apoptosis. Caspase 3 and 7 are effector caspases that exist as inactive pro-enzymes in the cell. During apoptotic pathway activation caspase pro-enzymes are cleaved to become active proteases. To monitor early apoptotic events in polymer modified PBMC, PBMC were incubated with a cell permeable peptide conjugated to a fluorescent probe (CellEvent® Caspase-3/7 Green flow cytometry assay kit, Molecular Probes Invitrogen, Eugene, OR, USA), according to manufacturer's protocol. Cleavage of the peptide conjugate by active caspase 3 or 7, results in release of the fluorescent moiety and production of a fluorescent signal that can be assessed by flow cytometry. Additionally, to examine late apoptotic events, cells were also stained with Sytox

(Molecular Probes Invitrogen, Eugene, OR, USA) according to manufacturer's protocol. Sytox is similar to 7AAD, both are DNA binding fluorescent probes that can permeate dead cell membranes and be evaluated by flow cytometry. Flow cytometric data acquisition and analysis was performed as previously described. A potent apoptosis inducer, anisomycin was added to PBMC cultures and served as the positive control.

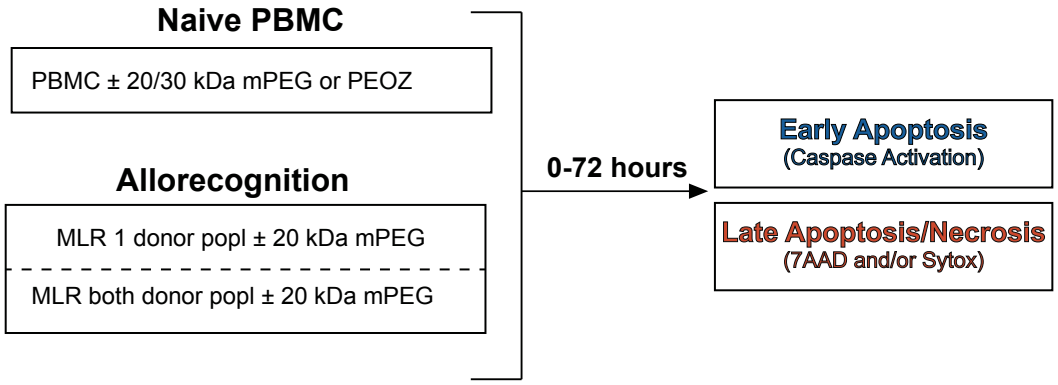

Figure 2.5 Experimental design for apoptosis study. Caspase 3/7 activation (early apoptosis) as well as 7AAD or Sytox incorporation (late apoptosis) were used to assess apoptotic events in polymer modified PBMC (0-4 mM) and during allogeneic (MLR) challenge over 72 hours.

2.17 IL2 Stimulation

IL2 is an important cytokine for lymphocyte activation, proliferation, and survival. To investigate whether reduced viability was a consequence of decreased IL2 stimulation in mPEG modified PBMC, the production and consumption of exogenous IL2 was examined in control and mPEG modified PBMC using Biosource IL2 EASIA kit (Life Technologies, Carlsbad, CA, USA). In addition, parallel samples of unmodified and PEGylated PBMC were used to assess the effect of exogenous IL2 on cell proliferation (CFSE assay) as well as apoptosis (caspase 3/7 activation) (**Figure 2.6)**. PBMC were isolated and modified with mPEG (20 kDa; 0-2 mM) as previously described, and plated in 48-well tissue culture plates (Becton Dickinson, Franklin Lakes, NJ, USA) to a final concentration of 2 x 10^6 cells/ml in AIM V Medium. Exogenous IL2 (R&D Systems, Minneapolis, MN, USA) was added at 25 and 250 U/ml. Cell culture supernatants and cells were harvested at 24 and 48 hours for EASIA and caspase activation

and on day 6 for proliferation. Prior to EASIA, cell culture medium was diluted to reach appropriate concentration within the reference curve (0-30 U/ml) and EASIA was performed according to manufacturer's protocol. Caspase and CFSE proliferation assays were performed as previously described.

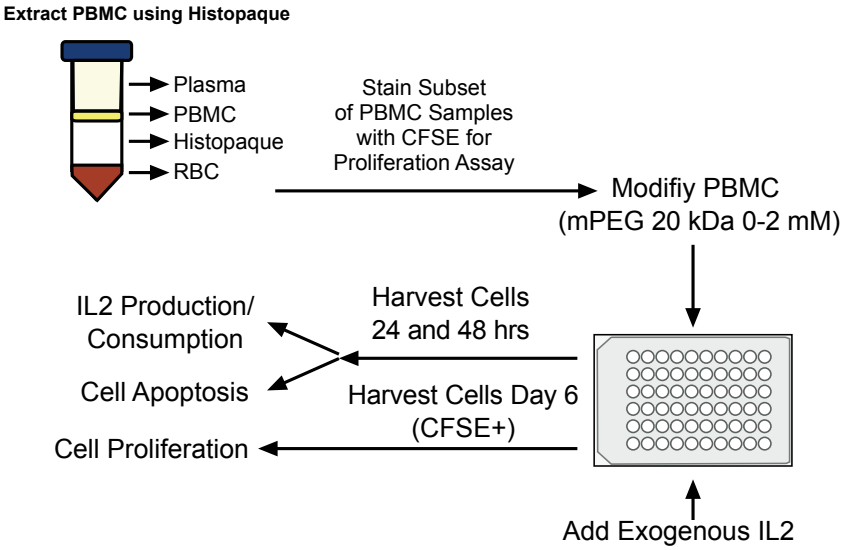

Figure 2.6 Experimental design for IL2 study. To investigate whether reduced PBMC viability was a consequence of decreased IL2 stimulation in mPEG-modified PBMC, the effect of exogenous IL2 on cell consumption/production, cell proliferation (CFSE assay) and apoptosis (Caspase 3/7 activation) was assessed. PBMC were isolated and modified with mPEG (20 kDa; 0-2 mM), and plated in 48-well tissue culture plates at a final concentration of 2 x 10^6 cells/ml. Exogenous IL2 was added at 25 and 250 U/ml. Cell culture supernatants and cells were harvested at 24 and 48 hours for EASIA and caspase activation and on day 6 for proliferation.

2.18 Statistical Analysis

All results were expressed as means ± standard error mean (SEM). A minimum of 3 independent replicates was completed for all studies in duplicate. In some instances representative images were presented (*i.e.,* microscopy). Data analysis was conducted using SPSS v.16.0 statistical software (Statistical Products and Services Solutions, Chicago, IL, USA). For significance, a minimum *p*-value of < 0.05 was used. For comparison of two mean values, an independent variable *t*-test was performed. For comparison of three or more means, a one-way analysis of variance (ANOVA) was performed followed by *Post hoc* analysis using the Tukey test.

3 CHAPTER 3: Comparative Efficacy of Methoxypoly(ethylene glycol) (mPEG) and Polyethyloxazoline (PEOZ) for Red Blood Cell and Leukocyte Modification

3.1 Overview

PEGylation of intact, biologically viable cells has demonstrated potential utility in transfusion and transplantation medicine, where prevention of immune responses to allogeneic tissues is critical [135,137,190]. However, despite the experimental and clinical success of PEGylation, some concerns exist as to the immunological recognition of PEG and the potential peroxidation of the PEG polymer itself, leading to unwanted biological consequences. A search for alternative polymers with improved pharmacological and biological properties relative to PEG may be beneficial for the development of new generations of immunocamouflaged proteins and cells.

A novel polymer class, polyoxazoline (POZ) may be suitable as an alternative polymer for the induction of immunocamouflage. Polyoxazolines exhibit lower viscosity, increased stability and lowered degradation potential compared to current mPEG polymers [150]. However, limited information exists as to the efficacy of polyoxazolines for the immunocamouflage of allogeneic cells [157]. Therefore, we examined the comparative efficacy of covalently grafted polyethyloxazoline (PEOZ) and mPEG on the direct and indirect immunocamouflage of human blood cells (RBC and leukocytes). PEOZ and mPEG were assessed, using various polymer lengths and grafting densities, for their effects on RBC structure and viability, immunocamouflage of blood group antigens (RhD and Kell), and the prevention of phagocytic recognition. Moreover, the differential efficacy of PEOZ and mPEG grafting to leukocytes was evaluated by their effects to cell viability, immunocamouflage of

cluster of differentiation (CD) markers, and the prevention of HLA-mediated allorecognition using mixed lymphocyte reactions (MLR).

3.2 Efficiency of Polymer Grafting

The differential grafting efficacy of mPEG and PEOZ was assessed *via* two-phase partitioning. As shown in **Figure 3.1A**, the transition of RBC to the upper PEG phase is a function of grafting concentration and polymer size. Quantitative analysis (**Figure 3.1B)** demonstrated that RBC modified with shorter polymers (2 and 5 kDa) were significantly less abundant in the upper phase compared to RBC modified with longer polymers (20 and 30 kDa) at matched grafting concentrations (≥ 0.5 mM; $p<0.05$) **(Figure 3.1B; Figure 3.1B insert)**. Comparing the longer 20 and 30 kDa lengths, there was a slight decrease in RBC migration to the upper phase using 20 kDa polymers *vs* 30 kDa polymers at low grafting concentrations (≤ 0.8 mM). However, as grafting concentration increased (≥ 1.0 mM) no significant difference in recovery was observed between the 20 and 30 kDa polymers with mPEG- or PEOZ-RBC ($p>0.05$). The size dependent migration to the upper phase was likely a consequence of the smaller number of ethoxy units per chain in the smaller polymers, resulting in decreased alteration of cell surface properties compared to the larger polymer chains at low grafting concentrations.

Comparing the degree of cell modification between mPEG and PEOZ, the percent hemoglobin recovered from the PEG layer indicated that both polymers had similar partitioning profiles. However, at low grafting concentrations (< 1.0 mM) mPEG-RBC demonstrated improved partitioning compared to RBC modified with corresponding PEOZ polymers (20 and 30 kDa; **Figure 3.1B** denoted by Δa and Δa', respectively). For example, at 0.5 mM mPEG-RBC showed 36% and 77% recovery, while PEOZ-RBC showed 11% and 25% recovery (20 and 30kDa respectively). In contrast, at 1.0 mM there was little difference between polymer species or polymer size. Interestingly, at the 2.0 mM grafting concentration, PEOZ-RBC showed slightly

improved recovery relative to mPEG-RBC (72% to 59%, 20 kDa; 71% to 56%, 30 kDa; **Figure 3.1B** Δ*b*) suggesting that mPEG could have some adverse effects on the RBC, although there were no significant differences between polymer species at matched polymer lengths (p>0.05).

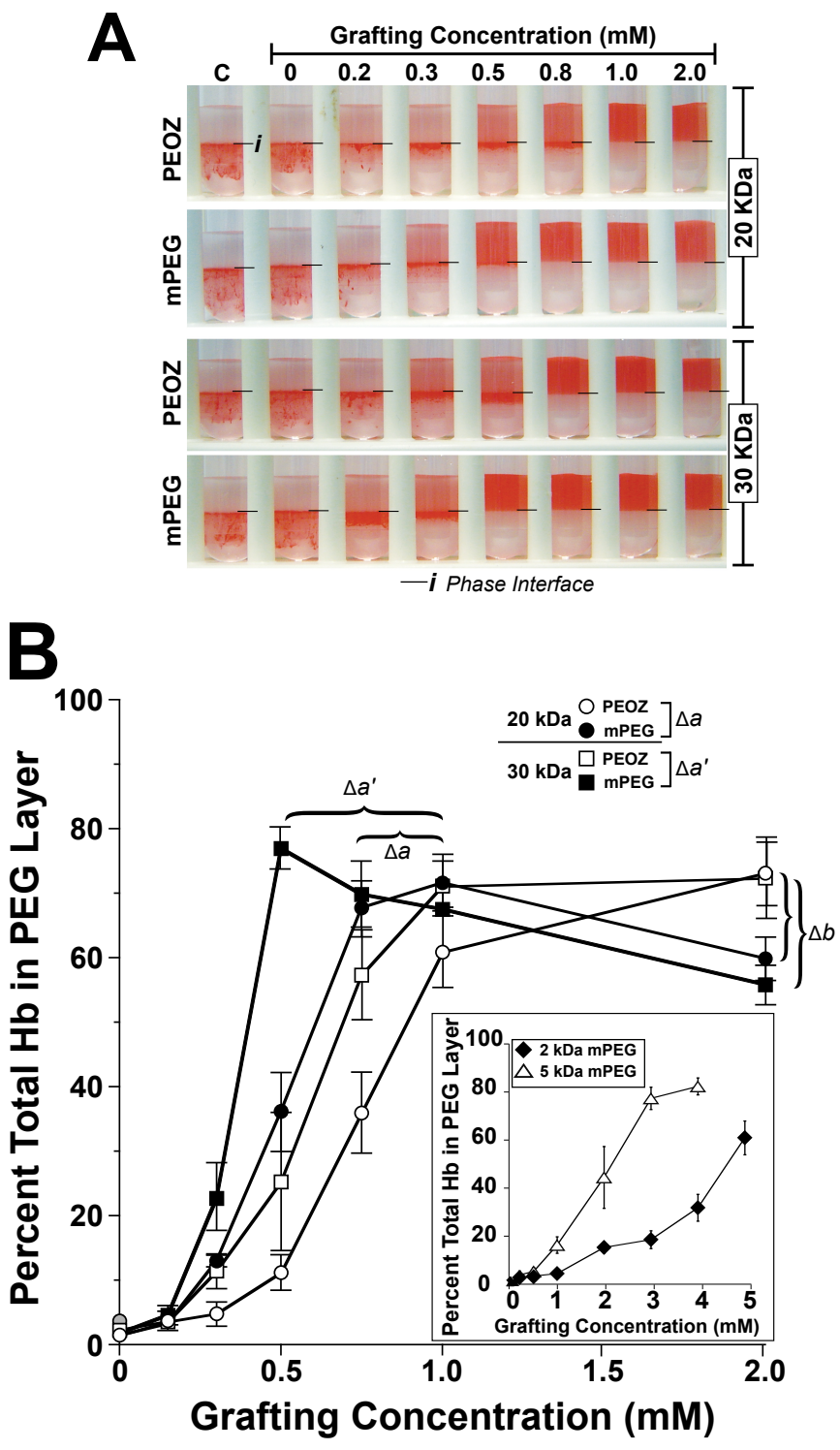

Figure 3.1 Grafting of PEOZ and mPEG yielded similar partitioning in a two-phase PEG-Dextran system. Polymer modified RBC migrate to the upper PEG layer whereas unmodified or poorly modified RBC preferentially partition to the lower Dextran layer or interface region**.** (A) Representative photos of phase separation of the 20 and 30 kDa PEOZ- and mPEG-RBC (0-2 mM). The migration of RBC to upper phase increased in a dose dependent manner. Both PEOZ- and mPEG-RBC showed comparable PEG phase separation. Photos were taken 20 minutes post mixing. (B) Phase separation is a function of polymer grafting concentration, size and species. Quantification of phase separation was done *via* hemoglobin concentration in the PEG layer. Results indicated differences in phase separation between large polymers (mPEG and PEOZ; 20 and 30 kDa) and small mPEG polymers (2 and 5 kDa) [insert]. The Δa (20 kDa) and Δa' (30 kDa) denotes the difference between the maximum phase separation for mPEG- and PEOZ-RBC at low grafting concentrations. The Δb denotes the difference between the 20 and the 30 kDa mPEG and PEOZ species at the 2.0 mM grafting concentration. Results (n=4) are expressed as mean ± SEM. Modified from Kyluik-Price 2014 [148].

3.3 Cell Morphology and Viability: Effect of Polymer Species, Grafting Concentration and Size

3.3.1 Red Blood Cell Morphology

RBC morphology is a sensitive indicator of RBC viability. To assess the effects of mPEG and PEOZ grafting on RBC viability *in vitro*, photomicrographs of control, mPEG and PEOZ-modified RBC were taken immediately post modification (**Figure 3.2**). RBC modified with the 20 kDa mPEG (**Figure 3.2C**) or PEOZ (**Figure 3.2E**) at ≤ 2.0 mM were similar in morphology to the sham treated, unmodified control cells (**Figure 3.2A**). Indeed, in support of this finding, previous studies of murine RBC modified at the 2.0 mM grafting concentration with 20 kDa mPEG showed normal *in vivo* survival [135]. In contrast, the 30 kDa mPEG-RBC modified at ≥ 2.0 mM showed significant morphological aberrations (**Figure 3.2D**) while the 30 kDa PEOZ-RBC showed slightly less morphological abnormalities (**Figure 3.2F**). Consistent with previous results using mPEG [136], higher polymer concentrations (4.0 mM grafting concentration shown) of both the 20 and 30 kDa mPEG or PEOZ gave rise to significant RBC morphological abnormalities compared to the control. However, at the 4.0 mM grafting concentration, less morphological defects were observed in PEOZ-modified RBC compared to the matched mPEG-RBC **(Figure 3.2).** Polymer length did have a clear effect on RBC morphology as demonstrated by the reduced morphological changes noted for RBC modified with the 5 kDa chains, even at high grafting concentrations (**Figure 3.2B**).

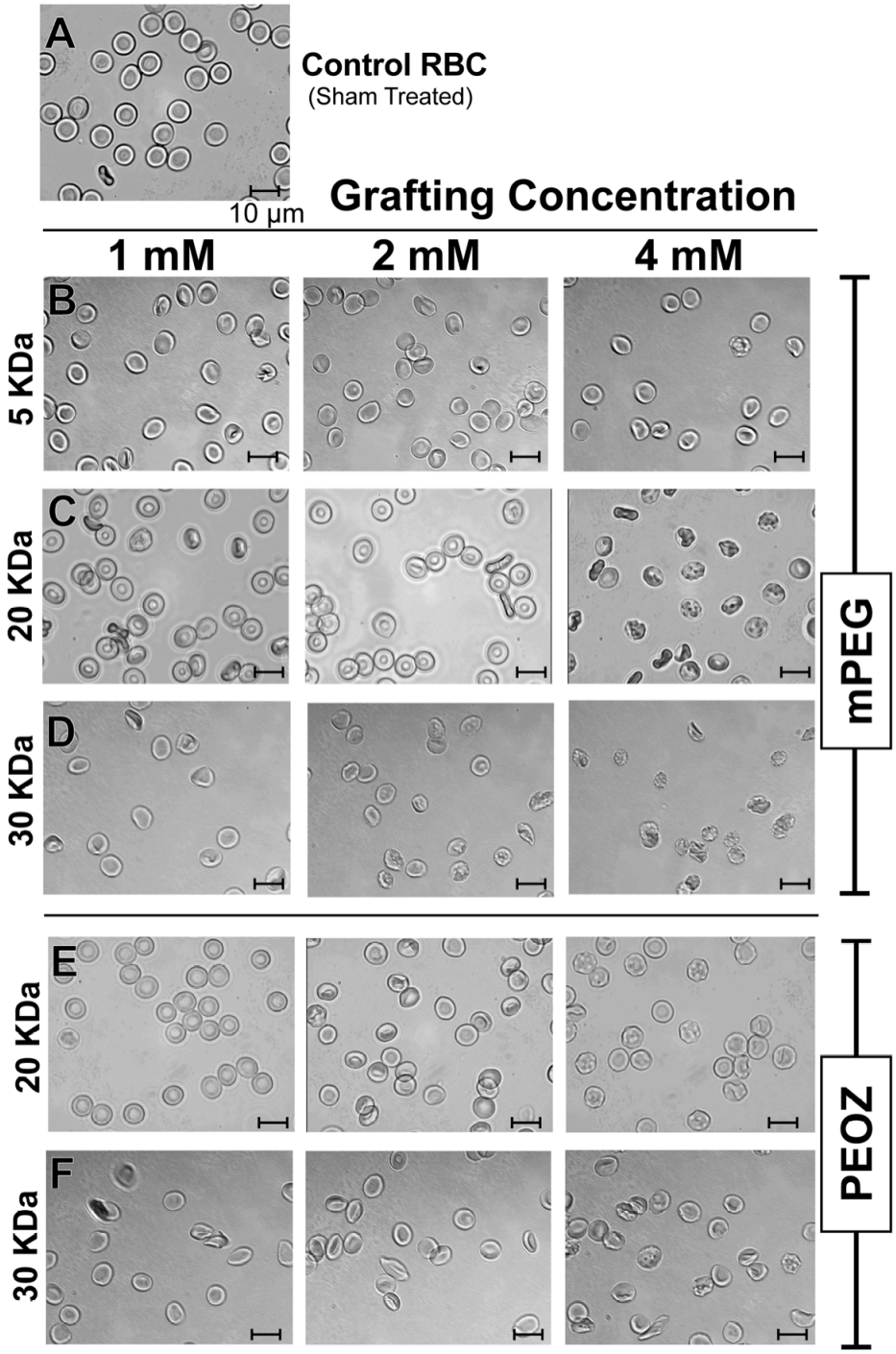

Figure 3.2 PEOZ grafting to RBC yielded improved morphology relative to mPEG at high grafting concentrations immediately post modification. Unmodified control RBC (A) are shown relative to RBC modified with increasing concentrations of 5, 20 or 30 kDa mPEG (B, C and D; respectively) or 20 or 30 kDa PEOZ (E and F; respectively). At higher concentrations (4.0 mM) morphological aberrations were observed in all modified cells, relative to the control cells, though this was most pronounced with the 30 kDa mPEG. PEOZ demonstrated improved morphological characteristics compared to the corresponding molecular weight mPEG at grafting concentrations ≥ 2.0 mM. Polymers were grafted to RBC as previously described and fixed in 4% methanol free formaldehyde. Representative RBC images (*n*=4) were taken at 1000x magnification. Size bar = 10 µm. From Kyluik-Price 2014 [148].

3.3.2 Osmotic Fragility and Hemolysis

The differential effects of mPEG and PEOZ grafting on RBC structure and viability was assessed by osmotic fragility and spontaneous lysis studies. Altered osmotic fragility profiles (left or right shift) and increased spontaneous lysis are indicative of decreased RBC viability. As

shown in **Figure 3.3**, there were no significant differences between mPEG- and PEOZ-RBC at equivalent polymer lengths, immediately post modification and after 24, 48 and 68 hours (p>0.05). Compared to the unmodified RBC, both polymers showed elevated spontaneous lysis immediately after modification (**Table 3.1**), which increased at later points (24, 48 and 68 hours) (0.9% saline; dotted box in **Figure 3.3)**. This suggests that both mPEG and PEOZ (20 and 30 kDa) may exert similar pro-lytic effects for a subset of cells under these metabolically harsh *in vitro* incubation conditions. Lysis was also a function of grafting concentration as shown by the rise in spontaneous lysis at higher grafting concentrations (0.5 *vs* 2.0 mM). However, the inflection point for rapid lysis (~0.4% saline at 0 hours) was similar for all of the polymer grafted-RBC and was comparable to unmodified RBC. Importantly, previous studies show that murine mPEG-RBC modified under identical conditions (*i.e*., 2.0 mM mPEG) exhibit normal *in vivo* survival (~50 days) when compared to unmodified murine RBC [136,195].

Table 3.1 Spontaneous Lysis (t=0) During Osmotic Fragility

Condition	**Percent Lysis**			
Sham Treated	0.98 ± 0.44			
Grafting Conc.	**mPEG-20 kDa**	**PEOZ-20 kDa**	**mPEG-30 kDa**	**PEOZ-30 kDa**
0.5 mM	2.35 ± 0.18	4.71 ± 0.19	4.19 ± 0.31	5.14 ± 0.13
2.0 mM	5.73 ± 0.20	8.86 ± 0.86	16.06 ± 1.26	10.33 ± 0.24

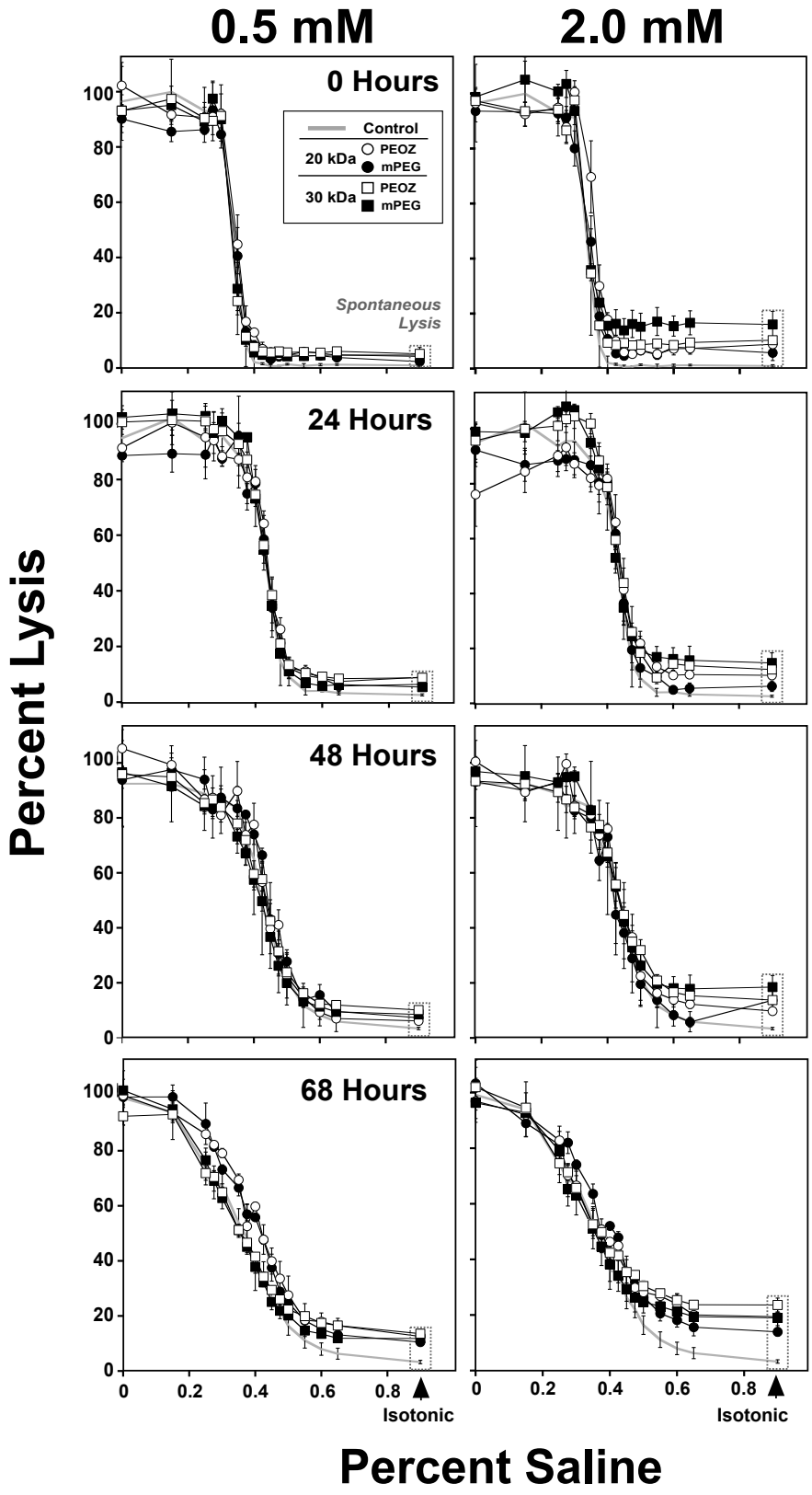

Figure 3.3 PEOZ- and mPEG-RBC showed similar osmotic fragility profiles compared to control RBC over a 68-hour incubation. However, at 0.9% saline, both mPEG-RBC and PEOZ-RBC (0.5 and 2.0 mM grafting concentration) exhibited elevated RBC spontaneous lysis (dashed box) relative to unmodified RBC. Percent lysis was determined by Drabkin's assay. Results (*n*=3) are expressed as mean ± SEM. Modified from Kyluik-Price 2014 [148].

3.3.3 Leukocyte Viability

The effects of polymer species on PBMC viability was measured by flow cytometry using 7AAD incorporation. Shown in **Figure 3.4A**, are the percentages of viable cells at various grafting concentrations using the 20 or 30 kDa polymers. PBMC modified with either mPEG or PEOZ demonstrated > 90% viability, even at high grafting concentrations (4.0 mM), with no significant differences from controls (p>0.05). Photomicrographs (**Figure 3.4B**) indicate no significant morphological changes observed in mPEG or PEOZ grafted PBMC with either polymer size when compared to unmodified control cells.

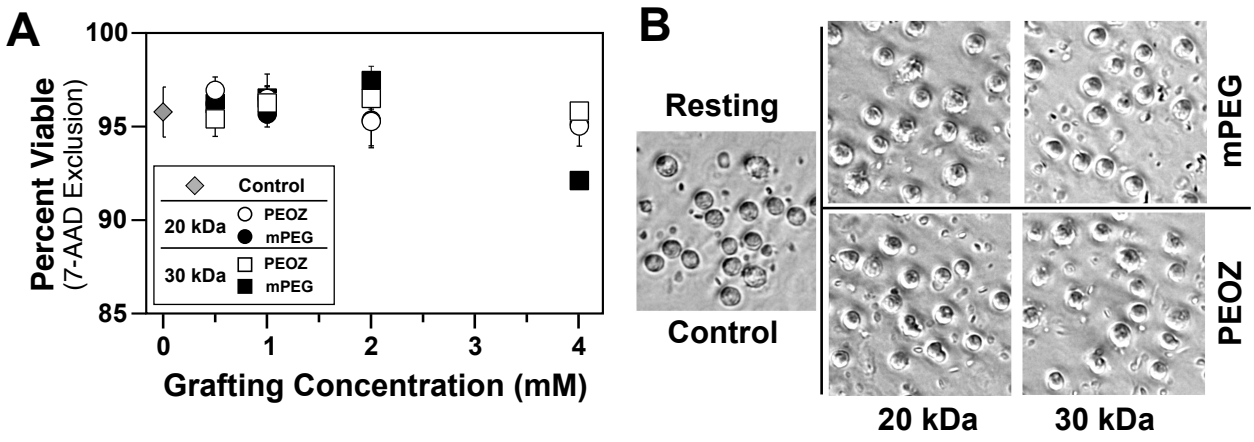

Figure 3.4 PEOZ and mPEG-modification yielded viable and morphologically normal PBMC over a grafting concentration of 0-4 mM. (A) Cell viability was determined by 7AAD exclusion. Cell viability was > 90% of control cells for all polymers and molecular weights assessed. Shown are the mean ± SEM. (B) Representative photomicrographs (n=4) are shown of control and polymer grafted PBMC fixed in 4% methanol free formaldehyde immediately post grafting. From Kyluik-Price 2014 [148].

3.4 Induction of Immunocamouflage: Effect of Grafting Concentration, Polymer Species and Size

3.4.1 Camouflage of RhD and Kell Antigens

The goal of immunocamouflaging RBC in transfusion medicine is to prevent immune recognition of mismatched non-ABO blood group antigens on donor RBC. Therefore, the differential efficacy of mPEG- and PEOZ-grafting on the immunocamouflage of RhD^+ and $Kell\text{-}k^+$ RBC was assessed using commercial antibodies. These antigens were chosen in part for their

topographic features (RhD is close to the membrane while the Kell protein extends well above the RBC surface) and for their known immunogenicity in clinical transfusion medicine (**Table 1.1**). As shown in **Figure 3.5**, the immunocamouflage of RhD^+RBC and k^+RBC was dose, size and polymer species specific as shown by both percent positive cells (PPC; as shown a +/- measure of bound antibody) and mean cell fluorescence (MCF; relative amount of bound antibody). All polymers induced significant immunocamouflage of RhD and k as measured by PPC ($p<0.05$ at 4.0 mM) and MCF ($p<0.05$ at ≥ 2.0 mM). For both RhD and k, mPEG provided significantly better immunocamouflage (PPC) than PEOZ at grafting concentrations > 1.0 mM with matched molecular weights ($p<0.05$). The superior immunocamouflage of both RhD and k by mPEG relative to PEOZ may be due to the improved charge camouflage of the protein surface arising from the heavily hydrated mPEG. Surprisingly, at high grafting concentrations (*i.e.,* ≥ 2.0 mM) of mPEG and PEOZ, the 20 kDa polymers demonstrated superior immunocamouflage, relative to the 30 kDa polymer, of RhD^+ and k^+ RBC despite similar grafting efficiency (**Figure 3.1**). This may reflect the tendency of initially bound large polymers to 'self-exclude' additional polymer binding, resulting in reduced polymer density.

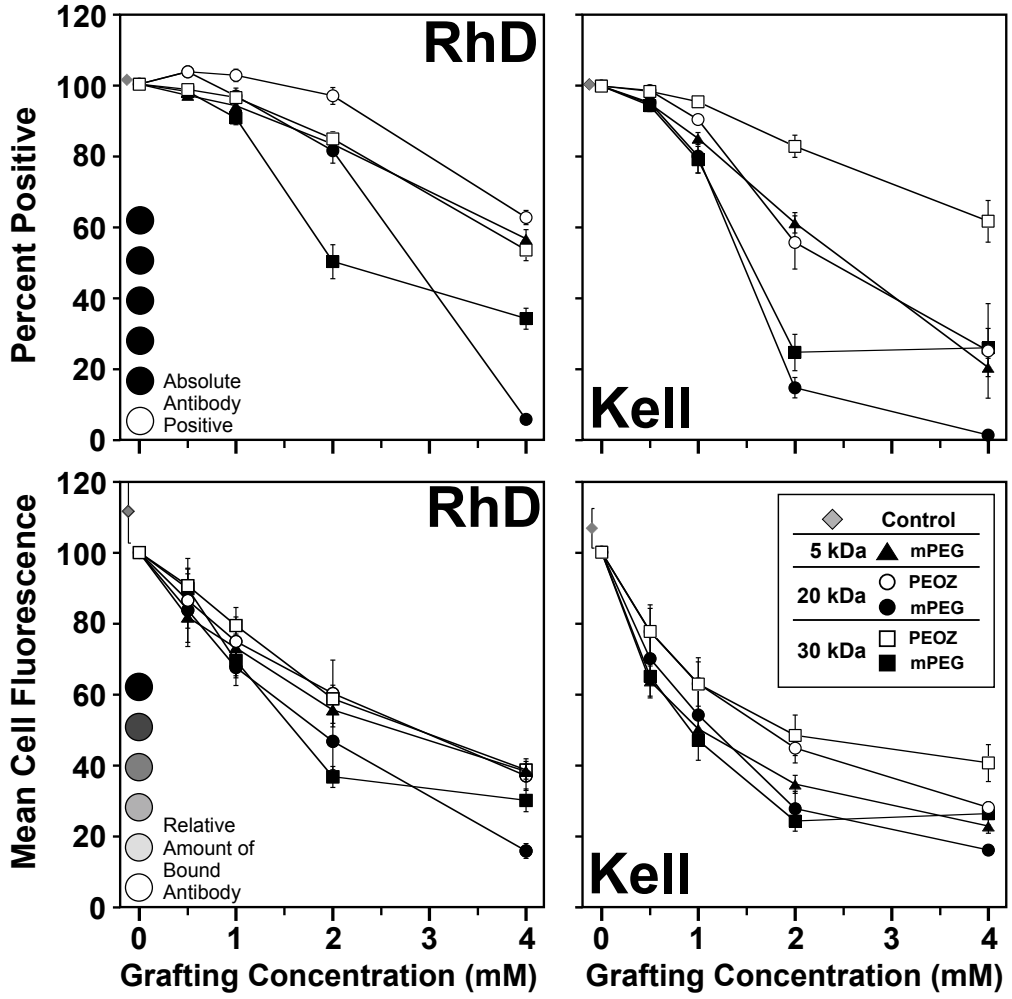

Figure 3.5 Both PEOZ and mPEG modified RBC exhibited a dose dependent decrease in percent positive cells (PPC) and mean cell fluorescence (MCF) of RhD and Kell (k) blood group antigens. mPEG demonstrated a significant decrease, relative to PEOZ, in PPC at high grafting concentrations (≥ 2.0 mM) with matched polymer lengths (p<0.05). However, both mPEG and PEOZ showed significant decreases in the amount of antibody bound (MCF) compared to the control, which may be a more biologically relevant measure of immunocamouflage. Results are expressed as the percent of unmodified cells (mean ± SEM) incubated with antibodies and set to equal 100%. Shown graphically is the interpretation of PPC and MCF; PPC is a measure of antibody positive *versus* antibody negative RBC, while the MCF value accounts for the mean amount of bound antibody for the total cell population. From Kyluik-Price 2014 [148].

3.4.2 Prevention of Phagocytic Recognition Using the Monocyte Monolayer Assay (MMA)

While flow cytometric analysis of blood group antigens provides valuable quantitative evidence for the efficiency of immunocamouflage, it was also necessary to assess the efficacy of mPEG and PEOZ grafting to RBC at a biological level. To accomplish this, the monocyte monolayer assay (MMA) was used. Previous studies have shown that a low monocyte

engulfment index (MI ≤ 5-6) is clinically correlated with good *in vivo* circulation and a low risk of an acute transfusion reaction [203,204]. As shown in **Figure 3.6**, anti-RhD opsonization of RhD^+ mPEG- and PEOZ-RBC demonstrated significantly different immunoprotective effects at comparable grafting concentrations (mPEG 20 or 30 kDa *vs* PEOZ 20 or 30 kDa; $p<0.01$). While mPEG-grafting with either the 20 or 30 kDa chains yielded RhD^+-RBC that could be deemed potentially safe (if other blood was not available) for transfusion into an alloimmunized RhD^- patient, PEOZ provided only a partial reduction in immunorecognition. Moreover, unlike mPEG, PEOZ demonstrated a size dependent effect with the 30 kDa polymer providing better, though again incomplete, protection from phagocytosis. The MMA findings agreed with the flow cytometric analysis of the efficacy of mPEG and PEOZ immunocamouflage of RhD; though neither polymer fully obscured RhD as measured by flow cytometry. The comparison of the flow cytometric and MMA data results clearly indicate the need to assess the biological efficacy of modified cells and not to solely rely upon more quantitative measures of immunocamouflage. In addition, this data suggests that the aggregate effects of immunocamouflage is not limited to camouflaging a specific antigen, but rather confers a more global immunocamouflage, thus preventing phagocytic recognition.

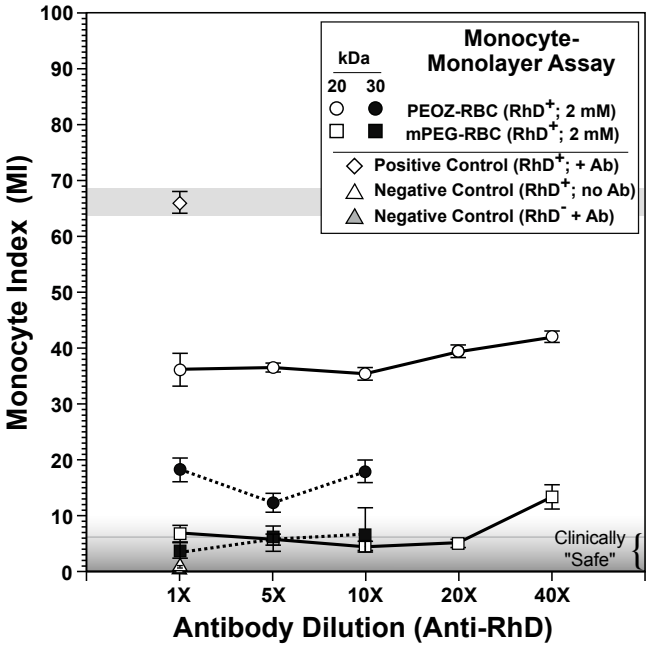

Figure 3.6 Opsonization (anti-RhD) of mPEG- and PEOZ-RhD+ RBC showed differential effects on immune recognition using the monocyte monolayer assay. At comparable levels of polymer grafting, mPEG yielded significantly greater ($p<0.01$) immunoprotection than PEOZ. The 2.0 mM mPEG grafting concentration of either the 20 or 30 kDa polymer gave rise to RBC that would, per clinical MMA studies, be deemed suitable for transfusion into an alloimmunized patient if other blood were not available. PEOZ grafting failed to reach a clinically significant level of protection, though the 30 kDa polymer showed significantly greater protection than the 20 kDa chain. Also shown are the effects of antibody opsonization of RhD^- RBC (negative control) and spontaneous phagocytosis of untreated RhD^+ blood. Results ($n=3$) are expressed as mean ± SEM. From Kyluik-Price 2014 [148].

3.4.3 Camouflage of CD Antigens

The immunocamouflage efficiency of mPEG and PEOZ was also explored for surface camouflage of leukocyte CD markers. The differential efficacy of mPEG and PEOZ grafted to leukocytes was assessed *via* flow cytometric detection of CD3, CD4 and CD28 – all of which are critical for allogeneic recognition. As with RBC blood group antigens (**Figure 3.5**) both mPEG and PEOZ resulted in significant immunocamouflage of the selected CD markers (**Figure 3.7**) as measured by both PPC and MCF. The efficacy of immunocamouflage was grafting concentration dependent and both the 20 and 30 kDa mPEG and PEOZ were highly effective in obscuring the CD markers at higher (e.g., ≥ 2.0 mM; $p<0.02$) grafting concentrations. This is shown at the 2.0 mM grafting concentration, where the PPC for CD3, CD4 and CD28 was reduced by 89 ± 1.3%, 98.4 ± 0.2%, and 94.2 ± 2.4% with 20kDa mPEG and 86.5 ± 1.4%, 97.0 ± 0.8% and 94.6 ± 1.6% with 20 kDa PEOZ. Overall, neither mPEG nor PEOZ demonstrated any reproducible superiority for the immunocamouflage of CD markers (0.2-4.0 mM; $p>0.05$). Comparable results were found when MCF was used as the measure of immunocamouflage (**Figure 3.7**). The MCF data showed that both mPEG and PEOZ could decrease antibody recognition of all three CD markers at very low grafting concentrations. While the PPC data demonstrated that at grafting concentrations ≤ 2.0 mM, a significant percentage of cells were detected as CD positive, the amount of antibody bound (*i.e.*, the MCF) was very low and would likely result in impaired allorecognition due to weak signaling.

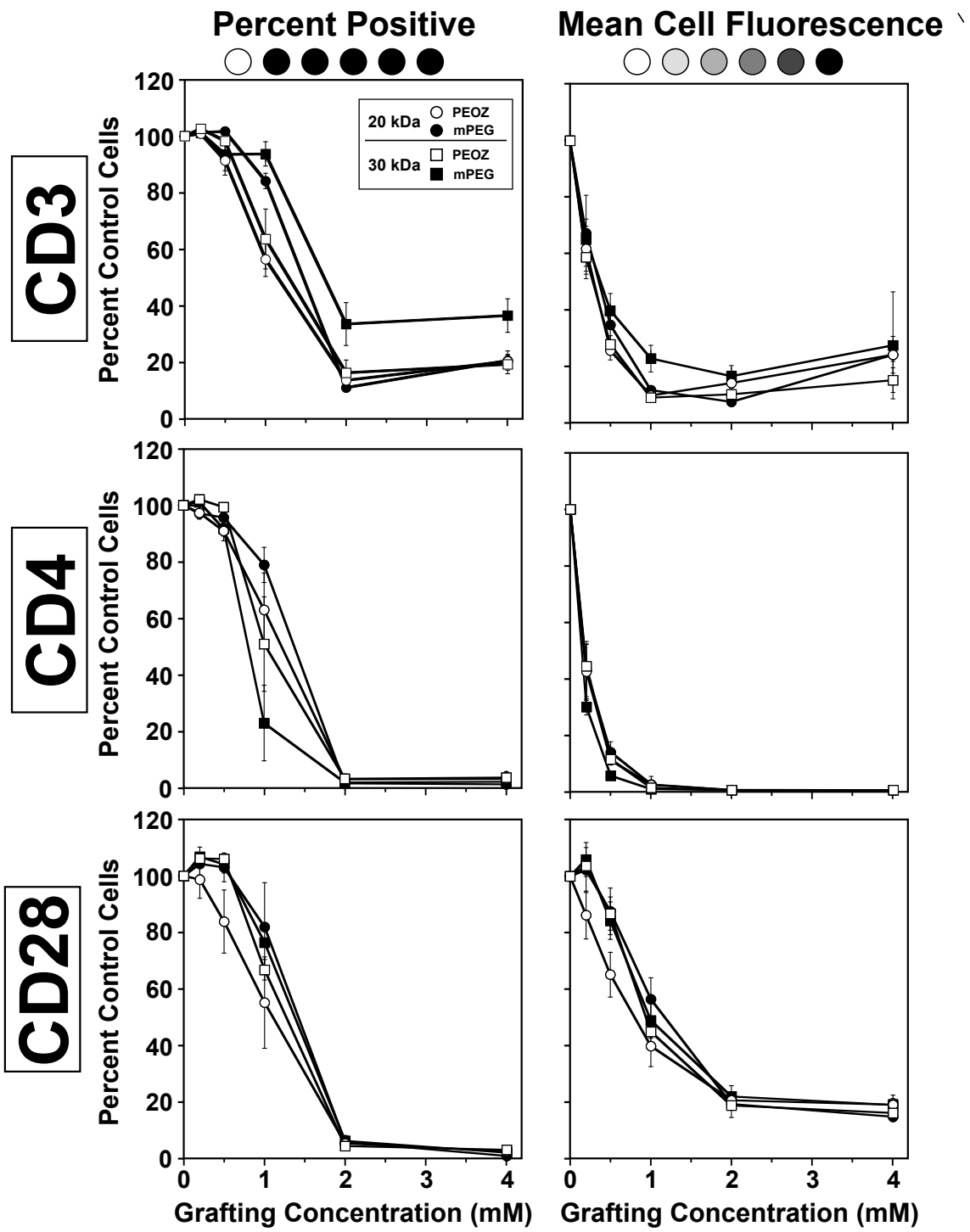

Figure 3.7 Both mPEG and PEOZ grafting resulted in significant immunocamouflage of leukocyte CD markers. The degree of CD immunocamouflage occurred in a dose-dependent manner that was similar using either mPEG or PEOZ. Shown are the effects of grafting concentration and polymer size on the percent positive cells (PPC) and mean cell fluorescence (MCF) of control and modified cells. Results (*n*=3) are expressed as the percent of unmodified cells (mean ± SEM) incubated with antibodies and set to equal 100%. Shown graphically is the interpretation of PPC and MCF; PPC is a measure of antibody positive *versus* antibody negative RBC while the MCF value accounts for the mean amount of bound antibody for the total cell population. Modified from Kyluik-Price 2014 [148].

3.4.4 Prevention of Leukocyte Proliferation During Mixed Lymphocyte Reaction (MLR)

The ability of both mPEG and PEOZ to prevent allorecognition was demonstrated in MLR studies. Efficient allorecognition requires substantive adhesion, recognition and costimulatory interactions between the disparate donor cells that can be readily disrupted by the bound polymers, thereby preventing allorecognition and cell proliferation. As shown in **Figure 3.8**, a dose-dependent decrease in proliferation (p<0.05 at ≥ 0.5 mM) was observed with both mPEG- and PEOZ-modified PBMC on day 14, as measured by a CFSE-dye dilution assay. No polymer size or species dependency was observed, suggesting that the global camouflage of multiple components of the adhesion, recognition and costimulation pathways was sufficient to impair successful allorecognition and proliferation. Moreover, as shown in **Figure 3.8B**, this finding was supported by the absence of proliferative foci in micrographs of mPEG-MLR and PEOZ-MLR, compared to foci present in the control MLR (black arrowheads). Indeed, modified-MLR closely resembled the resting naïve PBMC.

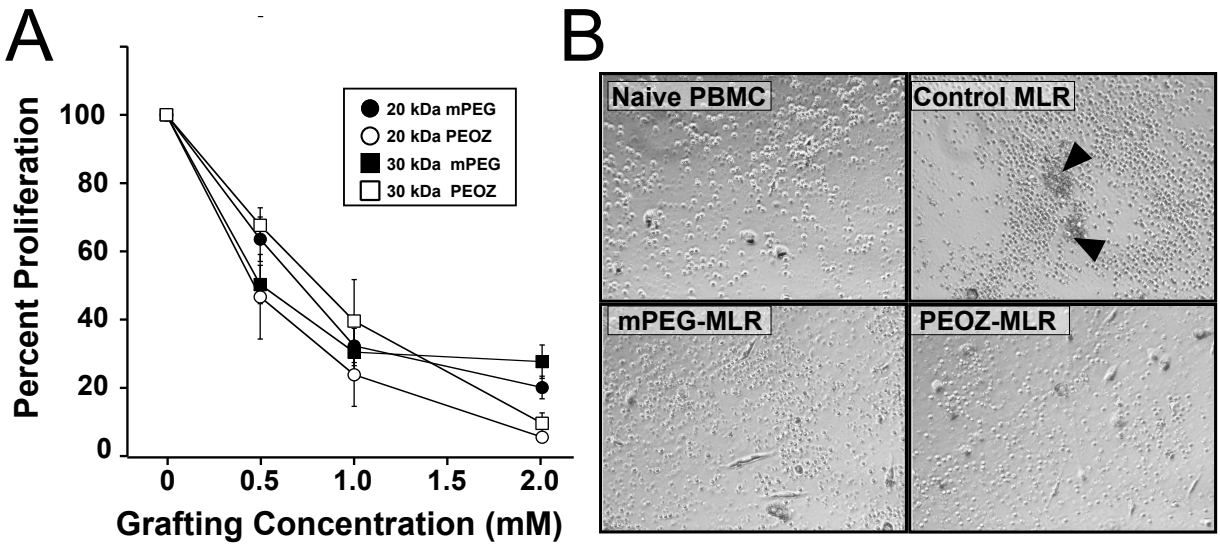

Figure 3.8 Polymer modification of lymphocytes resulted in a dose dependent decrease in allorecognition and proliferation. (A) As shown, on day 14 PEOZ- and mPEG-grafted PBMC resulted in similar inhibition of allorecognition as shown by the loss of cell proliferation. (B) Photomicrographs taken on day 14 showed foci of proliferating cells (arrow) in the control MLR, while both PEOZ- and mPEG-modification of one donor population inhibited proliferation and were morphologically similar to resting PBMC. The degree of $CD3^{+}CD4^{+}$ lymphocyte proliferation was measured by a decrease in CFSE (dye-dilution assay). Proliferation is expressed as the percent proliferation of control MLR (n=4; mean ± SEM), set to equal 100%. Modified from Kyluik-Price 2014 [148].

3.5 Conclusion

Polyoxazolines (e.g., PEOZ) are capable of mediating significant immunocamouflage of both human RBC and PBMC in a manner similar to grafted mPEG. Activated PEOZ and mPEG both demonstrated similar grafting efficacy and both polymers attenuated antibody recognition of blood group antigens and CD markers. Interestingly, mPEG and PEOZ exhibited some differential effects based on the type of cell being modified. While both polymers exhibited very similar immunocamouflage of human PBMC at both the antigenic (CD marker; **Figures 3.7**) and biological efficacy (MLR; **Figure 3.8**) level, RBC grafting exhibited some polymer-dependent effects. For example, phagocytic recognition (MMA) studies demonstrated that mPEG was vastly superior to PEOZ in preventing immune recognition and phagocytosis of anti-RhD opsonized RhD^{+}RBC (**Figure 3.6)**. While overall, mPEG appears to be superior to PEOZ in the immunocamouflage of cells, PEOZ may still be a valuable addition to the repertoire of immunomodulatory polymers used for the immunocamouflage of allogeneic cells in transfusion and transplantation medicine. Moreover, for the small subset of patients that may produce anti-PEG antibodies, PEOZ-modified cells (or proteins) could prove to be a highly useful alternative.

4 CHAPTER 4: The Effect of Methoxypoly(ethylene glycol) Grafting During Allogeneic Challenge

4.1 Overview

Our polymer comparison studies demonstrated the immunocamouflage potential of PEOZ. However, the RBC data indicated that PEOZ was significantly less effective than mPEG in preventing allorecognition. Therefore, the remainder of the thesis utilized the overall more efficacious mPEG polymers in order to fully explore the effects of surface immunocamouflage on downstream cellular events during allorecognition.

Tissue rejection occurs subsequent to the recognition of foreign antigens, *via* contact between APC and T cells. Initial cell contacts are achieved by various receptor and ligand interactions between these cells, resulting in initialization of signaling cascades and T cell proliferation. While previous PEGylation studies involved monitoring late events in T cell activation, such as decreased proliferation, little information has been provided concerning the early cellular events governing this response. Therefore, the effect of PEGylation was assessed by examining initial cell-cell interactions (camouflage of surface proteins, lymphocyte-APC conjugation events), changes to activation pathways (NFκB), and apoptosis to understand the role that each may play in the decreased proliferative response observed in modified cells during the course of an MLR. mPEG-modified PBMC resulted in significant immunocamouflage of lymphocyte surface proteins and decreased interactions with APC. Furthermore, mPEG-MLR exhibited decreased NFκB pathway activation, while exhibiting no significant differences in degree of cell death compared to the control MLR. Thus, the exclusion of immune cells and components by modified cells is an important factor leading to the decreased cell proliferation observed subsequent to allogeneic challenge.

4.2 Immunocamouflage of Surface Markers

To assess polymer mediated cell surface camouflage, we examined the effects of PEGylation on surface proteins involved in cellular adhesion (CD11a and CD62L), TCR signaling (CD3, CD4 and CD28) and receptors involved in activation and proliferation (CD25 and CD71). These proteins were assessed for immunocamouflage efficacy, in part, because of their importance during allorecognition, as drugs preventing their individual functions resulted in delayed rejection [206-208] and prolonged allograft survival [73,209-212]. The efficacy of polymer camouflage was examined by measuring the inhibition of antigen-antibody binding using fluorescently labeled antibodies. The amount of antibody bound was measured by flow cytometry and assessed as both percent positive cells (PPC) and mean cell fluorescence (MCF). Percent positive cells is a measure of the total percentage of cells in which any antibody is bound, whereas mean cell fluorescence is the average amount of antibody bound and was measured as MCF of the total population. PBMC were PEGylated with 5, 20 and 30 kDa SVA-mPEG at 0-4 mM grafting concentrations and the results were normalized to the value of the unmodified cells, set to equal 100%.

4.2.1 Adhesion Receptors CD11a and CD62L

mPEG modified PBMC demonstrated significant reduction in PPC for both CD11a and CD62L (p<0.01; 4.0 mM) for all polymer lengths, compared to the control (**Figure 4.1**). However, the longer polymers (20 and 30 kDa) resulted in significantly improved camouflage efficiency compared to the shorter (5 kDa) polymers at moderate grafting concentrations (2.0 mM). For example, detection of CD11a at 2.0 mM with the 5 kDa polymer resulted in a PPC of 57.2 ± 11.3%, while the 20 kDa and 30 kDa polymers reduced PPC to 30.7 ± 6.8% and 35.1 ± 8.4%, respectively. Similarly, the detection of CD62L at 2.0 mM grafting concentrations was 82.6 ± 4.5% using the 5 kDa, 31.2 ± 6.3% using the 20 kDa and 24.8 ± 6.6% using the 30 kDa polymer. The size dependent nature of immunocamouflage may be due to the topography of the

proteins as well as the Flory radius that governs the surface area of polymer exclusion. Both CD11a and CD62L have large extracellular domains with multiple lysine residues capable of polymer attachment. Therefore, the larger polymers may provide extended surface area coverage (R_F 20 kDa= 13.8 nm) compared to the smaller polymers (R_F 5 kDa= 6.0 nm). At high grafting concentrations (4.0 mM) there was no significant difference between polymer sizes (p>0.05), likely due to attachment of multiple small polymers near the antibody-binding site.

Mean cell fluorescence is a measure of the average amount of antibody bound and resulted in a steady decline of MCF intensity of the total cell population at lower concentrations relative to percent positive cells, which declined more abruptly at higher grafting concentrations. Compared to the control cells, the MCF values of CD11a and CD62L on modified cells showed a significant decrease in the amount of antibody bound that was apparent at low grafting concentrations for all polymer sizes assessed (p<0.05 at ≥ 1.0 mM) (**Figure 4.1**). The very large decrease in MCF seen at low grafting concentrations is influenced in part by the abundance of protein expression. Both CD11a and CD62L are highly expressed on human lymphocytes, exhibiting 4 x 10^4 integrin sites per cell [213]. Therefore, even low concentrations of bound polymer would likely result in attachment to or near these proteins.

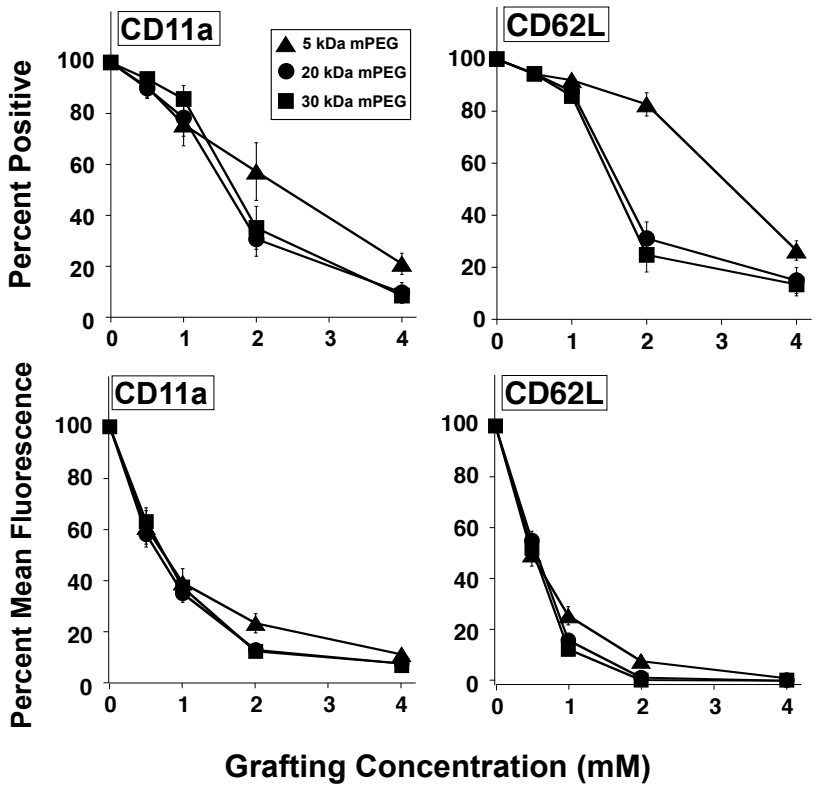

Figure 4.1 Immunocamouflage of lymphocyte adhesion receptors CD11a and CD62L. Covalent modification of PBMC with mPEG resulted in a dose and size dependent decrease in percent positive cells (PPC) and mean cell fluorescence (MCF). Results are expressed as mean ± SEM (*n*=3). Values are expressed as percent of unmodified cells incubated with antibody and set to equal 100%.

4.2.2 TCR Complex (CD3), Coreceptor (CD4) and Costimulatory Receptor (CD28)

The modification of PBMC with mPEG resulted in a polymer size and grafting concentration dependent decrease in the detection of CD3, CD4 and CD28 as measured by PPC (**Figure 4.2;** 20 and 30 kDa mPEG done previously for polymer comparison **Figure 3.7,** results shown for polymer size comparison). All polymers resulted in significantly decreased PPC compared to the control ($p<0.05$; ≥ 2.0 mM). The longer polymers (20 and 30 kDa) showed improved surface camouflage compared to the shorter 5 kDa chain at moderate grafting concentrations. For example CD3, CD4 and CD28 at 2.0 mM grafting concentrations resulted in the detection of 61.7 ± 7.0%, 50.5 ± 11.9% and 34.1 ± 6.5% using the 5 kDa polymer while the 20 kDa polymer resulted in detection of 11.0 ± 1.3%, 1.6 ± 0.2% and 5.84 ± 2.4% ($p<0.02$; 5 *vs* 20 kDa), respectively. While the difference in camouflage efficacy by polymer size can be explained in part by the height of the CD4 and CD28 receptors (7 and 13 nm from the membrane respectively) [214,215], CD3 is a relatively short protein (3 nm) [216]. Due to the short topography of CD3, it was expected that polymer length would not influence the degree of

immunocamouflage. However, the increased immunocamouflage efficacy observed for CD3 by the long polymers, may be due to CD3 close association with the TCR (approximately 7 nm in height) leading to the indirect camouflage of CD3 *via* the taller TCR. This would result in polymer size dependency as suggested previously [156]. In addition, for the camouflage of CD3, the 20 kDa polymer provided improved immunoprotection at higher grafting concentrations compared to the 30 kDa polymer. This could be a result of self-exclusion of the larger polymers binding to the TCR complex.

mPEG-modified cells also demonstrated a significant dose dependent decrease in the MCF for CD3, CD4 and CD28 **(Figure 4.2)**. However, the decreased MCF was initially more significant for CD3 and CD4 than for CD28. For example at 0.5 mM, the MCF was reduced to between 35-40% and 6-19% for CD3 and CD4 respectively ($p<0.05$), while CD28 was decreased to only 67-88% ($p>0.05$), compared to the controls. As previously discussed, protein expression may influence the MCF at low grafting concentrations. For example, CD3 and CD4 are highly expressed on the cell, approximately 3×10^5 and 1.5×10^5 [58,217], respectively, compared to CD28 with approximately 1.5×10^3 on naïve T cells [211]. As shown, all polymer-modified cells displayed significantly low MCF at grafting concentrations of ≥ 1.0 mM ($p<0.05$), compared to the controls.

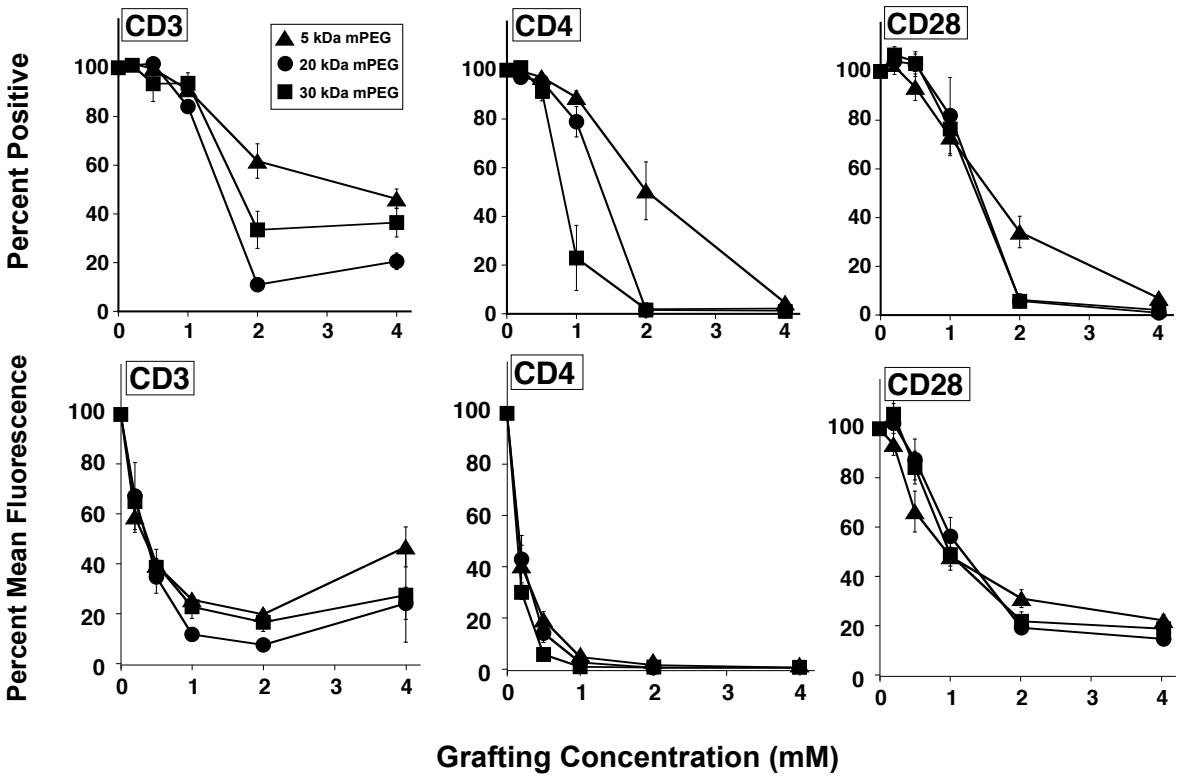

Figure 4.2 Immunocamouflage of lymphocyte TCR (CD3), coreceptor (CD4) and costimulatory receptor (CD28). Covalent modification of PBMC with mPEG resulted in a dose dependent decrease in percent positive cells (PPC) and mean cell fluorescence (MCF). The longer polymers (20 and 30 kDa) resulted in increased camouflage efficacy compared to the shorter (5 kDa) polymers. Results are expressed as mean ± SEM (*n*=3). Values are expressed as percent of unmodified cells incubated with antibody and set to equal 100%.

4.2.3 Activation Receptors CD25 and CD71

Similar to previous surface targets, polymer modification of PBMC also significantly reduced the detection of CD25 (high affinity IL2 receptor) and CD71 (transferrin receptor) in a dose and size dependent manner (**Figure 4.3**). Smaller polymers resulted in decreased camouflage efficacy compared to the larger polymer chains. At high grafting concentrations (4.0 mM) for most surface proteins assessed (CD4, CD11, CD25, CD28, CD62L), there were no significant differences between the polymer sizes ($p>0.05$), likely due to attachment of multiple small polymers on or near the antibody-binding site. However, the polymer size difference remained pronounced for CD71, even at high grafting concentrations (4.0 mM; $p<0.03$). For example at 4.0 mM, detection of CD71 positive cells was decreased to 55.5 ± 7.6%, 14.7 ± 3.5% and 19.5 ± 4.1% using the 5, 20 and 30 kDa polymer chains, respectively. The polymer

size dependency observed at high grafting concentrations may be influenced by the location of CD71. CD71, unlike many other proteins, are generally excluded from lipid rafts containing protein micro-domains and instead occurs as randomly organized single entities on the membrane [218-220]. Since CD71 has a fairly large extracellular domain, the results suggest that the smaller Flory radius of the 5 kDa may be hindered by its lower exclusion radius and lack of indirect camouflage provided by neighboring proteins, resulting in relatively higher detection of positive cells compared to the longer polymer chains.

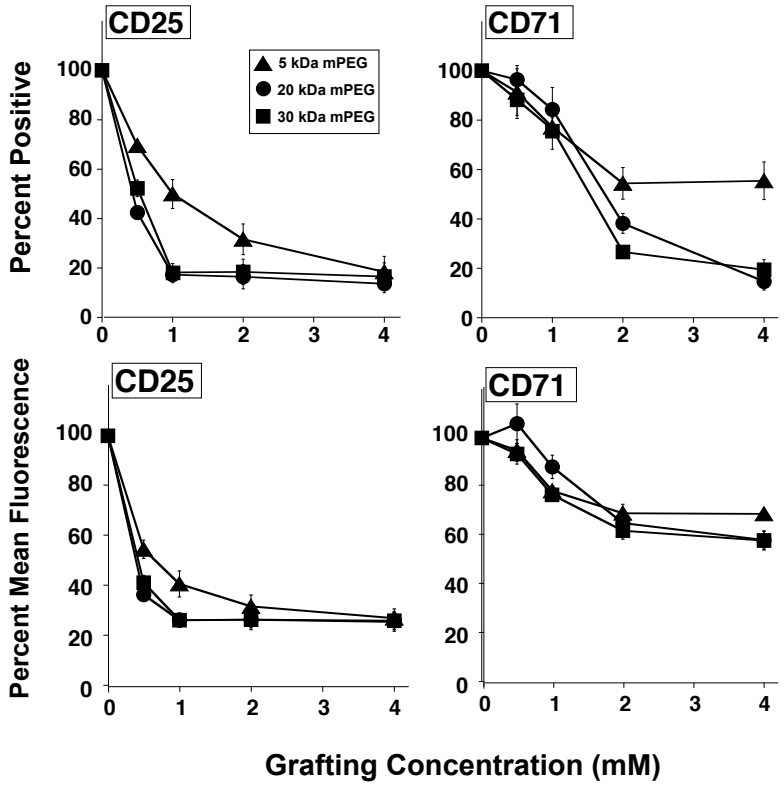

Figure 4.3 Immunocamouflage of lymphocyte CD25 and CD71. Similar to previous targets, the covalent modification of PBMC with mPEG resulted in a dose and size dependent decrease in percent positive cells (PPC) and mean cell fluorescence (MCF). The longer polymers (20 and 30 kDa) showed improved efficacy compared to the shorter (5 kDa) polymers. Results are expressed as mean ± SEM (*n*=3). Values are expressed as percent of unmodified cells incubated with antibody and set to equal 100%.

Similar to previous surface markers, MCF resulted in a significant dose dependent decrease in the relative amount of antibody bound to CD25 and CD71 (**Figure 4.3)**. For example, by 2.0 mM all polymer lengths resulted in significant reduction in MCF values for both CD71 and CD25, compared to the controls ($p<0.05$). However, in contrast to CD25, the MCF of CD71 did not decrease as abruptly. Although only a small number of cells in PBMC preparations express CD25 and CD71, the number of sites per cell on the CD25+ population is generally high (*i.e.*, Treg cells), compared to the very low expression of CD71 per cell.

4.2.4 Surface Marker Immunocamouflage Summary

Similar to RBC surface antigens in Chapter 3, the camouflage of leukocytes by polymer modification resulted in significantly decreased antibody binding compared to the unmodified control cells for all surface proteins assessed. For example, all polymer lengths resulted in significant decrease of PPC compared to the control ($p<0.05$; ≥ 4.0 mM). However, the longer polymers (20 and 30 kDa) resulted in increased camouflage capability compared to the shorter (5 kDa) polymers at moderate grafting concentrations. In addition, relative to the control cells, the MCF values showed a significant decrease in amount of antibody bound ($p<0.05$; ≥ 2.0 mM), and the decrease in MCF was apparent at lower grafting concentrations. The relationship between percent positive and MCF is somewhat complicated for assessing the efficacy of immunocamouflage. Cells that are deemed negative will have no significant MCF, while positive cells may exhibit low to high MCF consequent to the amount of polymer bound to an individual cell and therefore the amount of fluorescently labeled antibody that is capable of binding to receptors. As seen in CD3 immunocamouflage, a slight increase in MCF at high grafting concentrations (4.0 mM) reflects the presence of a very small subset of cells with low amounts of grafted polymer. However, the slight increase in MCF was not significantly different from the MCF at 2.0 mM for any polymer length examined ($p>0.05$). In contrast, a large percentage (~80%) of cells were CD62L positive at 1 mM, but the MCF value was significantly decreased (by ~90%), suggesting that cells were positive but were sufficiently camouflaged with polymer, resulting in very little bound antibody per cell. Therefore, it is crucial that both the percent positive and MCF values be properly evaluated in assessing the efficacy of immunocamouflage. Indeed, MCF may be of greater biological significance, as the large decrease in MCF indicates that cells modified with mPEG have surface proteins with very small amounts of antibody bound, even though they were considered positive as measured by PPC. Together, these studies suggest a very effective global immunocamouflage induced by mPEG grafting. The slight differences in immunocamouflage efficacy of surface proteins assessed can be attributed

to protein height, the number of lysine residues, membrane topography, protein abundance and the location of the antibody-binding site relative to the polymer-binding site.

4.3 Polymer Mediated Inhibition of Cell-Cell Interactions During a Two-Way Mixed Lymphocyte Reaction: Time-Lapse Microscopy

Immunocamouflage of cell surfaces was shown to significantly reduce antibody binding to RBC (**Figure 3.4)** and PBMC (**Figures 4.1-4.3**). Thus, PEGylation resulted in exclusion of small molecules such as antibodies that may lead to a reduction in immune responses to alloantigens. However, initial cell contacts between naïve lymphocytes and APCs are important events that mediate the alloresponse to foreign cells and tissues. To assess the effects of PEGylation on cell conjugation events between lymphocytes and APCs, time-lapse microscopy was utilized. Human monocyte derived dendritic cells (moDC) were matured, activated, and co-cultured with control or PEGylated allogeneic human PBMC to examine the effects of PEGylation on the direct allorecognition of foreign antigens. Co-cultures were plated on coverslips in a heated humidity chamber and micrographs were acquired every 20 seconds for 90 minutes. Representative micrographs from 0-90 minutes are shown in **Figure 4.4.** Within 30 minutes of acquisition in all replicates, unmodified (control) lymphocytes were observed forming prolonged contacts with MoDC (indicated by arrows in **Figure 4.4)**. In contrast, PEGylated lymphocytes (20 kDa; 2.0 mM) failed to generate sustained interactions with moDC over the time period assessed. While studies indicate that there may be a spectrum of behavior between antigen bearing DC and naïve T cells, which consist of both transient and prolonged contacts (minutes to hours) [72,221,222], very few interactions were observed between PEGylated cells and moDC. This suggests that PEGylation may prevent the direct recognition of foreign alloantigens by decreasing the stability and duration of initial cell-cell interactions.

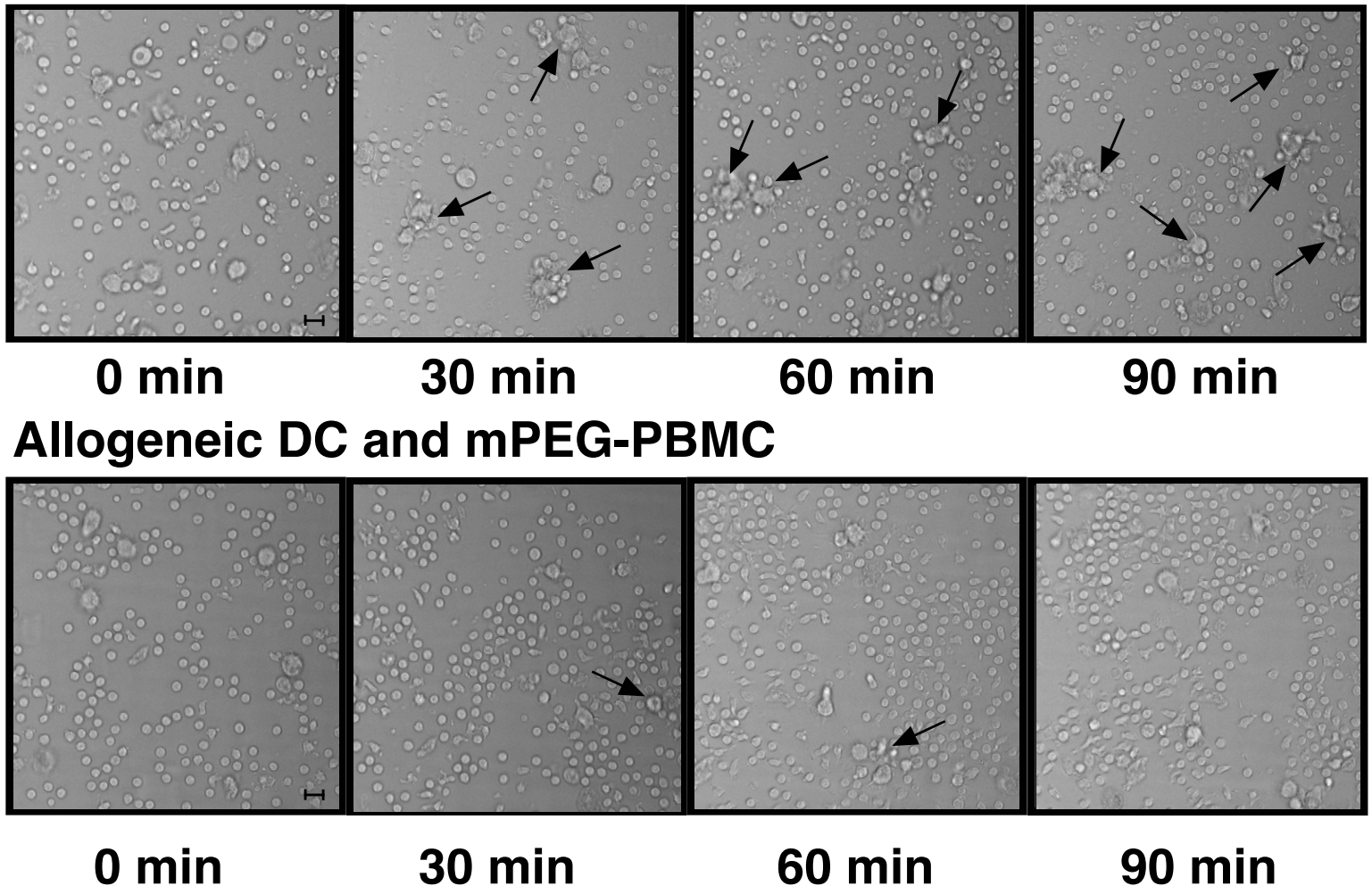

Figure 4.4 PEGylation decreased prolonged interactions between allogeneic cells. Shown in (A) are representative micrographs from 90 minute time-lapse (*n*=3). Within 30 minutes of acquisition, unmodified lymphocytes were seen forming prolonged contacts with moDC (indicated by arrows). In contrast, lymphocytes PEGylated with 20 kDa SVA-mPEG (2.0 mM) failed to generate sustained interactions with moDC over the time period assessed. Size bar = 10 μm.

Both APCs and lymphocytes are motile cells capable of covering fairly large distances in order to both present and detect foreign antigen *via* cell surface receptors. Studies show that 3-dimensional T cell velocities can be as high as 10 μm/minute [223], while dendritic cells have been shown to display high motility both *in vitro* and *in vivo*, averaging approximately 6.6 μm/minute [222,224]. However, upon cell-cell contact and recognition of foreign antigens, cell mobility decreases [72,225,226]. Therefore, to assess cell-cell interactions between PEGylated cells and APC during allogeneic challenge, the distances travelled by moDC were tracked for 90 minutes. Since PBMC preparations contain a heterologous population of cells, including T and B cells that are indistinguishable from each other microscopically, the velocities of moDC were examined to assess the extent of cell conjugation as reflected by the loss of cell motility. The superimposed trajectories of moDC movements in the control and PEGylated samples showed that DC movements were inversely correlated with antigen encounter (**Figure 4.5).** Indeed, the movements of moDC in control samples demonstrated an overall decrease in the 2-dimensional area covered, compared to moDC co-cultured with PEGylated PBMC, further demonstrating the loss of cell interactions between PEGylated lymphocytes and MoDC.

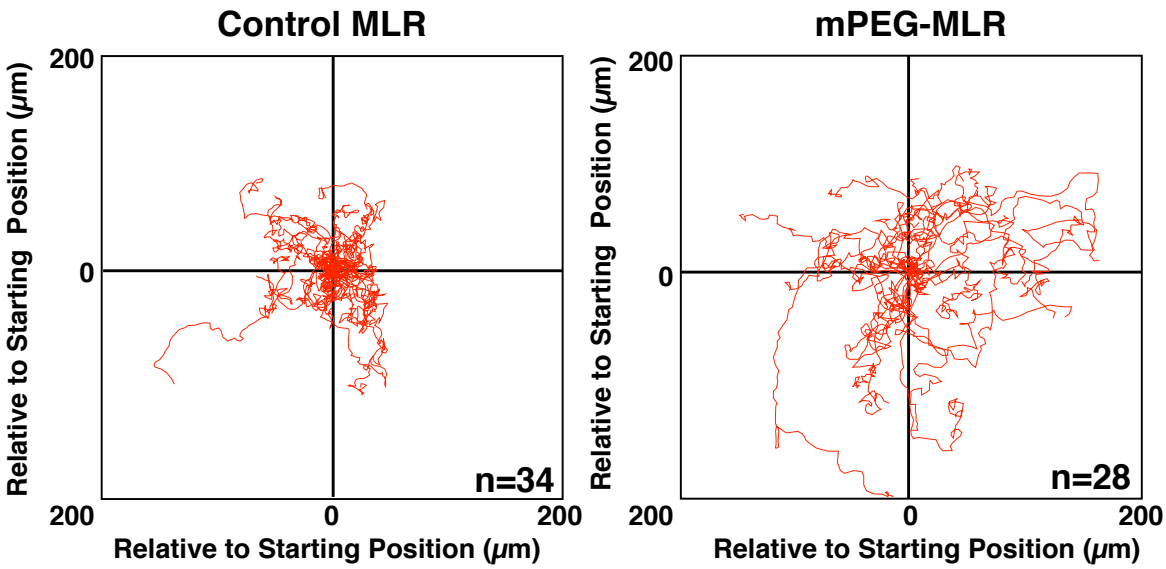

Figure 4.5 The superimposed trajectories of moDC movements in the control and PEGylated samples showed that DC movements were inversely correlated with antigen encounter. The movements of moDC in control samples showed an overall decrease in the 2-dimensional area covered compared to moDC co-cultured with PEGylated PBMC, demonstrating the loss of cell interactions between PEGylated lymphocytes and MoDC.

4.4 Polymer Mediated Prevention of Conjugate Formation Between Cells: Effect of Grafting Concentration and Polymer Size

To quantify cell interactions between control or PEGylated PBMC and MoDC, flow cytometry was utilized. PBMC and MoDC were labeled with distinct fluorescent dyes and, following a 20-minute co-incubation, the number of lymphocyte-moDC conjugates were quantified using two-color flow cytometry. Shown in **Figure 4.6** are the percentages of double staining cells over various polymer-grafting concentrations (0-4 mM) using 2 and 20 kDa mPEG. Results showed a significant dose dependent decrease in the number of cell conjugates, with both the 2 and 20 kDa polymers displaying similar efficacy (p<0.03 at ≥ 0.5 mM). For example, at 2.0 mM polymer grafting concentration percent conjugation was reduced to 1.07 ± 0.1% (2 kDa) and 1.04 ± 0.1% (20 kDa) compared to the control 2.36 ± 0.2%. In fact, the number of PEGylated PBMC and allogeneic moDC conjugates were not significantly different from the syngeneic co-culture (1.05 ± 0.1%) at all polymer lengths and concentrations assessed

(p>0.05). Furthermore, at very low grafting concentrations, the small polymer (2 kDa) showed a slightly greater decrease in conjugation events compared to the larger polymer chain (20 kDa), while at high grafting concentrations (4.0 mM) the larger polymers displayed somewhat better efficacy. Together, the results demonstrated that PEGylated cells led to decreased conjugate formation with allogeneic cells, in support of time-lapse microscopy studies.

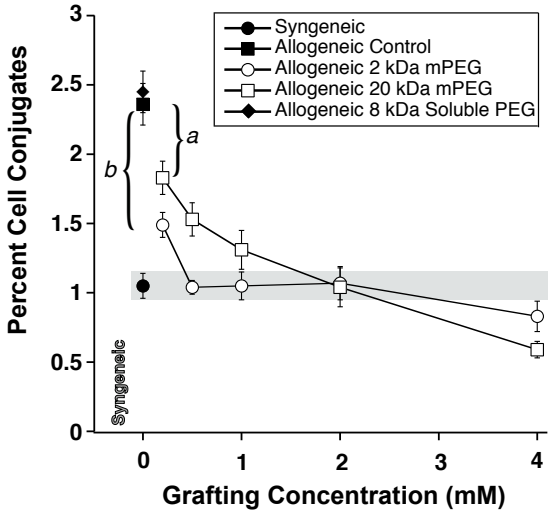

Figure 4.6 PEGylated PBMC demonstrated a significant dose dependent decrease in the number of cell conjugates (p<0.02 at ≥ 0.5 mM)**.** Cells were modified using the 20 kDa (*a*) and 2 kDa (*b*) polymers and compared to the control. Shown are the percentages of double staining cells over various polymer-grafting concentrations (0-4 mM). The number of PEGylated PBMC and allogeneic moDC conjugates were not significantly different from the syngeneic co-culture at all polymer lengths and concentrations (p>0.05). Results are expressed as mean ± SEM (n=4).

4.5 Inhibition of Lymphocyte Proliferation by PEGylation

To assess the downstream effects of surface camouflage, which prevented the approach of both cells and small molecules (antibodies), the proliferative response to allogeneic cells (MLR) and mitogens (PHA) was examined (**Figure 4.7)**. PEGylation of PBMC with 20 kDa mPEG (0-2 mM) resulted in a significant dose dependent decrease in the proliferation of CD3+/CD4+ lymphocytes. These results suggest that the camouflage of surface proteins can prevent activation *via* receptor ligand binding of either stimulatory cells (APC) or small activating mitogens (PHA). Furthermore, the decreased proliferation of PEGylated lymphocytes during an MLR was related to the decrease observed in cell conjugate studies (**Figure 4.6)**.

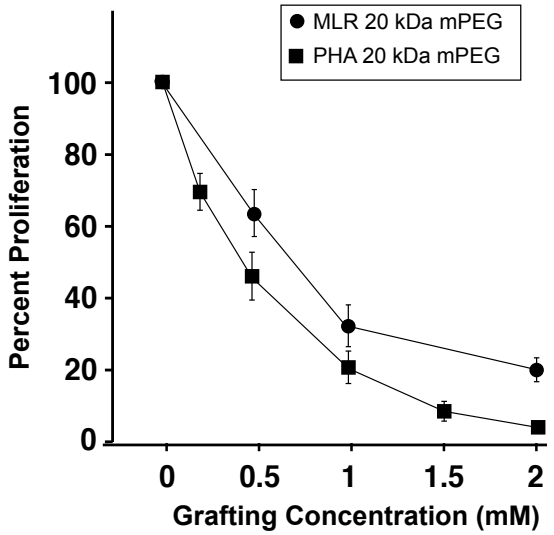

Figure 4.7 PEGylation of PBMC with 20 kDa mPEG resulted in a significant dose dependent decrease in the proliferation of lymphocytes during a MLR and upon mitogen (PHA) challenge. Cell proliferation was assessed on day 14 of a MLR and day 5 of PHA challenge. Results (*n*=4) are expressed as the percent of unmodified cell (mean ± SEM) proliferation set to equal 100%.

4.6 Effect of Polymer Grafting on Leukocyte Activation

Consequent to surface immunocamouflage studies, inhibition of cell interactions, and decreased proliferative response of modified PBMC during MLR, we investigated the consequence of polymer attachment to intracellular signaling events involved in cell activation. To assess the effects of polymer modification on cell activation pathways during allogeneic recognition, real-time PCR was performed using the human NFκB signaling targets RT^2 Profiler PCR arrays. mRNA targets of interest were further assessed for protein expression by western blot. NFκB is an important transcription factor for the activation of cells during an alloresponse. This includes the regulation and production of IL2 as well as other inflammatory molecules and growth factors. The importance of this pathway has been demonstrated by the induction of T cell hyporesponsiveness and prevention of GVHD in mice after NFκB blockade [227].

4.6.1 mRNA Expression of NFκB Pathway Target Genes During Mixed Lymphocyte Reaction: Effect of Polymer Modified Leukocytes

To examine the intracellular effects of mPEG-PBMC modification during MLRs, the mRNA expression of genes transcribed during NFκB pathway activation were examined in control and mPEG modified MLRs (20 kDa; 2.0 mM) as well as unmodified 'resting' PBMC at 2, 6 and 24 hours. Changes in fold regulation are shown as heat maps in **Figure 4.8**, which

compared control MLR *vs* resting PBMC (**Figure 4.8- a, d** and **g)**, mPEG-MLR *vs* resting PBMC (**Figure 4.8- b, e** and **h)** and mPEG-MLR *vs* control MLR (**Figure 4.8- c, f** and **i)** for each timepoint assessed. Genes responsive to NFκB signal transduction include those involved in inflammation, immune response, differentiation and apoptosis and the heat map is organized according to these functional gene groupings. Results showed similar mRNA profiles at 2 hours for resting PBMC, control MLR and mPEG-MLRs (**Figure 4.8 a-c**). However at 6 and 24 hours, control MLR mRNA expression increased compared to resting PBMC (**Figure 4.8 d and g**) indicating activation of cells as a result of allorecognition. In addition, mPEG-MLR profiles show a considerable decrease in mRNA expression of several NFκB targets compared to control MLRs (**Figure 4.8 f and i**). Indeed, mPEG-MLR profiles were more similar to resting PBMC profiles (**Figure 4.8 e and h**). Together this suggests a considerable loss of activation in mPEG modified MLRs compared to the control. However, the activation NFκB pathways were not completely abrogated in mPEG-MLRs, as mRNA expression remained somewhat increased compared to resting PBMC.

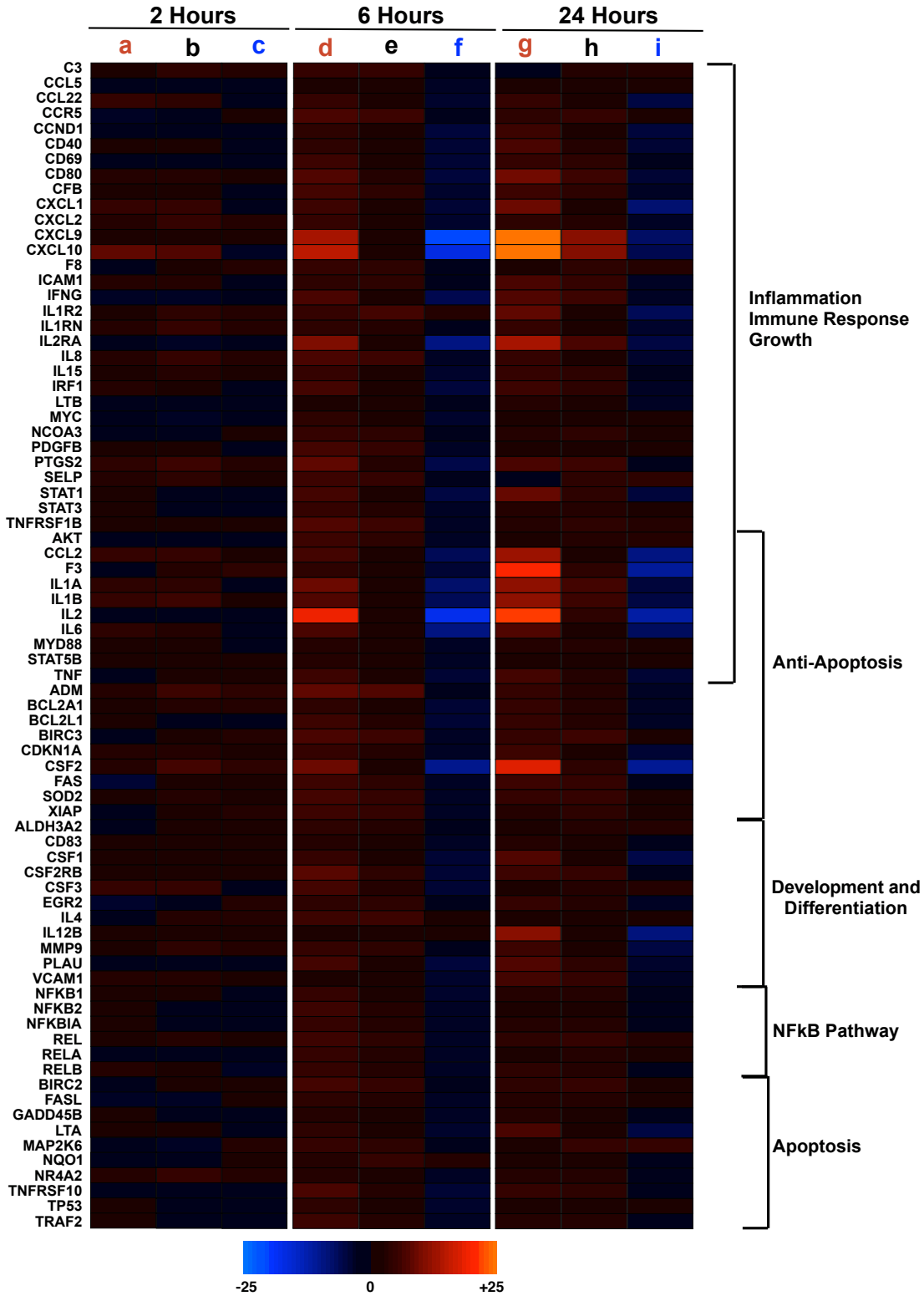

Figure 4.8 mPEG-MLR demonstrated decreased expression of mRNA involved in NFκB signal transduction. Mean changes in fold regulation (*n*=3) are shown as heat maps, comparing control MLR *vs* resting PBMC (a,d and g), mPEG-MLR *vs* resting PBMC (b,e and h) and mPEG-MLR *vs* control MLR (c,f and i) for each timepoint (2, 6 and 24 hours). Genes (listed in left column) responsive to NFκB signal transduction include those involved in inflammation, immune response, differentiation and apoptosis.

To illustrate the differences between control MLR and mPEG-modified MLRs, volcano plots are shown for 6 and 24 hour timepoints in **Figure 4.9**. Volcano plots illustrate both fold-change and significance (x- and y-axes, respectively) between control and mPEG-MLRs. Although the results suggest that mRNA expression of many inflammatory cytokines and chemokines characteristically upregulated during MLRs were considerably decreased in mPEG-MLRs at both 6 and 24 hours, only a small number of targets were statistically significant ($p<0.05$; $n=3$). For example at 6 hours, IL2 and CSF3 produced by lymphocytes and monocytes, respectively, were significantly downregulated in mPEG-MLR. While at 24 hours, IL1R2, STAT1, IL2 and F3 mRNA were all significantly decreased in mPEG-MLR. Although fold-expression of multiple mRNA targets were downregulated in mPEG-MLR, the relatively low statistical significance observed may be due to the increased variability in the alloresponse of disparate donor PBMC populations during MLRs (ranging from 1-10% of cells). However, biologically, the decreased mRNA expression of various inflammatory chemokines and cytokines may be cumulative, creating a decreased inflammatory milieu during the MLR and decreased cell proliferation.

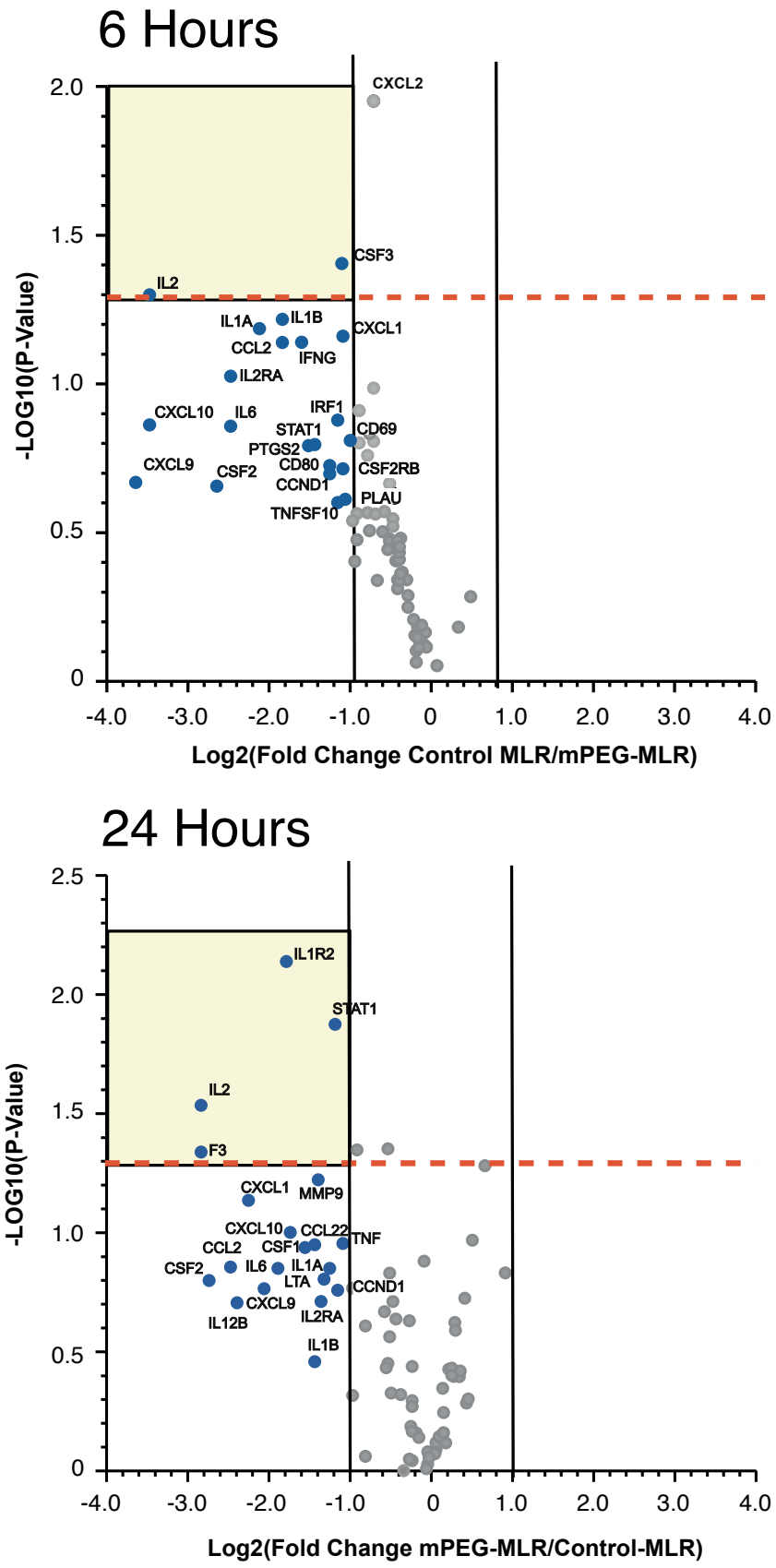

Figure 4.9 Inflammatory cytokines and chemokines characteristically upregulated during MLRs were considerably decreased in mPEG-MLRs at both 6 and 24 hours. Volcano plots illustrate both fold change and significance (x- and y-axes, respectively) between control and mPEG-MLRs. Yellow shaded area shows targets that displayed both large magnitude fold changes and statistical significance. Dashed line specifies where p=0.05.

4.6.2 Protein Expression During Mixed Lymphocyte Reaction: Effect of Polymer-Modified Leukocytes

Subsequent to mRNA expression profiles, we determined the level of protein expression of various mRNA targets that were significantly downregulated in mPEG-MLRs compared to control MLRs. Since PBMC preparations contain a heterologous population of cells, proteins of interest to further pursue were chosen based on the significance to naïve lymphocyte activation and inflammatory response subsequent to allorecognition (*i.e.,* IL2, STAT1, IL1R2).

The protein expression of IL2 and STAT1, both of which promote inflammation and proliferation, have been investigated previously showing that both IL2 and cytokines (INFγ) that promote and are the product of STAT1 activation, were significantly downregulated in mPEG-MLR [190]. Therefore, we chose to pursue the differential expression of IL2 receptors (α and β) in mPEG-MLR compared to control. Increased expression of high affinity IL2Rα is indicative of the response to IL2 production as well as an indicator of cell activation subsequent to the stimulation of the auto- and paracrine action of IL2.

The western blots and analyzed band intensities on day 4 and 7 of IL2Rα and IL2Rβ for resting PBMC, control MLR and mPEG-MLR are shown in **Figure 4.10 A** and **B**. Results indicate a significant increase in IL2Rα expression on day 7 in control MLR compared to mPEG-MLR (**Figure 4.10A**) ($p<0.05$). Conversely, no significant differences were seen in the expression of IL2Rα between mPEG-MLR and resting PBMC on either day 4 or 7. These results corresponded with mRNA data that indicated an upregulation in IL2Rα in control MLR compared to mPEG-MLR and suggests an increased receptor expression response to IL2. As expected, no significant differences were seen in the constitutively expressed IL2Rβ between mPEG-MLR, control MLR or the resting PBMC population on day 4 or 7 ($p>0.05$) (**Figure 4.10B**).

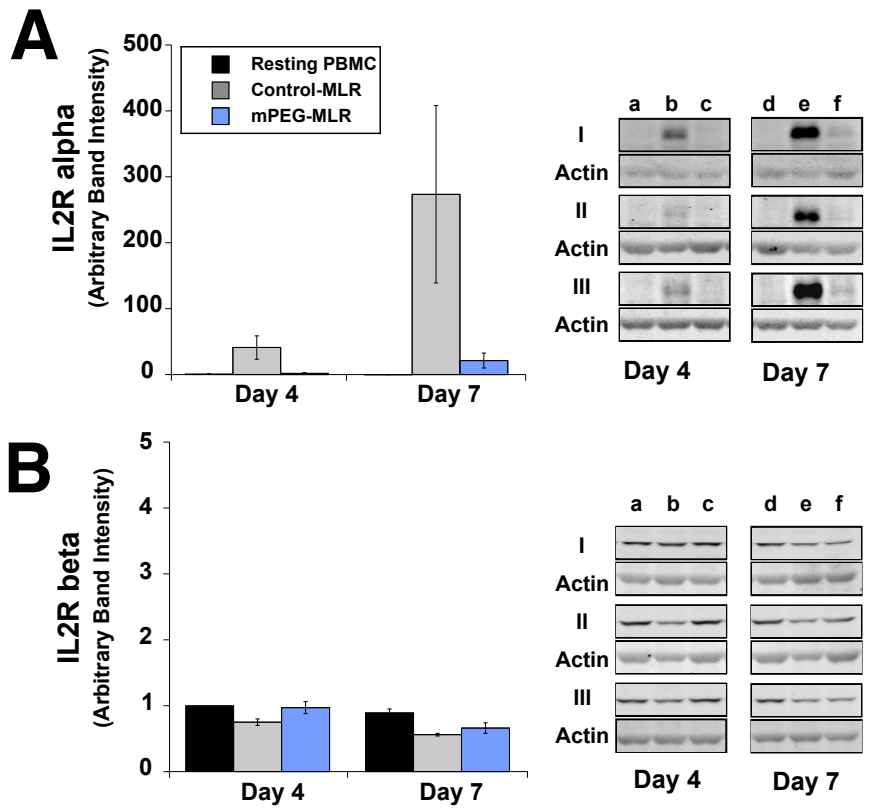

Figure 4.10 (A) The expression of IL2Rα was significantly decreased ($p<0.05$) in mPEG-MLR compared to the control-MLR on day 7. (B) Conversely, no significant differences were observed between mPEG-MLR and control MLR for IL2Rβ. Shown are western blot results of triplicate experiments (I-III) and the corresponding actin loading controls of resting PBMC (a,d), control-MLR (b,e) and 2.0 mM mPEG-MLR (c,f) on day 4 and 7. Values analyzed by densitometry are expressed relative to unmodified control day 4 and set to equal 1. Results are expressed as mean ± SEM.

While mRNA profiles indicated that IL1R2 was not upregulated in control MLRs compared to mPEG-MLR at 6 hours, IL1R2 was significantly upregulated at 24 hours (**Figure 4.9**). IL1R2 is an early response protein expressed by many cells including lymphocytes and monocytes that acts as a decoy receptor. IL1R2 is upregulated in response to inflammatory cytokines *via* NFκB transduction, to control the biological effects of IL1 during an inflammatory immune response [228]. Thus, IL1R2 protein expression can be indicative of NFκB activation and inflammatory responses.

To assess the expression of IL1R2 subsequent to mRNA experiments, the protein expression of decoy receptor IL1R2 was examined on day 4 and 7 of an MLR. Since IL1R2 is expressed on both the cell membrane as well as in secreted form, control-MLR, mPEG-MLR,

and resting PBMC were assessed for IL1R2 in both membrane and supernatant components. The western blot results showed a small increase in the expression of IL1R2 on both the membrane (day 4 and 7) (**Figure 4.11A**) as well as the secreted protein (day 7) (**Figure 4.11B**) in control MLR compared to mPEG-modified MLR, however there was no statistical significance noted between mPEG-MLR and control MLR at either location or timepoints assessed, suggesting a post-transcriptional inhibition of IL1R2.

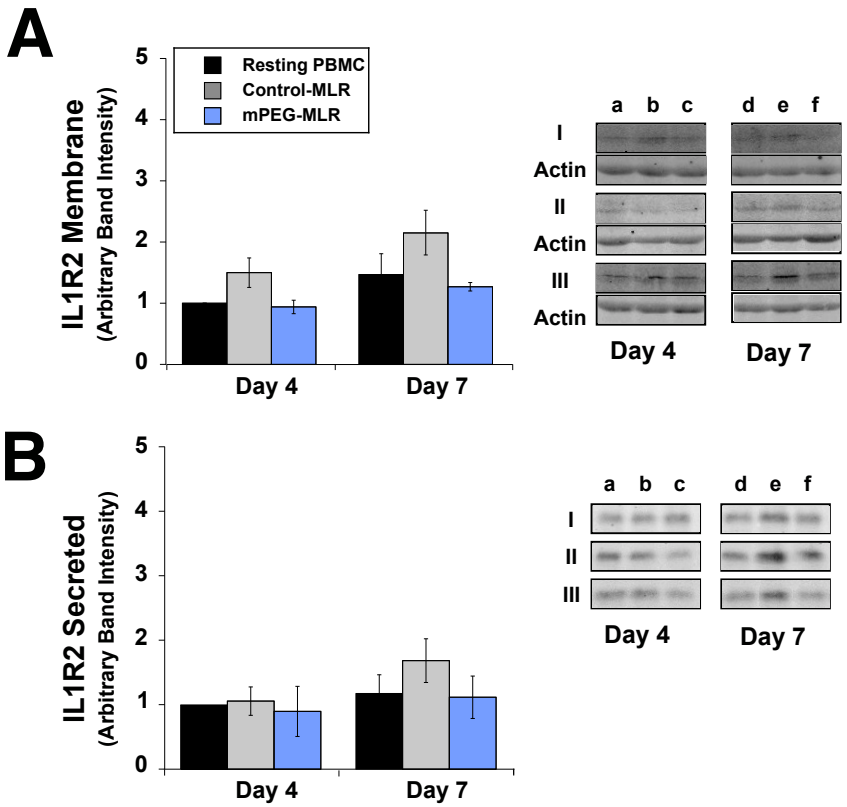

Figure 4.11 No significant differences were observed between mPEG-MLR and control-MLR for membrane expressed IL1R2 (A) or secreted IL1R2 (B). Shown are western blot results of triplicate experiments (I-III) and the corresponding actin loading controls of resting PBMC (a,d), control-MLR (b,e) and 2.0 mM mPEG-MLR (c,f) on day 4 and 7. Values analyzed by densitometry are expressed relative to unmodified control day 4 and set to equal 1. Results are expressed as mean ± SEM.

4.7 Influence of Polymer Grafting on Apoptosis

Previous studies have suggested a small decrease in cell viability of polymer modified PBMC over time [229] and during an MLR [138] *in vitro*. Therefore, we sought to determine whether apoptosis was increased in polymer-modified cells and whether the loss of viability played a role in the decreased proliferative response seen in mPEG modified MLRs (**Figure**

4.7). Decreased viability of mPEG-modified cells may be due to subthreshold or weak cell stimulation by allogeneic cells during an MLR or by loss of survival factor stimulation in modified cells. Both early apoptotic events (caspase 3/7 activation) as well as late apoptotic/necrotic (Sytox staining) were used to assess the cell viability of resting PBMC (0-72 hours), PBMC during the course of an MLR (2-72 hours) as well as the ability of survival cytokine (IL2) to rescue mPEG-modified cells from apoptosis.

4.7.1 Viability of Leukocytes During a Mixed Lymphocyte Reaction

To determine whether mPEG-modified cells resulted in decreased viability during allogeneic challenge, control and mPEG-modified MLR (20 kDa; 0-2 mM) were assessed at 2, 6, 24, 48 and 72 hours for caspase 3/7 activation (early apoptosis) and degree of membrane permeabilization characteristic of late apoptosis/necrosis (Sytox staining). The viability studies can be separated into two components, cell viability during the early activation phase of an MLR 2-24 hours and the proliferation phase of an MLR 24-72 hours (**Figure 4.12A)**. Cell death as a result of weak activation events may be more pronounced during the early activation phase. Results of both early and late apoptotic events during the early activation phase of an MLR (≤ 24 hours) showed a small increase in cell death in mPEG-MLR compared to the control MLR that was somewhat more pronounced with higher grafting concentrations (2.0 mM). While, this slight increase was statistically significant at 2 hours ($p<0.05$), there was no significant difference from control MLR at any subsequent timepoints assessed. Furthermore, there were no substantial differences between early and late apoptotic markers, suggesting that the small number of apoptotic cells all progress to the late apoptotic (*i.e.*, secondary necrotic cell) stage. Similarly, results corresponding to the proliferative phase of an MLR (48-72 hours) demonstrated no increase in the degree of apoptosis in modified cells compared to control MLR, and no significant differences between early and late apoptotic markers.

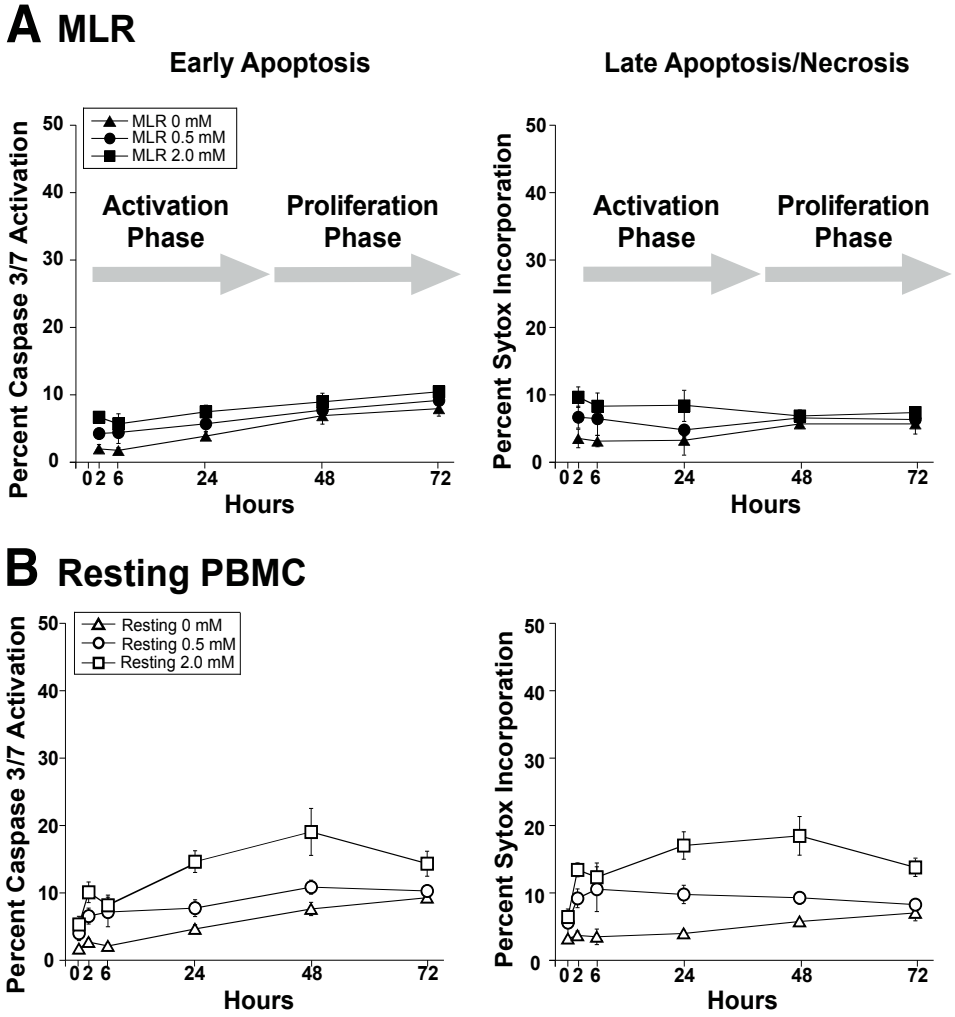

Figure 4.12 The slight increase in cell death of mPEG-modified cells during an MLR was not a consequence of weak costimulatory events, but likely resulted from polymer modification itself. (A) Cell death was slightly increased in mPEG-MLR ≤ 24 (activation phase), but not significantly different from control MLR at > 2 hours (p>0.05). (B) Conversely, unstimulated resting mPEG-PBMC demonstrated a small, but significant increase of both early and late apoptotic markers compared to the resting unmodified control PBMC at ≥ 2 hours. The differences in cell viability between mPEG modified resting cells and mPEG-MLR may be due to the proportion of cells modified. PBMC in the modified resting samples were all modified, whereas in the MLR only one disparate donor population was modified, resulting in only half the total cells with polymer attached. Results are expressed as mean ± SEM (n=3).

The small decrease to the viability of mPEG modified cells observed during an MLR may not be a consequence of weak costimulatory events as previously proposed, but instead a result of polymer modification itself. As shown in **Figure 4.12B**, resting mPEG-PBMC demonstrated a small, but significant increase in both early and late apoptotic markers compared to the resting unmodified control PBMC at ≥ 2 hours. Although, similar to previous viability data (**Figure 3.4**), immediately post modification, polymer modified cells show no significant difference from

controls. The differences in viability between mPEG modified cells during a MLR and modified resting PBMC likely occurred due to the proportion of cells modified. For example, PBMC in the modified resting samples were all modified, whereas in the MLR only one disparate donor population was modified, resulting in only half the total cells with polymer attached.

The differences in viability observed between mPEG-resting PBMC and mPEG-MLR was further investigated by comparing MLRs in which one, or both, populations were PEGylated (20 kDa; 0.5 and 2.0 mM). The results (**Figure 4.13**) suggest that the degree of cell death (caspase activation) is increased in a simply additive manner. For example, MLR in which both populations were modified showed increased apoptosis compared to samples in which only one donor was modified, and caspase activation was not significantly different from the unmodified resting PBMC at corresponding grafting concentrations (**Figure 4.12B**).

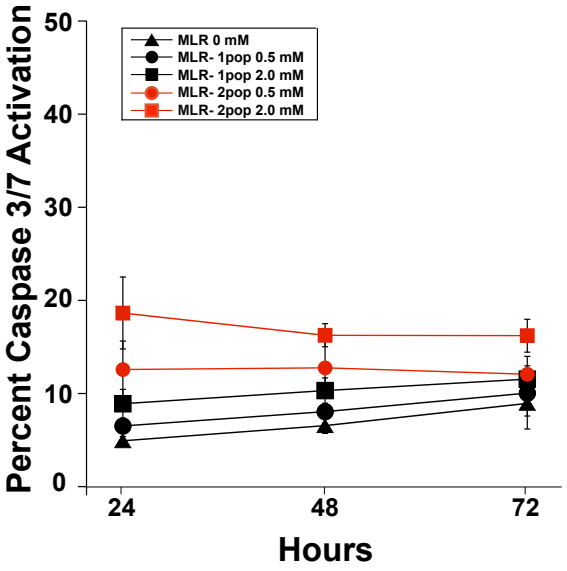

Figure 4.13 The degree of cell death (caspase activation) increased in an additive manner in mPEG-modified cells. MLRs in which both populations were modified (● 0.5 mM, ■ 2.0 mM) showed increased caspase activation compared to samples in which only one donor was modified (● 0.5 mM, ■ 2.0 mM). Caspase activation, when both populations were modified, was not significantly different from the unmodified resting PBMC at corresponding grafting concentrations (**Figure 4.12B**). Results are expressed as mean ± SEM (*n*=3).

In summary, while there was a significant degree of cell death in resting mPEG-PBMC compared to unmodified resting controls, there was no meaningful increase in modified cells during the course of an MLR (activation or proliferation phases) compared to control-MLR. This suggests that cell death may be a result of polymer modification itself, rather than weak interactions between polymer-modified cells. Taking into account the small difference in the extent of apoptotic cells in mPEG modified cells during an MLR (*i.e.*, less than 7% compared to

control cells), apoptosis is not likely a major contributor to the loss of proliferative response seen in mPEG-modified MLRs (**Figure 4.7**). The small loss of cell viability seen in mPEG-modified PBMC may be due to immunocamouflage of surface receptors required for the binding of essential growth factors.

4.7.2 Response of PEGylated Leukocytes to IL2 Stimulation: Effect on IL2 Production, Apoptosis and Proliferation

We next investigated whether growth factor deprivation occurs in highly modified cells, where growth factors and cytokines may be unable to penetrate the PEG layer. IL2 is an important growth factor cytokine, responsible for survival of effector cells and for promoting survival of resting human T cell populations. Consequently, IL2 deprivation can result in the induction of passive cell death by cytokine withdrawal, and upon exogenous IL2 addition has been shown to rescue T cells from apoptosis [230]. To assess if IL2 deprivation may be a contributing factor to the cell death observed in polymer modified resting cells, IL2 production and consumption was examined as well as the ability of exogenously added IL2 to rescue cells from apoptosis and promote cell stimulation (proliferation) in control and mPEG-modified PBMC.

To examine whether IL2 is produced or consumed differently in polymer modified cells compared to control PBMC, an EASIA was done on the supernatant of control and modified resting PBMC, 24 and 48 hours after IL2 media supplementation. As shown in **Figure 4.14A**, no significant differences in endogenous IL2 levels could be detected at 24 or 48 hours of PBMC cell culture. Furthermore, no significant differences could be detected in consumption of exogenously added IL2 (25 U/ml) after 24 or 48 hours. These results may be due to the confounding effects of both consumption and production of IL2 by stimulated cells [231].

To evaluate whether addition of IL2 could rescue polymer-modified cell from apoptosis, both early and late apoptotic events were assessed using high concentrations of IL2 (25 and 250 U/ml) (**Figure 4.14B**). Additionally, to monitor the stimulatory effects of exogenously added

IL2, cell proliferation was monitored on day 6 by CFSE staining (**Figure 4.14C**). High levels of exogenously added IL2 were used, as previous studies have determined that these concentrations may both rescue apoptotic cells as well as stimulate resting cell cultures. This allowed an evaluation, by the degree of proliferation, of the capacity of IL2 to penetrate the PEG layer. Results shown in **Figure 4.14B**, indicated that IL2 may have some inhibitory effects on the degree of cell death in PEGylated cells at very high levels of exogenous IL2 (250 U/ml). However, even at these very high levels of IL2, only a slight decrease in the degree of cell death was detected in modified PBMC, at either 24 or 48 hours. Furthermore, the degree of cell death in polymer-modified cells at high grafting concentrations (2.0 mM) remained significantly increased compared to resting cell controls. The failure to rescue modified cells from cell death and return viability to control cell levels was not due to exclusion of these high levels of IL2 by the mPEG layer, as mPEG-modified PBMC demonstrated a similar degree of proliferation compared to the control PBMC as assessed on day 6 ($p>0.05$) (**Figure 4.14C**). This indicated that the function of IL2 as a survival cytokine/growth factor was not the contributing factor to the small increase in apoptosis seen in polymer modified cells and rather, suggests that a small number of modified cells are likely irreversibly damaged during polymer grafting.

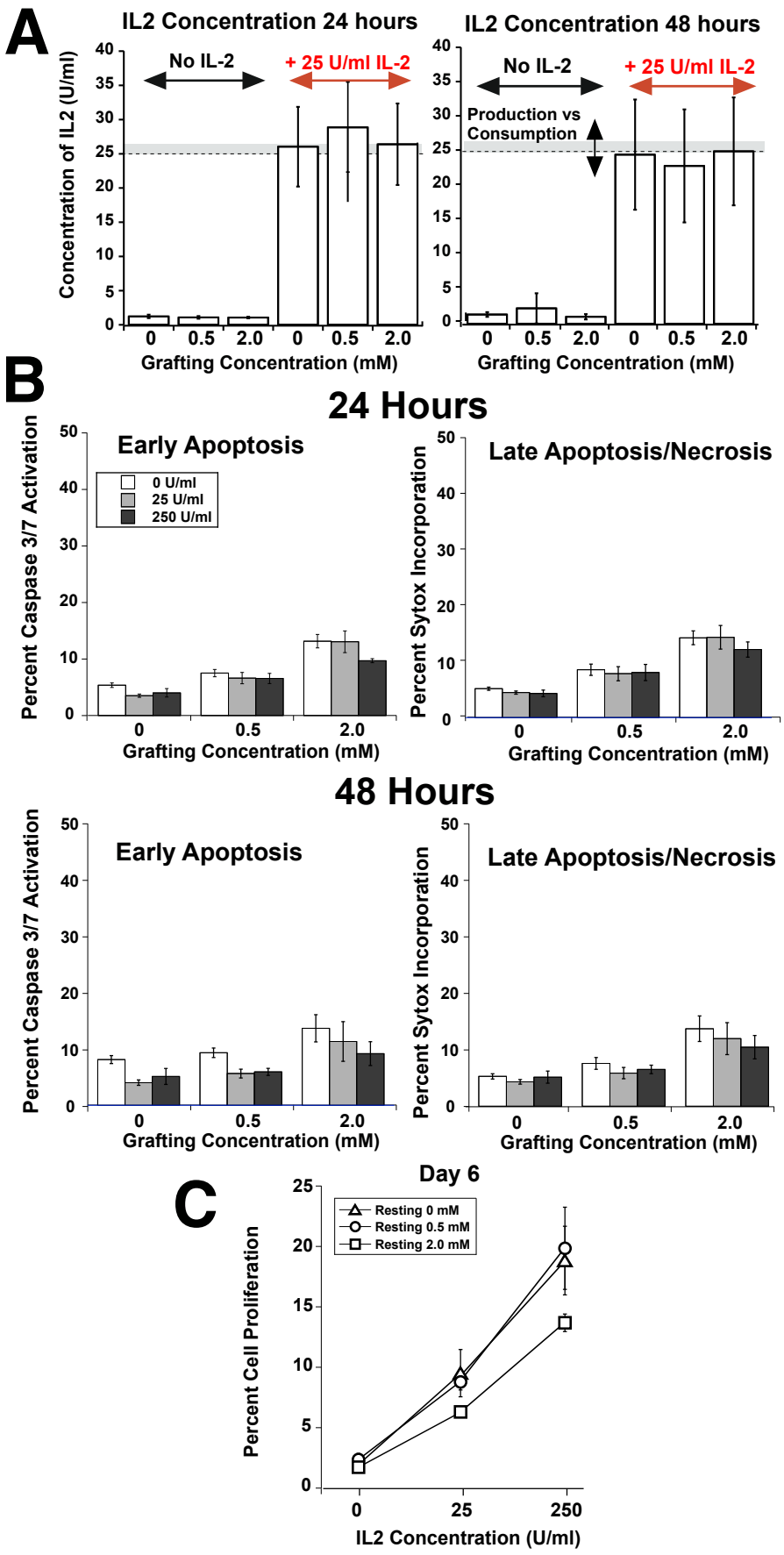

Figure 4.14 IL2 deprivation was not the contributing factor to the small increase in apoptosis observed in polymer-modified cells. (A) No significant differences in endogenous IL2 levels were detected at 24 or 48 hours of PBMC cell culture (± 25 U/ml) after 24 or 48 hours. (B) IL2 may have a slight inhibitory effect on the degree of cell death in PEGylated cells at very high levels of exogenous IL2. However, even at very high levels of IL2 (250 U/ml) only a slight decrease in the degree of cell death was observed in modified PBMC, at either 24 or 48 hours. Furthermore, the increased cell death of polymer-modified cells at high grafting concentrations (2.0 mM) remained significantly increased compared to resting cell controls. (C) The failure to rescue modified cells from cell death and return viability to control cell levels was not due to exclusion of these high levels of IL2 by the mPEG layer, as mPEG-modified PBMC demonstrated a similar degree of proliferation compared to the control PBMC as assessed on day 6 (p>0.05). Results are expressed as mean ± SEM (n=3).

4.8 Conclusion

Studies often involve monitoring late events in T cell activation such as proliferation and cytokine secretion. Although valuable, these studies cannot provide the dynamic information on early T cell activation events. Therefore we sought to evaluate the relationship between surface camouflage, cell-cell interactions, intracellular activation pathway (NFκB), and cell death to the decreased proliferative response seen during allogeneic challenge.

The covalent attachment of mPEG to PBMC resulted in significant immunocamouflage of various surface receptors involved in adhesion, TCR signaling and activation. This suggests that moderate polymer grafting concentrations (≥ 2.0 mM) impart global camouflage effects, rendering modified cells unable to form the cell interactions necessary for activation during allogeneic challenge. This is supported by the dose dependent decrease in proliferation of modified cells during MLRs. Further investigation into the intracellular events of modified PBMC during allogeneic challenge showed that NFκB was downregulated, but not fully abrogated, resulting in the decreased transcriptional regulation of inflammatory cytokines. An important cytokine involved in allorecognition is IL2. mRNA expression studies showed a significant decrease of IL2 in mPEG-MLR compared to control MLR. These results were confirmed in both previous studies and in the decreased expression of the high affinity IL2Rα, which unlike IL2Rβ, is upregulated in response to increased production and consumption of IL2. Furthermore, the decrease in proliferation of modified PBMC during allogeneic challenge was not due to cell death, as no significant loss in cell viability was observed in modified cells over 72 hours of an MLR. Although a small subset of modified PBMC demonstrated loss of viability, this was not attributed to weak signaling events during an MLR or deprivation of survival cytokine IL2, but likely a consequence of irreversible damage to cells during modification. However, this small decrease in viability would not be sufficient to mediate the significant loss in proliferation observed. Thus, immunocamouflage of PBMC creates stealth cells that are prevented from foreign recognition and activation, with minimal effect on cell viability.

5 CHAPTER 5: Discussion

5.1 Overview

For purposes of clarity the discussion is divided into two sections, the effects of polymer species on the efficacy of immunocamouflage, and the consequences of surface modification during allorecognition. In the first section, we compared a traditionally utilized polymer (mPEG), to a novel polymer species (PEOZ), to explore the efficacy of immunocamouflage. The differential effects of mPEG and PEOZ were examined using two cell models (RBC and WBC) to explore the effects of polymer grafting on cell structure, function, viability and allorecognition. Consequent to the polymer comparison studies, we utilized the overall more efficacious mPEG to examine the consequences of surface modification on cell interactions and intracellular events during allorecognition. We examined mPEG-modified cells in terms of changes to cell interactions, intracellular activation pathways (NFκB) and apoptosis during mixed lymphocyte reactions (MLR). The discussion addresses how these events may contribute to the decreased proliferation of leukocytes during allogeneic challenge.

5.2 Comparative Efficacy of Methoxypoly(ethylene glycol) (mPEG) and Polyethyloxazoline (PEOZ) on Red Blood Cell and Leukocyte Modification

The immunocamouflage of cells and tissues by the bioengineering of cell membranes with low-immunogenic polymers may be clinically useful for preventing adverse immunological events. While PEG and PEG-derivatives (e.g., mPEG in particular) have been the gold standard in both the research laboratory and the clinic for several decades, a limited number of studies have indicated that PEG may have some immunological and chemical characteristics that could be improved upon. Therefore, examination of alternative low-immunogenic polymers that exhibit improved clinical utility and/or greater immunocamouflage efficacy is of potential clinical value. To this end, the differential effects of PEOZ relative to mPEG on cell structure, function, viability,

and allorecognition was examined. As demonstrated in these studies, PEOZ shows some strengths and weaknesses relative to mPEG for the immunocamouflage of allogeneic cells.

Although structurally distinct (**Figure 2.1)**, the PEOZ polymer shares many chemical, physical, immunological, and economic characteristics with PEG. Both are relatively simple polymers, easily and cheaply synthesized, are known to be of low immunogenic potential, have large hydrodynamic volumes consequent to intra-chain rotational flexibility, and very low toxicity. Similarly to PEG, PEOZ has historically been synthesized for use as a food and cosmetic additive [150]. In contrast to the hydrophilic and viscous mPEG, PEOZ is characterized by low viscosity and, unlike mPEG, does not form potentially toxic peroxides during storage. From a cellular bioengineering perspective, it was hypothesized that the low viscosity and decreased hydrophilicity of PEOZ could offer some biological and therapeutic advantages; especially at the higher grafting concentrations required for the immunocamouflage of cells and tissues.

Overall, both polymers displayed significant efficacy for the immunocamouflage of RBC and WBC. However, mPEG and PEOZ exhibited differential effects based on the type of cell being modified. While both polymers exhibited very similar immunocamouflage of human PBMC at both the antigenic (CD marker; **Figures 3.7**) and biological efficacy (MLR; **Figure 3.8**) level, RBC grafting demonstrated some polymer-dependent differential effects. Indeed, our results demonstrated that mPEG was more effective for RBC camouflage compared to PEOZ.

The difference in the efficacy of immunocamouflage, relative to cell type, may be related to the membrane protein distribution on RBC and WBC, and the structural differences of polymers. For example, large protein macrocomplexes are found on the RBC membrane, composed of multiple proteins that interact with each other and cytoskeletal components [232]. Conversely, the membrane protein distribution of quiescent lymphocytes are more diffuse, with proteins found as smaller nanoclusters or monomeric proteins. These small protein units diffuse across the membrane forming larger micro-clusters upon antigen stimulation or interactions with APC [233]. Thus, polymers bound to large protein clusters on RBC may ‘self-exclude’ additional

polymer attachment due to steric hindrance in these protein dense domains. Therefore, the camouflage of RhD and Kell antigens found in these large complexes could be more dependent on indirect coverage, compared to the modification of more diffuse protein structures such as CD4, CD28 and the TCR (CD3).

Due to the dense protein distribution of RBC complexes, camouflage efficacy would be influenced by the polymer's ability to impart indirect camouflage to neighboring proteins. The Flory radius (R_F) influences the efficacy of indirect camouflage, which is a function of both polymer length and flexibility. While the grafting efficacy of PEOZ and mPEG to RBC were similar (**Figure 3.1**), though mPEG showed improved grafting at lower concentrations, differences between polymer species may be a consequence of the slightly decreased rotational capabilities of PEOZ compared to mPEG. The smaller intra-chain rotational flexibility of PEOZ, due to the side chain moiety (**Figure 2.1**), may decrease the degree of indirect camouflage, essential for the protein dense macroclusters on the RBC. This is supported by studies using branched polymers that show decreased camouflage efficacy compared to more highly flexible linear polymers [156].

Our RBC data further demonstrated the differential effects of direct and indirect immunocamouflage of antigenic sites. Based on the linker chemistries used in the activated mPEG and PEOZ, external lysine residues were targeted for the covalent grafting of the polymer. As shown in **Figure 5.1A**, the RhD carrier protein is lysine poor containing only 3 potential lysine targets per molecule with 2 of the residues being present at the protein-lipid bilayer interface. The scarcity of lysine residues makes the direct immunocamouflage of the RhD protein virtually impossible to achieve when viewed in the context of the radius of gyration (R_F: Flory Radius) of grafted polymers [234-236]. However, as shown experimentally in this study, grafted polymers did significantly attenuate both flow cytometric (**Figure 3.5**) and biologic (MMA; **Figure 3.6**) immunological recognition of RhD^+-RBC. This demonstrates that indirect immunocamouflage plays a critical role in preventing the detection of RhD (as well as other

blood group antigens, leukocyte cluster of differentiation). In contrast to RhD, the Kell carrier protein contains 20 external lysine residues, many in very close proximity to multiple Kell blood group antigens (including *k* used in this study), making it more likely to be directly modified by the added polymers (**Figure 5.1B**). Indeed, as shown in **Figure 3.5**, polymers exhibited superior immunocamouflage of kell relative to RhD at equivalent polymer grafting concentrations. Shown in **Figure 5.1B** are the theoretical effects of alloantibody (as exemplified by Kp^{a-c} and the K/k antigens; arrows) binding to the Kell protein consequent to the direct grafting of increasing concentrations of 2, 5 or 20 kDa polymers (increased polymer concentration are noted by dashed circles; **Figure 5.1c-f**) to an unfolded protein chain. Although, the unfolded Kell protein model is biologically unrealistic in that not all lysines would be available for grafting in a folded state (globular structure shown in **Figure 5.1B**), nor does it take into account that proteins rarely exist in an isolated form on the cell surface.

Considering the topography of RBC protein complexes, not all proteins would be equally accessible to the activated polymer as schematically illustrated in **Figure 5.1C**. For example, the lysine-poor RhD is buried within RBC complexes while the lysine-rich Kell protein is more accessible to the activated polymer. These data support the contention that indirect immunocamouflage maybe a critical mechanism for many blood group antigens (or clusters of differentiation). Our RhD data suggests that this is the case and that polymers grafted to topologically superior proteins on the RBC (e.g*.,* CD47, ICAM4, Kell, glycophorin A/B) may prevent immunological recognition of RhD in the MMA. This is also supported by CD3 immunocamouflage, based on the proximity to the membrane, the low number of lysine residues, and the size dependent camouflage efficacy demonstrated by our data, all suggests that polymer attachment to the TCR results in indirect immunocamouflage of CD3.

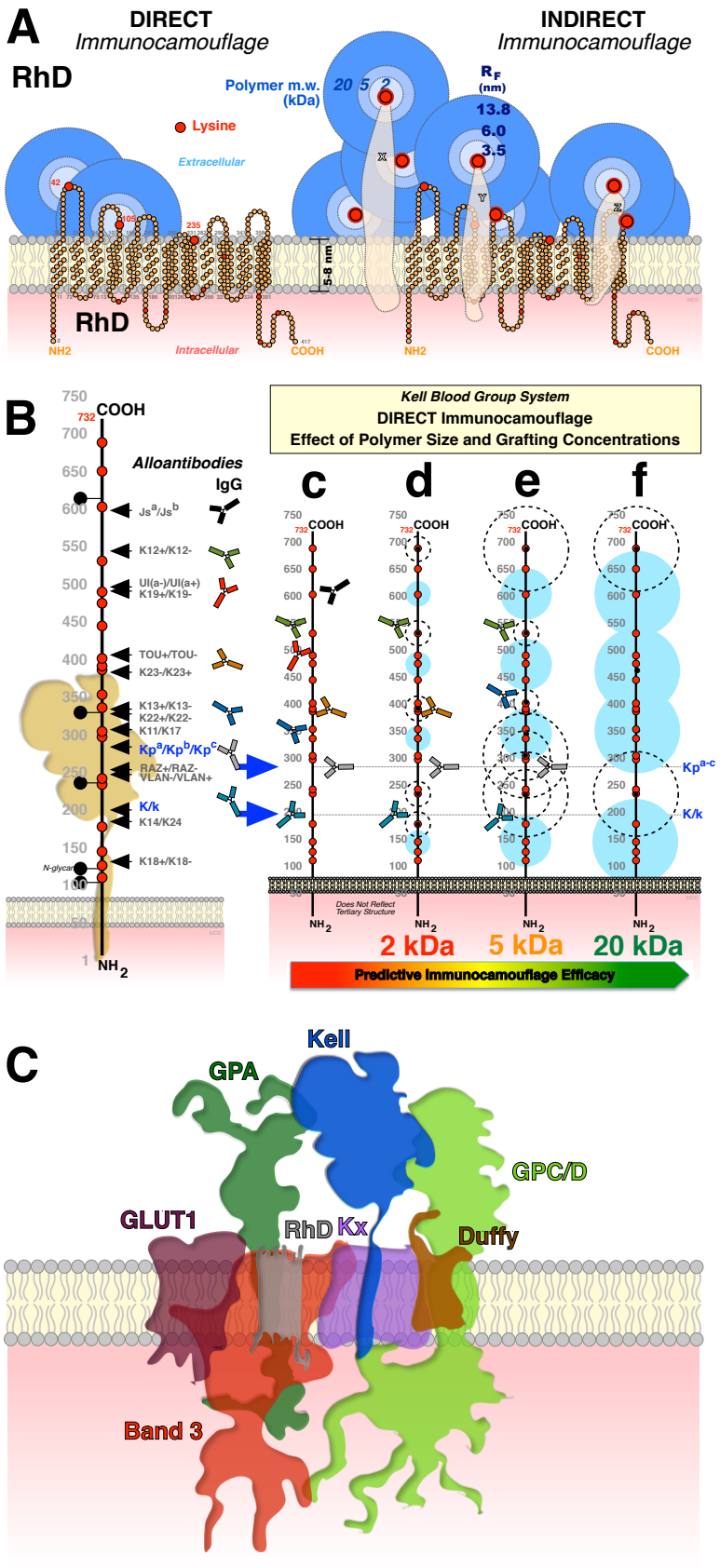

Figure 5.1 Immunocamouflage of membrane proteins occurs *via* both direct and indirect camouflage. (A) Direct polymer grafting to RhD would provide modest camouflage. Only 2-3 available lysine sites are on the exterior face of the protein and reside very close to the membrane surface, making RhD less susceptible to direct polymer modification. However, other proteins may serve as binding sites for the activated polymers, leading to indirect immunocamouflage. The circles shown bound to protein lysine residues illustrate the Flory radii of the covalently bound polymers. The R_F (in nm) values for 2, 5 and 20 kDa polymers are also shown. Lysine residues of RhD are noted in red. (B) The Kell protein contains 20 exterior lysine residues (noted in red), many in very close proximity to specific Kell blood group antigens. Shown (c-f) are the theoretical effects of the direct grafting of 2, 5 and 20 kDa polymers (increasing concentration are denoted by dashed circles) on alloantibody binding to the Kell protein. Approximate protein folding is also illustrated. (C) While most commonly studied as simple, isolated protein structures; membrane proteins on cells exist as complexes. This is readily observed on RBC. Not all proteins in the complex topology will be equally accessible to the activated polymer (e.g., RhD is buried in the complex unlike Kell). Thus, indirect immunocamouflage may be more critical for many blood group proteins. Modified from Kyluik-Price 2014 [148].

Complex modeled on: Mankelow et al. *Blood Cells, Molecules, and Diseases.* 2012;49:1–10.

Conversely, the structural and chemical attributes of PEOZ relative to mPEG, may confer some biomechanical benefits. For example, at high polymer concentrations, the 20 and 30 kDa mPEG-modified RBC exhibited some RBC morphological changes, in agreement with previous studies using mPEG [136], not observed in the PEOZ-RBC (**Figure 3.2**). Indeed, consequent to the hydrophilicity and viscosity of the grafted mPEG, mechanical instability could arise in the modified RBC due to changes in fluid transport (*i.e.*, water balance and lipid bilayer microenvironment dehydration) and membrane dynamics (e.g*.,* lipid and protein raft movements, protein-protein interactions). Importantly however, murine studies demonstrate that the 20 kDa mPEG modified RBC (2.0 mM grafting concentration) show normal *in vivo* circulation even after repeated transfusions (**Figure 1.9**) [136,198]. These transient hydrodynamic changes could also underlie some of the molecular weight (*i.e.,* 20 *vs* 30 kDa) and polymer species disparities seen between mPEG and PEOZ for the immunocamouflage of RhD and Kell proteins (**Figure 3.5**). For example, morphological aberrations observed at high grafting concentrations of the 30 kDa could expose antigenic sites of the protein and result in increased antibody binding.

As shown in the MMA using IgG-opsonized RhD^+ RBC, mPEG confers significantly superior biological immunocamouflage (**Figure 3.6**). While it is important to note that direct antibody binding does not always correlate with immunological recognition, a good correlation did exist between the direct antibody detection of RhD and protection from phagocytosis of RhD^+ cells in the MMA (**Figures 3.5** and **3.6**). Moreover, to achieve this biological immunocamouflage, it is not necessary for the grafted mPEG to fully camouflage RhD from antibody binding. As assessed *via* flow cytometry, PPC measurements indicated that a small percentage of cells remained RhD positive, however, MCF data showed that cells had relatively low amounts of bound antibody. Indeed, studies suggest that there is a relationship between the quantity of antibody bound and RBC clearance [237,238]**.** Furthermore, studies have clearly documented that significant numbers of normal human RBC have bound antibodies, but this

does not appear to effect *in vivo* viability, suggesting that a *'threshold'* effect for immune recognition may exist [239]. This threshold effect may be critical, as unlike other non-primate RBC, the human RBC is a critical component in the trafficking and removal of immune complexes *via* the complement receptor 1 (CR1) on the RBC membrane [240,241]. The biological viability of antibody-positive RBC also arises from the fact that the majority of IgG alloantibodies are not complement fixing thus do not cause direct lysis of the RBC (**Table 1.3**). Hence biological allorecognition, as measured by the MMA, may be a better determinant of the utility of grafted polymers to mediate effective immunocamouflage of an allogeneic cell. Consequent to the MMA findings, mPEG appears to be vastly superior to PEOZ for the immunocamouflage of RBC. This may result from the greatly enhanced charge and steric camouflage of the heavily hydrated and flexible mPEG polymer [156] relative to PEOZ.

5.3 Summary of Discussion on Comparative Efficacy of mPEG and PEOZ

Polyoxazolines (e.g., PEOZ) mediate significant immunocamouflage of both human RBC and leukocytes (PBMC). However, phagocytic recognition (MMA) studies demonstrated that mPEG was vastly superior to PEOZ in preventing immune recognition and phagocytosis of anti-RhD opsonized RhD^{+}RBC. Conversely, both polymers very effectively prevented leukocyte allorecognition. Furthermore, the role of polymers in the direct and indirect immunocamouflage of cells suggests that indirect camouflage (steric and charge camouflage of unmodified antigenic sites) may be more critical than the direct modification of an antigenic site. However, PEOZ may be a useful addition to the repertoire of polymers (e.g., mPEG and HPG) that can be used for the immunocamouflage of allogeneic cells in transfusion and transplantation medicine. Moreover, in the small subset of patients who exhibit anti-PEG antibodies, PEOZ-modified cells (or proteins) could prove to be a highly useful alternative.

5.4 The Effect of Methoxypoly(ethylene glycol) Grafting During Allogeneic Challenge

While our polymer comparison studies demonstrated the immunocamouflage potential of PEOZ, the RBC MMA data indicated that PEOZ was significantly less effective than mPEG for preventing allorecognition. Therefore, the remainder of the thesis focused on mPEG in order to fully explore the effects of surface immunocamouflage on downstream cellular events during allorecognition. Using various polymer sizes and grafting concentrations of mPEG to modify human PBMC, extensive studies were conducted to determine the efficacy of global cell surface camouflage, focusing on a number of receptors involved in cell adhesion, T cell receptor signaling, as well as activation and proliferation. The surface CD markers examined, consisted of proteins of various heights, differing numbers of modifiable lysine residues, as well as proteins found either in multi-protein complexes or as isolated entities on the membrane.

The results demonstrated a very effective camouflage of all surface proteins, which increased with grafting concentration and polymer size (**Figure 4.1-4.3)**. The size dependent nature of immunocamouflage was due to the decreased Flory radius of small polymers compared to longer polymers. The longer polymers provided increased surface area coverage compared to shorter chains, resulting in improved exclusion of antibodies using the longer polymers even if the lysine-binding site of the polymer was distant from the antibody-binding site.

The size dependent nature of immunocamouflage was also a function of protein topography, which was consistent with previous data [137,156]. For example, CD4, CD11a, CD28, CD62L, and CD71 have large extracellular domains with multiple lysine residues capable of polymer attachment, whereas CD3 has a relatively short extracellular domain and few lysine residues. However, the results indicated that even CD3 demonstrated polymer size dependency (**Figure 4.2)**. This may be due to the close association of CD3 with the TCR (approximately 7

nm in height), leading to indirect camouflage of CD3 *via* the taller TCR [156]. This indirect camouflage may occur in a manner similar to RhD proteins discussed previously. The lack of indirect camouflage may also be responsible for the relatively small decrease observed for the immunocamouflage of CD71 (**Figure 4.3)**. CD71 is generally excluded from lipid rafts containing protein micro-domains, and often occur as randomly organized components on the membrane [218-220]. Thus, the efficacy of surface coverage would be more dependent on the location of the lysine-binding site in relation to the antibody-binding site, with little additional surface camouflage provided by the attachment of polymers to nearby proteins. However, for most proteins modified at higher grafting concentrations, the size dependent nature of immunocamouflage was less significant. This may be due to the additional attachment of short chain polymers on or near the antibody-binding site.

The modification of PBMC with mPEG demonstrated a global camouflage of cell surfaces that was proficient in obscuring topographically complex and protein dense cell surfaces. Previous biophysical studies indicate that surface camouflage is achieved through both charge and steric camouflage of cell surfaces owing to the large hydrodynamic shielding capability of the neutral water binding PEG, as well as steric repulsion governed by the polymer occupying a large 3D surface area [141,156]. Thus, the attachment of polymers to surface proteins results in the exclusion of immune components (as shown by inhibition of antibody binding) (**Figure 4.1-4.3**) [156,242]; viruses [141]; and RBC, as shown previously by decreased RBC rouleaux formation [195]. Moreover, our studies showed decreased recognition of allogeneic cells, demonstrated in both the RBC model (MMA**; Figure 3.6**) and leukocyte model (cell conjugates; **Figure 4.4-4.6**, MLR**; Figure 4.7**).

The interaction of cells with allogeneic immune components (i.e., receptor-ligand, antibodies) is not the only factor that influences leukocyte activation. As shown schematically in **Figure 5.2A**, the protein distribution on quiescent lymphocyte membranes take the form of small nanoclusters or monomers. During cell conjugation and cell activation events, surface receptors

often form complexes, coming together to form larger micro-domains that add to the strength and extent of cell contacts, thereby increasing signaling intensity and duration [233,243] (**Figure 5.2B**). Efficient TCR signaling often involves the clustering of CD3, CD4, and CD28, as well as adhesion molecules (*i.e.,* CD11a) [244,245]. For example, studies have shown that prevention of micro-cluster formation leads to reduced contact times between APC and lymphocytes, decreased activation signals, and decreased IL2 production [246,247]. Thus, surface camouflage prevents the approach of cells bearing receptors and ligands **(Figure 5.2C-a)**, but would also inhibit the formation of clustered micro-domains due to both steric and charge camouflage exerted by polymers when bound to surface proteins **(Figure 5.2C-b)**. Therefore, disturbances of both 'vertical' (the approach of immune cells and components) and 'horizontal' (protein-protein interactions on the membrane) interactions would likely both contribute to the decreased cell contacts, activation signaling (NFκB), IL2 production, and proliferation during an MLR observed in our studies. Disturbances in the horizontal interactions of skeletal or membrane proteins may also lead to instability and alterations to RBC membrane morphology. Indeed, as demonstrated by Bradley *et al*, polymer grafting interfered with the lateral mobility of the complement binding receptor (CR1), preventing CR1 capping and complex binding [240]. This 'horizontal' hindrance may also be supported in part by RBC morphology studies done in Chapter 3. Protein interactions would likely be disrupted to a greater extent with longer polymers than with short chain polymers. As shown in **Figure 3.2**, longer chain polymers demonstrated increased morphological aberrations compared to short chain polymers at high grafting concentrations.

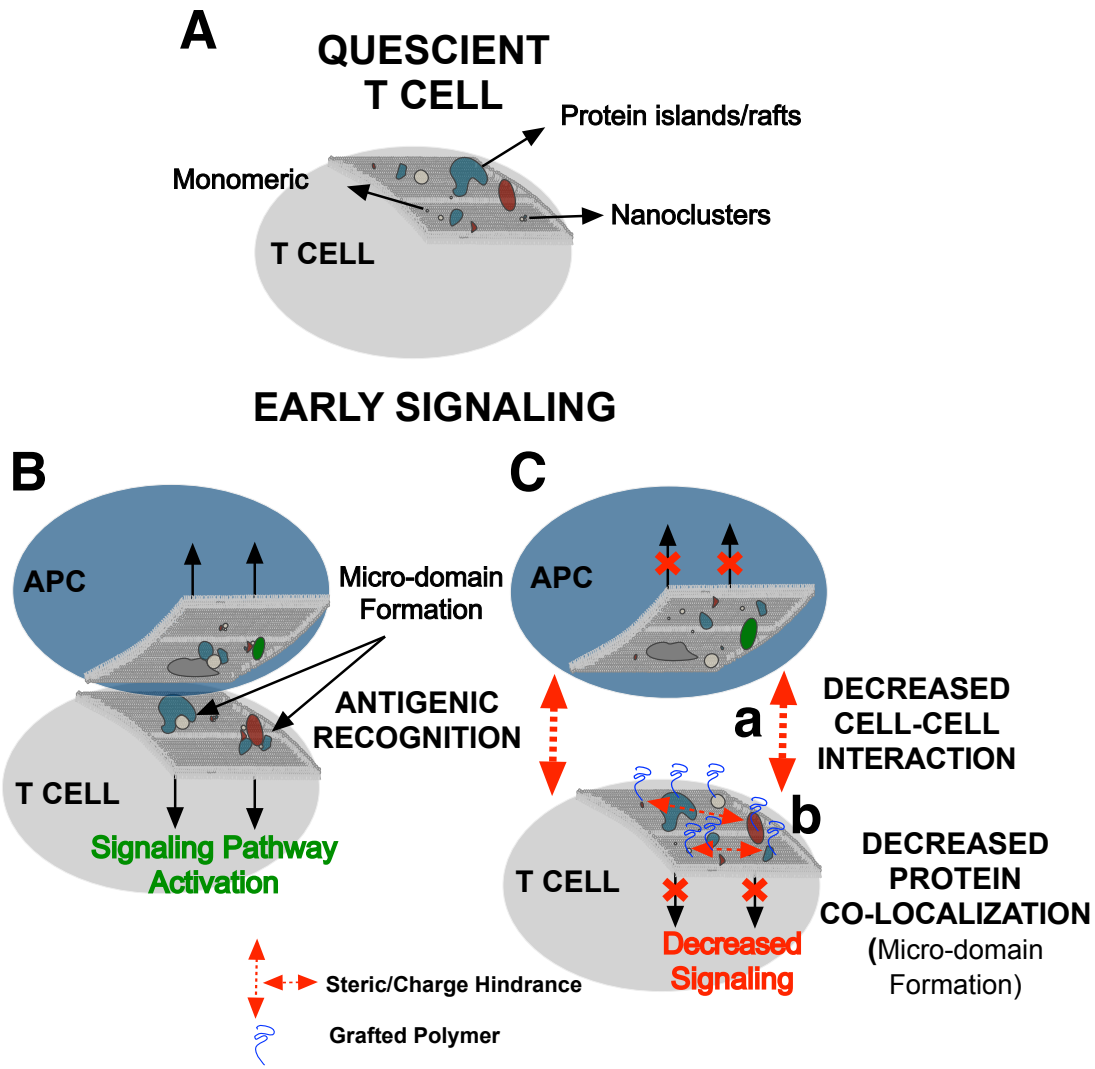

Figure 5.2 Protein distribution during cell activation. (A) Quiescent cells have surface proteins consisting of segregated protein islands, nanoscale clusters or monomers. (B) Upon antigen recognition, reorganization of signaling proteins takes place, which often involves assembly of multi-protein signaling complexes. (C) The attachment of polymers to cell surfaces prevents signaling and proliferation during allogeneic challenge due to steric hindrance and charge camouflage of receptor-ligand interactions and prevents cell approach. Additionally, steric and charge camouflage by polymers may also sustain the segregation of signaling proteins into distinct components, preventing the formation of protein signaling complexes necessary for cell activation. Lymphocyte protein distribution modeled on Klammt 2012 [248] and Lillemeier 2010 [233].

Upon examining conjugation events between APC and lymphocytes, results demonstrated a significant dose dependent inhibition of prolonged cell contacts during allorecognition (**Figure 4.6)**. Surprisingly, the short chain polymers were as effective as the long chain polymers for preventing cell conjugation as assessed by flow cytometry. This is contrary to results showing decreased immunocamouflage of surface proteins by short chain polymers

(**Figure 4.1-4.3)**, and to previous MLR data showing that short chain polymers were less effective for preventing proliferation than long chain polymers [156,242]. While our model focused on prolonged or static contacts between cells at certain timepoints during allorecognition, several studies have shown that prolonged cell interactions, and decreased cell mobility, may not always be necessary to achieve lymphocyte activation both *in vitro* [221,222,249] and *in vivo* [72]. In these studies, short-lived interactions with APC resulted in the expression of activation markers on T cells, suggesting that TCR signaling was occurring. Thus, the decreased number of prolonged cell contacts observed may not be solely indicative of cell signaling abrogation. Indeed, this suggests that short chain polymers may not effectively prevent transient interactions. As shown in **Figure 5.3**, the decreased camouflage of surface protein receptors, when modified with small polymers (**Figure 5.3B)**, may allow transient interactions between cells, resulting in proliferation during the MLR. The long chain polymers, shown to effectively camouflage cell surfaces, may lead to reduced transient interactions and decreased proliferation observed during the MLR (**Figure 5.3C**).

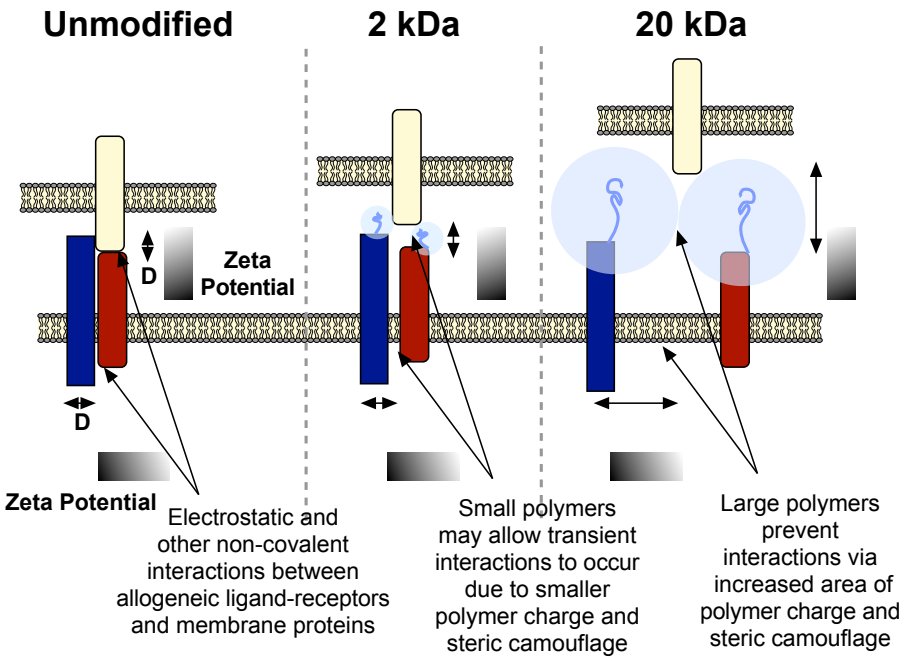

Figure 5.3 mPEG modification of cell surfaces camouflages the charge of proteins and sterically inhibits protein interactions. (A) Protein-protein interactions are a result of non-covalent interactions, forming contacts between both receptor-ligand (between cells) and protein interactions on the membrane. (B) Short polymers may not prevent transient interactions, compared to longer polymers (C) due to increased Flory radius of longer polymers, resulting in surface extension of the zeta potential and hydrodynamic shielding. D=distance.

MLR studies showed that even with long chain polymers, cell-cell interactions, NFκB signaling, and proliferation, were not completely abrogated compared to resting PBMC (**Figure 4.8**). However, mRNA profiles did indicate that both inflammatory and growth cytokines were decreased at ≥ 6 hours during modified-MLR compared to control-MLR. While only a few genes were significantly different, possibly due to the variation in the intensity of allogeneic responses (1-10% of cells respond depending on the disparate donor MHC mismatches) [250], IL2 was consistently and significantly downregulated at both 6 and 24 hours in the modified-MLR (**Figure 4.9)**. Since IL2 is produced almost exclusively by T cells in response to antigenic stimulation, the observed decrease of IL2 in the mPEG-MLR is an important indicator of decreased T cell activation during allogeneic challenge. The decreased mRNA regulation of IL2 demonstrated in this thesis is supported by previous data showing a significant decrease in IL2 release during mPEG-MLR compared to controls [190]. Furthermore, western blot analysis of the expression of IL2Rα, a receptor upregulated during inflammation and in response to IL2, was significantly decreased in mPEG-MLR compared to control-MLR. Moreover, in mPEG-MLRs IL2Rα was not significantly different from resting PBMC populations at all timepoints assessed (**Figure 4.10A)**. The regulated expression of IL2Rα in response to IL2 is supported by several studies showing that TCR ligation triggers the transcription of genes, including both IL2 and IL2Rα [251,252], and that decreased IL2Rα expression is correlated with decreased lymphocyte proliferation [253].

Furthermore, the significant decrease in the proliferation of modified PBMC during a MLR was not due to cell death, as no significant increase was observed in modified cells over 72 hours of an MLR. Although a very small subset of modified cells demonstrated a loss in viability, this was not attributed to weak signaling events during an MLR, or deprivation of survival cytokines (IL2), but likely a consequence of irreversible damage to cells during modification. We propose that this decrease in cell viability would not be a major contributor to the significant loss in proliferation observed during an MLR, and this is based on several

assumptions. Firstly, the small (< 7%) loss of viability compared to the control MLRs is not large enough to produce the significant decrease in proliferation seen in mPEG-MLRs. Secondly, during a two-way MLR, non-viable cells are still able to act as stimulator cells. Indeed, one-way MLRs used to assess MHC disparity are done where one population is irradiated.

Our results showed that modification of cells with polymers led to a global camouflage of cell surfaces, which resulted in decreased activation and proliferation upon allogeneic challenge. We investigated NFκB because of its role in T cell receptor signaling, and its importance in transducing signals *via* environmental stimuli (cytokines and nutrients). Thus, NFκB is an important pathway for both cell activation and survival. Although other pathways were not specifically assessed in this thesis, the transcription of many cytokines that were downregulated in the mRNA analysis, including IL2, are also controlled by other major pathways [254]. For example, as discussed in the Introduction, the regulation of IL2 is controlled by several transcription factors such as AP-1 and NFAT, in addition to NFκB (**Figure 1.4**). Thus, the coordination of several pathways contributes to the activation threshold of the cell, which would ultimately determine the degree of IL2 release. Therefore, the global camouflage of cell surfaces would likely affect several activation pathways, making it a viable alternative to the singular blockade of activation pathways by current immunosuppressive drugs (**Figure 5.4)**. Indeed, the use of singular IL2 pathway blocking agents has been shown to reduce acute rejection and improve short-term graft survival, but exhibit acute kidney toxicities and fail to prevent chronic rejection [255]. Additionally, therapies blocking adhesion or costimulatory receptors are often inadequate alone, due to the redundancy of these pathways. Therefore, combination therapy is often utilized. Although some combinations have shown a synergistic effect, certain drug combinations show no improvement, or even contradict each other [256,257]. Furthermore, most currently utilized drugs and combinations thereof elicit serious side effects and may increase rates of infections and malignancies**.** Thus, the global camouflage of allogeneic cell surfaces *via* polymer modification may be a viable and non-toxic therapeutic

strategy for transfusion and transplantation medicine, preventing allorecognition through the inhibition of adhesion, costimulation, recognition and activation pathways as shown in **Figure 5.4**.

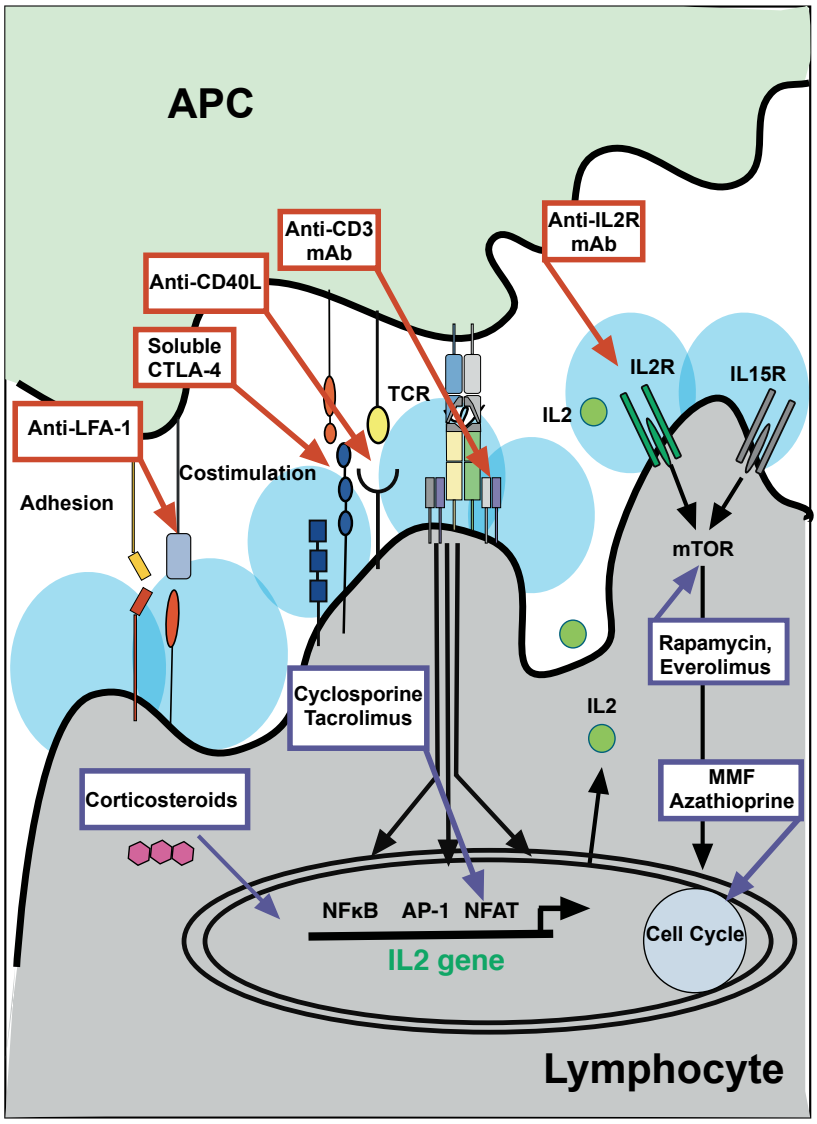

Figure 5.4 Global camouflage of surface proteins may be a viable therapeutic alternative to the singular blockade of stimulatory pathways and receptors. Current immunosuppressive drugs specifically target individual surface receptors (red box) or broadly prevent late stages of T cell activation (purple box). Conversely, the global camouflage of cell proteins (shaded blue areas) inhibits cell interactions, cell adhesion, antigen recognition and costimulation necessary for cell signaling and activation. This may be of significance for therapeutic purposes, as the biological redundancy of surface adhesion, costimulatory and growth receptors inhibit the long-term efficacy of many drugs, which are specific to one receptor or specific pathway. This approach would prevent systemic cytotoxic events and may enhance allospecific tolerance.

5.5 Summary of Discussion on mPEG Grafting During Allogeneic Challenge

Significant global immunocamouflage of surface proteins was achieved by the covalent attachment of polymers to PBMC. Overall, longer polymers resulted in improved inhibition of antibody binding compared to short chain polymers. Moreover, the efficacy of immunocamouflage was governed by the topography of surface proteins, the number of lysine

residues, the location of antibody binding sites as well as the degree of direct and indirect surface camouflage.

In addition to the exclusion of antibodies, our results demonstrated a significant polymer mediated exclusion of cells, as shown by the decreased conjugation events between allogeneic cells. The exclusion of allogeneic APC was likely a result of polymer mediated 'vertical' and 'horizontal' hindrance of protein interactions. However, contrary to our cell conjugation studies, polymer size dependent proliferation was observed in previous MLR studies, suggesting that transient interactions may be occurring to a greater extent in cells modified with short chain polymers. Our results demonstrated decreased pathway activation (NFκB), inflammatory cytokine release (IL2) and receptor expression (IL2Rα), leading to reduced cell proliferation (MLR), using the 20 kDa mPEG polymer.

Furthermore, while cell viability studies demonstrated a small degree of cell death in polymer modified cells, this was not a consequence of weak signaling events during an MLR or deprivation of survival cues, but likely a consequence of cell damage during modification. However, the slight decrease in cell viability would not be sufficient to explain the significant decrease observed during MLR. Rather, the global camouflage of surface proteins likely results in decreased activation of numerous pathways responsible for cell proliferation, making PEGylation a viable non-toxic alternative to current immunosuppressive therapies.

5.6 Future Directions

Future PEGylation studies should be aimed at the clinical applications of polymer technology for prevention of allorecognition in transfusion and transplantation. The preliminary structural and functional studies, which assessed the use of a potential novel polymer PEOZ *in vitro,* could be further characterized *in vivo* to bring about a more fulsome analysis of its potential applications. While, *in vivo* studies have been done showing that PEOZ exhibits low toxicity and decreased tendency to elicit anti-polymer antibodies [150,258], experiments to

explore the efficacy and survival of PEOZ-modified cells in a PEG-sensitized animal model would be beneficial. Indeed, the use of this novel polymer may be especially valuable for patients with anti-PEG antibodies.

Furthermore, we utilized the MMA to assess the polymer-mediated prevention of phagocytosis using opsonized RhD+ RBC with commercial antibody. However, ongoing work is being done using the MMA to determine the efficacy of immunocamouflage on additional non-ABO antigens, using alloantibodies from patient serum. This is important to predictably map the efficacy of immunocamouflage for non-ABO antigens. Similarly, this could be applied to allogeneic immunized transplant patients. Antibodies to HLA in transplant patients have been shown to be composed of multiple isotypes and have the ability to fix complement [259]. Thus, the efficacy of polymers to prevent antibody binding to allogeneic tissues using alloimmunized transplant patient serum, could be used to explore the efficacy of immunocamouflage in a more biologically relevant context.

The use of mPEG-modified leukocytes to prevent allorecognition and induce tolerance is based on results indicating a decreased inflammatory milieu and decreased proliferative response. However, previous studies (both *in vitro* and *in vivo*) also demonstrated altered cell differentiation during mPEG-MLRs [190]. Cell differentiation studies would be important for the translation of polymer-modified leukocytes into therapeutic tools to induce transplantation tolerance. Further investigation of intracellular pathways that are more specifically involved in cell differentiation, such a mechanistic target of rapamycin (mTOR) pathway, may be beneficial. Recently, it has been shown that (mTOR) pathway has a critical role in determining the outcome of TCR recognition. mTOR is important for the coordination of extracellular cues (cytokines, ligand-receptor interactions and nutrients) that promote and guide the outcome of antigen recognition. Studies show that absence of mTOR signaling leads to the generation of Treg cells [260,261]. This pathway may be important to further define the effects of polymer modification for prevention of allorecognition, as previous studies demonstrated increased Treg generation

during mPEG-MLRs both *in vitro* and *in vivo* [190]. An increased understanding of the molecular mechanisms of the mPEG induced immunotolerant state is important for the development of novel polymer therapeutics.

Indeed, developing therapies to induce donor specific tolerance to foreign tissues would reduce the need for broad and generalized immunosuppression and the associated toxic side effects of currently utilized therapeutics. Cell-based therapies can be used to deliver antigens with regulatory signals to reduce the immune response and elicit antigen specific tolerance. This may be effective therapy for preventing both acute and chronic rejection, unlike current immunotherapies. Previous research has shown that the transfusion of polymer modified murine splenocytes decreased the induction of inflammatory cytokine and cells (*i.e.,* Th17) while increasing suppressive cells (*i.e.,* Treg). Furthermore, these immunomodulatory effects were long-lived and were sustained even upon rechallenge with unmodified splenocytes [190]. It would be valuable to assess the efficacy of modified allogeneic splenocytes for the prevention of transplant rejection and further studies could be employed to assess the use of polymers for the prevention/treatment of allograft rejection. For example, studies consisting of injections of mPEG-modified haplotype-mismatched splenocytes prior to transplantation (such as skin or cardiac allografts) in a murine model, may determine whether rejection could be prevented or delayed. These studies could be done using various polymer lengths and concentrations as well as using both long and short course treatment regimes with polymer modified splenocytes. Moreover, additional studies could be done to examine the antigen specificity of polymer modified cell therapies. For example, subsequent to injection of polymer modified allogeneic splenocytes, injections of unmodified splenocytes consisting of a third murine haplotype could be utilized to assess the specificity of polymer-induced tolerance.

5.7 Conclusions and Overall Significance

The structural and functional characterization of a novel polymer species showed that PEOZ mediated significant immunocamouflage of both RBC and leukocytes in a similar manner to grafted mPEG. For polymer comparison studies, it was our hypothesis that owing to the structural and chemical attributes inherent to PEOZ that this polymer may result in improved immunocamouflage utility. Preliminary structural and functional studies showed that PEOZ demonstrated some improved utility, in regards to morphological studies, although mPEG did show improved efficacy in RBC allorecognition studies. PEOZ, however, would be a useful addition to the repertoire of polymers for the immunocamouflage of cells, especially for a subset of patients that may exhibit anti-PEG antibodies.

Moreover, the analysis of initial cell events during allorecognition in polymer modified leukocytes helped to define the mechanisms of cell surface immunocamouflage and how it was related to the decrease proliferation and immunotolerance observed during allogeneic challenge. In support of our hypothesis, it was shown that surface immunocamouflage was dose dependent and was more effective using longer chain polymers. Furthermore, immunocamouflage of surface proteins led to significantly decreased prolonged cell interactions. It was also demonstrated that an important pathway during allorecognition (NFκB) was decreased in polymer-modified cells during an MLR. Although NFκB was not completely abrogated, both IL2 production and high affinity receptor (IL2Rα) were significantly downregulated, indicating a decrease in TCR signaling. Since optimal IL2 production is the result of coordinated pathway expression and nonspecific global camouflage of cells by polymer grafting, this likely prevents several activation pathways. Immunocamouflage may be of significance for therapeutic purposes as the biological redundancy of surface adhesion, costimulatory and growth receptors inhibit the long-term efficacy of many drugs, which are often specific to one receptor or one specific pathway. In addition, the prevention of allorecognition by

inhibition of cell interactions or binding of immune components may be superior to the majority of current immunosuppressants that target downstream events such as T cell activation and proliferation. This approach would prevent systemic cytotoxic events and may enhance allospecific tolerance.

These findings demonstrated the therapeutic potential of both traditional mPEG and novel polymer alternatives. Furthermore, this work defined several mechanisms responsible for the decreased alloresponse of immunocamouflaged cells. Our results showed the clear potential for polymer-based bioengineering to modulate the immune response to allogeneic cells and would be useful for the prevention of allorecognition in transplantation and transfusion medicine.

Bibliography

[1] Azizi M-H, Nayernouri T, Azizi F. A brief history of the discovery of the circulation of blood in the human body. Arch Iran Med 2008;11:345–50.

[2] Ribatti D. William Harvey and the discovery of the circulation of the blood. J Angiogenes Res 2009;1:3.

[3] Tubbs RS, Loukas M, Shoja MM, Ardalan MR, Oakes WJ. Richard Lower (1631–1691) and his early contributions to cardiology. Int J Cardiol 2008;128:17–21.

[4] Fastag E, Varon J, Sternbach G. Richard lower: the origins of blood transfusion. J Emerg Med 2013;44:1146–50.

[5] Giangrande PL. The history of blood transfusion. Br J Haematol 2000;110:758–67.

[6] Learoyd P. The history of blood transfusion prior to the 20th century--part 1. Transfusion Med 2012;22:308–14.

[7] Baskett TF. James Blundell: the first transfusion of human blood. Resuscitation 2002;52:229–33.

[8] Blundell J. Experiments on the transfusion of blood by the syringe. Medico-Chirurgical Transactions 1818;9:56–92.

[9] Landsteiner K. On agglutination of normal human blood. Transfusion 1961;1:5–8.

[10] Hektoen L. Isoagglutination of human corpuscles. J Infect Dis 1907;48:1739–40.

[11] Ottenberg R. Studies in Isoagglutination : I. Transfusion and the question of intravascular agglutination. J Exp Med 1911;13:425–38.

[12] Weil R. Sodium citrate in the transfusion of blood. J Am Med Assoc 1915;LXIV:425–6.

[13] Landsteiner K, Wiener AS. An agglutinable factor in human blood recognized by immune sera for rhesus blood. Exp Biol and Med 1940;43:223–3.

[14] Voronoy U. Sobre bloqueo del aparato reticuloendotelial del hombre en algunas formas de intoxicacion por el sublimado y sobre la transplantacion del rinon cadaverico como metodo de tratamiento de la anuria consecutiva a aquella intoxicacion. (Blocking the reticuloendothelial system in man in some forms of mercuric chloride intoxication and the transplantation of the cadaver kidney as a method of treatment for the anuria resulting from the intoxication.). Siglo Med 1937;97:296–7.

[15] Medawar PB. The behaviour and fate of skin autografts and skin homografts in rabbits: A report to the War Wounds Committee of the Medical Research Council. J Anat 1944;78:176–99.

[16] Gibson T, Medawar PB. The fate of skin homografts in man. J Anat 1943;77:299–294.

[17] Mitchison NA. Passive transfer of transplantation immunity. Proc R Soc Lond, B, Biol Sci 1954;142:72–87.

[18] Gorer P. The genetic and antigenic basis of tumour transplantation. J Pathol 1937;44:691-7.

[19] Gorer PA, Lyman S, Snell GD. Studies on the genetic and antigenic basis of tumour transplantation. Linkage between a histocompatibility gene and “fused” in mice. Proc R Soc B: Biol Sci 1948;135:499–505.

[20] Dausset J. Iso-leuco-anticorps. Acta Haematol 1958;20:156–66.

[21] van Rood JJ, van Leeuwen A. Leukocyte grouping. A method and its application. J Clin Invest 1963;42:1382.

[22] Merrill JP, Murray JE, Harrison JH, Guild WR. Successful homotransplantation of the human kidney between identical twins. J Am Med Assoc 1956;160:277–82.

[23] Gatti RA, Meuwissen HJ, Allen HD, Hong R, Good RA. Immunological reconstitution of sex-linked lymphopenic immunological deficiency. Lancet 1968;2:1366–9.

[24] Murray JE, Merrill JP, Harrison JH, Wilson RE, Dammin GJ. Prolonged survival of human-kidney homografts by immunosuppressive drug therapy. N Engl J Med 1963;268:1315–23.

[25] Hardy JD, Webb MS, Dalton ML, Walker GR. Lung homotransplantation in man. JAMA 1963;186:1065–74.

[26] Kelly WD, Lillehei RC, Merkel FK, Idezuki Y, Goetz FC. Allotransplantation of the pancreas and duodenum along with the kidney in diabetic nephropathy. Surgery 1967;61:827–37.

[27] Starzl TE, Groth CG, Brettschneider L, Penn I, Fulginiti VA, Moon JB, et al. Orthotopic homotransplantation of the human liver. Ann Surg 1968;168:392–415.

[28] Barnard MS. Heart transplantation: an experimental review and preliminary research. S Afr Med J 1967;41:1260–2.

[29] Borel JF, Feurer C, Magnee C, Stähelin H. Effects of the new anti-lymphocytic peptide cyclosporin A in animals. Immunology 1977;32:1017–25.

[30] Cohen DJ, Loertscher R, Rubin MF, Tilney NL, Carpenter CB, Strom TB. Cyclosporine: a new immunosuppressive agent for organ transplantation. Ann Intern Med 1984;101:667–82.

[31] Kino T, Hatanaka H, Hashimoto M, Nishiyama M, Goto T, Okuhara M, et al. FK-506, a novel immunosuppressant isolated from a Streptomyces. I. Fermentation, isolation, and physico-chemical and biological characteristics. J Antibiot 1987;40:1249–55.

[32] Sayegh MH, Carpenter CB. Transplantation 50 years later — progress, challenges, and promises. N Engl J Med 2004;351:2761–6.

[33] Todo S, Tzakis A, Starzl TE. Preservation of livers with UW or Euro-Collins' solution. Transplantation 1988;46:925–6.

[34] Yoglu M, Stratta R, Hoffmann R, Sollinger H, D'Alessandro A, Pirsch J, et al. Extended preservation of the liver for clinical transplantation. Lancet 1988;331:617–9.

[35] Ploeg RJ, Goossens D, McAnulty JF, Southard JH, Belzer FO. Successful 72-hour cold storage of dog kidneys with UW solution. Transplantation 1988;46:191–6.

[36] Global database on blood safety and availability 2012. World Health Organization; 2014.

[37] Maria J. International figures on donation and transplantation. vol. 18. Global Observatory

on Donation and Transplantation. World Health Organization; 2013.

[38] Canadian blood services annual report. Canadian Blood Services; 2012.

[39] Canadian organ replacement register annual report: treatment of end-stage organ failure in canada, 2001 to 2010. Canadian Institute for Health Information; 2011.

[40] United states organ transplantation: 2012 annual data report. Health Resources and Services Administration; 2014.

[41] Reid ME, Lomas-Francis C. The blood group antigen factsbook. 2nd ed. San Diego: Academic Press; 2004.

[42] Gunson HH, Stratton F, Cooper DG, Rawlinson VI. Primary immunization of Rh-negative volunteers. Br Med J 1970;1:593–5.

[43] Pollack W, Ascari WQ, Crispen JF, OConnor RR, Ho TY. Studies on Rh prophylaxis: II Rh immune prophylaxis after transfusion with Rh-positive blood. Transfusion 1971;11:340–4.

[44] A S, AL K, MR S, U S. Incidence and persistence of anti-kell after transfusion of kell-positive blood. Beitr Infusionsther Transfusionsmed 1994;32:175–8.

[45] Norol F, Nadjahi J, Bachir D, Desaint C. Transfusion and alloimmunization in sickle cell anemia patients. Transfusion Clinique Et Biologique 1994;1:27.

[46] Schonewille H, van de Watering LMG, Brand A. Additional red blood cell alloantibodies after blood transfusions in a nonhematologic alloimmunized patient cohort: is it time to take precautionary measures? Transfusion 2006;46:630–5.

[47] Schonewille H. Red blood cell alloimmunization after blood transfusion. Leiden University, 2008.

[48] Issitt PD. Race-related red cell alloantibody problems. Br J Biomed Sci 1994;51:158–67.

[49] Vichinsky EP, Earles A, Johnson RA, Hoag MS, Williams A, Lubin B. Alloimmunization in sickle cell anemia and transfusion of racially unmatched blood. N Engl J Med 1990;322:1617–21.

[50] Yazdanbakhsh K, Ware RE, Noizat-Pirenne F. Red blood cell alloimmunization in sickle cell disease: pathophysiology, risk factors, and transfusion management. Blood 2012;120:528–37.

[51] LaSalle-Williams M, Nuss R, Le T, Cole L, Hassell K, Murphy JR, et al. Extended red blood cell antigen matching for transfusions in sickle cell disease: a review of a 14-year experience from a single center. Transfusion 2011;51:1732–9.

[52] Choo SYS. The HLA system: genetics, immunology, clinical testing, and clinical implications. Yonsei Med J 2007;48:11–23.

[53] Holling TM, Schooten E, van Den Elsen PJ. Function and regulation of MHC class II molecules in T-lymphocytes: of mice and men. Hum Immunol 2004;65:282–90.

[54] Navarrete C. Human leukocyte antigens. 3rd ed. Oxford: Wiley-Blackwell; 2009.

[55] Robinson J, Halliwell JA, McWilliam H, Lopez R, Parham P, Marsh SGE. The IMGT/HLA database. Nucleic Acids Res 2012;41:D1222–7.

[56] Prugnolle F, Manica A, Charpentier M, Guégan JF, Guernier V, Balloux F. Pathogen-driven selection and worldwide HLA class I diversity. Curr Biol 2005;15:1022–7.

[57] Sanchez-Mazas A, Lemaître J-F, Currat M. Distinct evolutionary strategies of human leucocyte antigen loci in pathogen-rich environments. Philos Trans R Soc Lond, B, Biol Sci 2012;367:830–9.

[58] Murphy K. Janeway's immunobiology, 8th Edition - Kenneth M. Murphy. 8 ed. New York: Garland Science; 2011.

[59] Afzali B, Lechler RI, Hernandez-Fuentes MP. Allorecognition and the alloresponse: clinical implications. Tissue Antigens 2007;69:545–56.

[60] Benichou G, Valujskikh A, Heeger PS. Contributions of direct and indirect T cell alloreactivity during allograft rejection in mice. J Immunol 1999;162:352–8.

[61] Manning DD, Reed ND, Shaffer CF. Maintenance of skin xenografts of widely divergent phylogenetic origin of congenitally athymic (nude) mice. J Exp Med 1973;138:488–94.

[62] Gras S, Kjer-Nielsen L, Chen Z, Rossjohn J, McCluskey J. The structural bases of direct T-cell allorecognition: implications for T-cell-mediated transplant rejection. Immunol Cell Biol 2011;89:388–95.

[63] Sherman LA, Chattopadhyay S. The molecular basis of allorecognition. Ann Rev Immunol 1993;11:385–402.

[64] Suchin EJ, Langmuir PB, Palmer E, Sayegh MH, Wells AD, Turka LA. Quantifying the frequency of alloreactive T cells in vivo: new answers to an old question. J Immunol 2001;166:973–81.

[65] Smith C, Miles JJ, Khanna R. Advances in direct T-cell alloreactivity: function, avidity, biophysics and structure. Am J Transplant 2011;12:15–26.

[66] Roopenian D, Choi EY, Brown A. The immunogenomics of minor histocompatibility antigens. Immunol Rev 2002;190:86–94.

[67] Artyomov MN, Lis M, Devadas S, Davis MM, Chakraborty AK. CD4 and CD8 binding to MHC molecules primarily acts to enhance Lck delivery. Proc Natl Acad Sci USa 2010;107:16916–21.

[68] Garcia KC, Scott CA, Brunmark A, Carbone FR, Peterson PA, Wilson IA, et al. CD8 enhances formation of stable T-cell receptor/MHC class I molecule complexes. Nature 1996;384:577–81.

[69] Killeen N, Stuart SG, Littman DR. Development and function of T cells in mice with a disrupted CD2 gene. Embo J 1992;11:4329–36.

[70] Bachmann MF, Barner M, Kopf M. CD2 sets quantitative thresholds in T cell activation. J Exp Med 1999;190:1383–92.

[71] Sasada T, Yang H, Reinherz EL. CD2 facilitates differentiation of CD4 Th cells without affecting Th1/Th2 polarization. J Immunol 2002;168:1113–22.

[72] Mempel TR, Henrickson SE, Andrian Von UH. T-cell priming by dendritic cells in lymph nodes occurs in three distinct phases. Cell Mol Immunol 2004;427:154–9.

[73] Li N, Zhu F, Gao F, Wang Q, Wang X, Li H, et al. Blockade of CD28 by a synthetical peptoid inhibits T-cell proliferation and attenuates graft-versus-host disease. Cell Mol Immunol 2010;7:133–42.

[74] Lenschow DJ, Walunas TL, Bluestone JA. CD28/B7 system of T cell costimulation. Ann Rev Immunol 1996;14:233–58.

[75] Mesturini R, Nicola S, Chiocchetti A, Bernardone IS, Castelli L, Bensi T, et al. ICOS cooperates with CD28, IL-2, and IFN-gamma and modulates activation of human naïve CD4+ T cells. Eur J Immunol 2006;36:2601–12.

[76] Zavazava N, Kabelitz D. Alloreactivity and apoptosis in graft rejection and transplantation tolerance. J Leukoc Biol 2000;68:167–74.

[77] Gimmi CD, Freeman GJ, Gribben JG, Gray G, Nadler LM. Human T-cell clonal anergy is induced by antigen presentation in the absence of B7 costimulation. Proc Natl Acad Sci USa 1993;90:6586–90.

[78] Walunas TL, Lenschow DJ, Bakker CY, Linsley PS, Freeman GJ, Green JM, et al. CTLA-4 can function as a negative regulator of T cell activation. Immunity 1994;1:405–13.

[79] Trivedi HL. Immunobiology of rejection and adaptation. Transplant Proc 2007;39:647–52.

[80] Nishimura H, Nose M, Hiai H, Minato N, Honjo T. Development of lupus-like autoimmune diseases by disruption of the PD-1 gene encoding an ITIM motif-carrying immunoreceptor. Immunity 1999;11:141–51.

[81] Lin H, Rathmell JC, Gray GS, Thompson CB, Leiden JM, Alegre ML. Cytotoxic T lymphocyte antigen 4 (CTLA4) blockade accelerates the acute rejection of cardiac allografts in CD28-deficient mice: CTLA4 can function independently of CD28. J Exp Med 1998;188:199–204.

[82] Duke RC, Cohen JJ. IL-2 addiction: withdrawal of growth factor activates a suicide program in dependent T cells. Lymphokine Res 1986;5:289–99.

[83] Kuroda K, Yagi J, Imanishi K, Yan XJ, Li XY, Fujimaki W, et al. Implantation of IL-2-containing osmotic pump prolongs the survival of superantigen-reactive T cells expanded in mice injected with bacterial superantigen. J Immunol 1996;157:1422–31.

[84] Le Gros G, Ben-Sasson SZ, Seder R, Finkelman FD, Paul WE. Generation of interleukin 4 (IL-4)-producing cells in vivo and in vitro: IL-2 and IL-4 are required for in vitro generation of IL-4-producing cells. J Exp Med 1990;172:921–9.

[85] Lighvani AA, Frucht DM, Jankovic D, Yamane H, Aliberti J, Hissong BD, et al. T-bet is rapidly induced by interferon-gamma in lymphoid and myeloid cells. Proc Natl Acad Sci USA 2001;98:15137–42.

[86] Zhou L, Ivanov II, Spolski R, Min R, Shenderov K, Egawa T, et al. IL-6 programs TH-17 cell differentiation by promoting sequential engagement of the IL-21 and IL-23 pathways. Nat Immunol 2007;8:967–74.

[87] Veldhoen M, Hocking RJ, Atkins CJ, Locksley RM, Stockinger B. TGFβ in the Context of an inflammatory cytokine milieu supports de novo differentiation of IL-17-producing T cells. Immunity 2006;24:179–89.

[88] Piccotti JR, Chan SY, VanBuskirk AM, Eichwald EJ, Bishop DK. Are Th2 helper T lymphocytes beneficial, deleterious, or irrelevant in promoting allograft survival? Transplantation 1997;63:619–24.

[89] Nickerson P, Steiger J, Zheng XX, Steele AW, Steurer W, Roy-Chaudhury P, et al. Manipulation of cytokine networks in transplantation: false hope or realistic opportunity for tolerance? Transplantation 1997;63:489–94.

[90] Moore KW, de Waal Malefyt R, Coffman RL, O'Garra A. Interleukin-10 and the interleukin-10 receptor. Ann Rev Immunol 2001;19:683–765.

[91] Li MO, Sanjabi S, Flavell RA. Transforming growth factor-β controls development, homeostasis, and tolerance of T cells by regulatory T cell-dependent and -independent mechanisms. Immunity 2006;25:455–71.

[92] Kang SM, Tang Q, Bluestone JA. CD4+CD25+ regulatory T cells in transplantation: progress, challenges and prospects. Am J Transplant 2007;7:1457–63.

[93] Di Ianni M, Falzetti F, Carotti A, Terenzi A, Castellino F, Bonifacio E, et al. Tregs prevent GVHD and promote immune reconstitution in HLA-haploidentical transplantation. Blood 2011;117:3921–8.

[94] Rathmell JC, Thompson CB. Pathways of apoptosis in lymphocyte development, homeostasis, and disease. Cell 2002;109:S97–S107.

[95] Fujiki M, Esquivel CO, Martinez OM, Strober S, Uemoto S, Krams SM. Induced tolerance to rat liver allografts involves the apoptosis of intragraft T cells and the generation of CD4(+)CD25(+)FoxP3(+) T regulatory cells. Liver Transpl 2010;16:147–54.

[96] Sun E, Gao Y, Chen J, Roberts AI, Wang X, Chen Z, et al. Allograft tolerance induced by donor apoptotic lymphocytes requires phagocytosis in the recipient. Cell Death Diff 2004;11:1258–64.

[97] Colvin RB, Smith RN. Antibody-mediated organ-allograft rejection. Nat Rev Immunol 2005;5:807–17.

[98] Lanzavecchia A. Antigen-specific interaction between T and B cells. Nature 1985;314:537–9.

[99] Game DS, Lechler RI. Pathways of allorecognition: implications for transplantation tolerance. Transpl Immunol 2002;10:101–8.

[100] Lechler RI, Batchelor JR. Immunogenicity of retransplanted rat kidney allografts. Effect of inducing chimerism in the first recipient and quantitative studies on immunosuppression of the second recipient. J Exp Med 1982;156:1835–41.

[101] Lechler RI, Batchelor JR. Restoration of immunogenicity to passenger cell-depleted kidney allografts by the addition of donor strain dendritic cells. J Exp Med 1982;155:31–41.

[102] Lafferty KJ, Cooley MA, Woolnough J, Walker KZ. Thyroid allograft immunogenicity is reduced after a period in organ culture. Science 1975;188:259–61.

[103] Pietra BA, Wiseman A, Bolwerk A, Rizeq M, Gill RG. CD4 T cell-mediated cardiac allograft rejection requires donor but not host MHC class II. J Clin Invest 2000;106:1003–10.

[104] Conlon TM, Saeb-Parsy K, Cole JL, Motallebzadeh R, Qureshi MS, Rehakova S, et al.

Germinal center alloantibody responses are mediated exclusively by indirect-pathway CD4 T follicular helper cells. J Immunol 2012;188:2643–52.

[105] Chen AM, Scott MD. Current and future applications of immunological attenuation via pegylation of cells and tissue. BioDrugs 2001;15:833–47.

[106] Pilmore HL, Painter DM, Bishop GA, McCaughan GW, Eris JM. Early up-regulation of macrophages and myofibroblasts: a new marker for development of chronic renal allograft rejection. Transplantation 2000;69:2658–62.

[107] Wyburn KR, Jose MD, Wu H, Atkins RC, Chadban SJ. The role of macrophages in allograft rejection. Transplantation 2005;80:1641–7.

[108] Hancock WW, Thomson NM, Atkins RC. Composition of interstitial cellular infiltrate identified by monoclonal antibodies in renal biopsies of rejecting human renal allografts. Transplantation 1983;35:458–63.

[109] Cutbush M, Mollison PL. Relation between characteristics of blood-group antibodies in vitro and associated patterns of red-cell destruction in vivo. Br J Haematol 1958;4:115–37.

[110] Hughes Jones NC, Mollison PL, Veall N. Removal of incompatible red cells by the spleen. Br J Haematol 1957;3:125–33.

[111] Stowell SR, Winkler AM, Maier CL, Arthur CM, Smith NH, Girard-Pierce KR, et al. Initiation and regulation of complement during hemolytic transfusion reactions. Clin Dev Immunol 2012;2012:1–12.

[112] Platt JL. Antibodies in transplantation. Discovery Medicine 2010;10:125.

[113] Doxiadis II, Smits JM, Schreuder GM, Persijn GG, van Houwelingen HC, van Rood JJ, et al. Association between specific HLA combinations and probability of kidney allograft loss: the taboo concept. Lancet 1996;348:850–3.

[114] Schonewille H, Haak HL, van Zijl AM. RBC antibody persistence. Transfusion 2000;40:1127–31.

[115] Reverberi R. The persistence of red cell alloantibodies. Blood Transfusion 2008;6:225.

[116] Kacker S, Ness PM, Savage WJ, Frick KD, Shirey RS, King KE, et al. Cost-effectiveness of prospective red blood cell antigen matching to prevent alloimmunization among sickle cell patients. Transfusion 2014;54:86–97.

[117] Ho VT, Soiffer RJ. The history and future of T-cell depletion as graft-versus-host disease prophylaxis for allogeneic hematopoietic stem cell transplantation. Blood 2001;98:3192–204.

[118] Barnes PJ. Corticosteroid effects on cell signalling. Eur Respir J 2006;27:413–26.

[119] Smith L. Corticosteroids in solid organ transplantation: update and review of the literature. J Pharm Pract 2003;16:380–7.

[120] Tiede I, Fritz G, Strand S, Poppe D, Dvorsky R, Strand D, et al. CD28-dependent Rac1 activation is the molecular target of azathioprine in primary human CD4+ T lymphocytes. J Clin Invest 2003;111:1133–45.

[121] van Sandwijk MS, Bemelman FJ, Berge Ten IJM. Immunosuppressive drugs after solid organ transplantation. Neth J Med 2013;71:281–9.

[122] Clipstone NA, Crabtree GR. Identification of calcineurin as a key signalling enzyme in T-lymphocyte activation. Nature 1992;357:695–7.

[123] Nourse J, Firpo E, Flanagan WM, Coats S, Polyak K, Lee MH, et al. Interleukin-2-mediated elimination of the p27Kip1 cyclin-dependent kinase inhibitor prevented by rapamycin. Nature 1994;372:570–3.

[124] Battaglia M, Stabilini A, Migliavacca B, Horejs-Hoeck J, Kaupper T, Roncarolo M-G. Rapamycin promotes expansion of functional CD4+CD25+FOXP3+ regulatory T cells of both healthy subjects and type 1 diabetic patients. J Immunol 2006;177:8338–47.

[125] Pilat N, Sayegh MH, Wekerle T. Costimulatory pathways in transplantation. Semin Immunol 2011;23:293–303.

[126] Kirk AD, Harlan DM, Armstrong NN, Davis TA, Dong Y, Gray GS, et al. CTLA4-Ig and anti-CD40 ligand prevent renal allograft rejection in primates. Proc Natl Acad Sci USA 1997;94:8789–94.

[127] Levisetti MG, Padrid PA, Szot GL, Mittal N, Meehan SM, Wardrip CL, et al. Immunosuppressive effects of human CTLA4Ig in a non-human primate model of allogeneic pancreatic islet transplantation. J Immunol 1997;159:5187–91.

[128] Suntharalingam G, Perry MR, Ward S, Brett SJ, Castello-Cortes A, Brunner MD, et al. Cytokine storm in a phase 1 trial of the anti-CD28 monoclonal antibody TGN1412. N Engl J Med 2006;355:1018–28.

[129] Abuchowski A, van Es T, Palczuk NC, Davis FF. Alteration of immunological properties of bovine serum albumin by covalent attachment of polyethylene glycol. J Biol Chem 1977;252:3578–81.

[130] Abuchowski A, McCoy JR, Palczuk NC, van Es T, Davis FF. Effect of covalent attachment of polyethylene glycol on immunogenicity and circulating life of bovine liver catalase. J Biol Chem 1977;252:3582–6.

[131] Hershfield MS, Buckley RH, Greenberg ML, Melton AL, Schiff R, Hatem C, et al. Treatment of adenosine deaminase deficiency with polyethylene glycol-modified adenosine deaminase. N Engl J Med 1987;316:589–96.

[132] Mehvar R. Modulation of the pharmacokinetics and pharmacodynamics of proteins by polyethylene glycol conjugation. J Pharm Pharm Sci 2000;3:125–36.

[133] Greenwald RB, Choe YH, McGuire J, Conover CD. Effective drug delivery by PEGylated drug conjugates. Adv Drug Deliv Rev 2003;55:217–50.

[134] Harris JM, Chess RB. Effect of pegylation on pharmaceuticals. Nat Rev Drug Discov 2003;2:214–21.

[135] Scott MD, Murad KL, Koumpouras F, Talbot M, Eaton JW. Chemical camouflage of antigenic determinants: stealth erythrocytes. Proc Natl Acad Sci USA 1997;94:7566–71.

[136] Murad KLK, Mahany KLK, Brugnara CC, Kuypers FAF, Eaton JWJ, Scott MDM. Structural and functional consequences of antigenic modulation of red blood cells with methoxypoly(ethylene glycol). Blood 1999;93:2121–7.

[137] Murad KLK, Gosselin EJE, Eaton JWJ, Scott MDM. Stealth cells: prevention of major histocompatibility complex class II-mediated T-cell activation by cell surface modification. Blood 1999;94:2135–41.

[138] Chen AM, Scott MD. Immunocamouflage: prevention of transfusion-induced graft-versus-host disease via polymer grafting of donor cells. J Biomed Mater Res A 2003;67:626–36.

[139] Lee DY, Park SJ, Nam JH, Byun Y. A combination therapy of PEGylation and immunosuppressive agent for successful islet transplantation. J Control Release 2006;110:290–5.

[140] McCoy JR, Scott MD. Antiviral drug discovery for emerging diseases and bioterrorism threats. Hoboken: John Wiley & Sons; 2005.

[141] Sutton TC, Scott MD. The effect of grafted methoxypoly(ethylene glycol) chain length on the inhibition of respiratory syncytial virus (RSV) infection and proliferation. Biomaterials 2010;31:4223–30.

[142] Maruyama K, Okuizumi S, Ishida O, Yamauchi H, Kikuchi H, Iwatsuru M. Phosphatidyl polyglycerols prolong liposome circulation in vivo. Int J Pharm 1994;111:103–7.

[143] Oudshoorn MHM, Rissmann R, Bouwstra JA, Hennink WE. Synthesis and characterization of hyperbranched polyglycerol hydrogels. Biomaterials 2006;27:5471–9.

[144] Stiriba S-E, Kautz H, Frey H. Hyperbranched molecular nanocapsules: comparison of the hyperbranched architecture with the perfect linear analogue. J Am Chem Soc 2002;124:9698–9.

[145] Rossi NAA, Constantinescu I, Kainthan RK, Brooks DE, Scott MD, Kizhakkedathu JN. Red blood cell membrane grafting of multi-functional hyperbranched polyglycerols. Biomaterials 2010;31:4167–78.

[146] Chapanian R, Constantinescu I, Brooks DE, Scott MD, Kizhakkedathu JN. In vivo circulation, clearance, and biodistribution of polyglycerol grafted functional red blood cells. Biomaterials 2012;33:3047–57.

[147] Chapanian R, Constantinescu I, Rossi NAA, Medvedev N, Brooks DE, Scott MD, et al. Influence of polymer architecture on antigens camouflage, CD47 protection and complement mediated lysis of surface grafted red blood cells. Biomaterials 2012;33:7871–83.

[148] Kyluik-Price DL, Li L, Scott MD. Comparative efficacy of blood cell immunocamouflage by membrane grafting of methoxypoly(ethylene glycol) and polyethyloxazoline. Biomaterials 2014;35:412–22.

[149] Mero A, Fang Z, Pasut G, Veronese FM, Viegas TX. Selective conjugation of poly(2-ethyl 2-oxazoline) to granulocyte colony stimulating factor. J Control Release 2012;159:353–61.

[150] Viegas TX, Bentley MD, Harris JM, Fang Z, Yoon K, Dizman B, et al. Polyoxazoline: chemistry, properties, and applications in drug delivery. Bioconjugate Chem 2011;22:976–86.

[151] Knop K, Hoogenboom R, Fischer D, Schubert US. Poly(ethylene glycol) in drug delivery: pros and cons as well as potential alternatives. Angew Chem Int Ed 2010;49:6288–308.

[152] Roberts MJ, Bentley MD, Harris JM. Chemistry for peptide and protein PEGylation. Adv Drug Deliv Rev 2002;54:459–76.

[153] Parveen S, Sahoo SK. Nanomedicine: clinical applications of polyethylene glycol conjugated proteins and drugs. Clin Pharmacokinet 2006;45:965–88.

[154] Veronese FM. Peptide and protein PEGylation: a review of problems and solutions. Biomaterials 2001;22:405–17.

[155] Nelson DL, Cox MM. Lehninger principles of biochemistry. W. H. Freeman; 2013.

[156] Le Y, Scott MD. Immunocamouflage: the biophysical basis of immunoprotection by grafted methoxypoly(ethylene glycol) (mPEG). Acta Biomater 2010;6:2631–41.

[157] Mero A, Pasut G, Via LD, Fijten MW, Schubert US, Hoogenboom R, et al. Synthesis and characterization of poly(2-ethyl 2-oxazoline)-conjugates with proteins and drugs: suitable alternatives to PEG-conjugates? J Control Release 2008;125:87–95.

[158] Manjula BN, Tsai A, Upadhya R, Perumalsamy K, Smith PK, Malavalli A, et al. Site-specific PEGylation of hemoglobin at Cys-93(beta): correlation between the colligative properties of the PEGylated protein and the length of the conjugated PEG chain. Bioconjugate Chem 2003;14:464–72.

[159] Torchilin VP, Trubetskoy VS. Which polymers can make nanoparticulate drug carriers long-circulating? Adv Drug Deliv Rev 1995;16:141–55.

[160] Zhang N. Molecular Brushes of Poly(2-oxazoline)s. Technische Universitat Munchen, 2010.

[161] Chen FP, Ames AE, Taylor LD. Aqueous solutions of poly (ethyloxazoline) and its lower consolute phase transition. Macromolecules 1990;23:4688–95.

[162] de Gennes P. Conformations of polymers attached to an interface. Macromolecules 1980;13:1069–75.

[163] Goddard P, Hutchinson LE, Brown J, Brookman LJ. Soluble polymeric carriers for drug delivery. Part 2. Preparation and in vivo behaviour of N-acylethylenimine copolymers. J Control Release 1989;10:5–16.

[164] Gaertner FC, Luxenhofer R, Blechert B, Jordan R, Essler M. Synthesis, biodistribution and excretion of radiolabeled poly(2-alkyl-2-oxazoline)s. J Control Release 2007;119:291–300.

[165] Webster R, Didier E, Harris P, Siegel N, Stadler J, Tilbury L, et al. PEGylated proteins: evaluation of their safety in the absence of definitive metabolism studies. Drug Metab Dispos 2007;35:9–16.

[166] Yamaoka T, Tabata Y, Ikada Y. Distribution and tissue uptake of poly(ethylene glycol) with different molecular weights after intravenous administration to mice. J Pharm Sci 1994;83:601–6.

[167] Chen AM, Scott MD. Comparative analysis of polymer and linker chemistries on the efficacy of immunocamouflage of murine leukocytes. Artif Cells Blood Substit Immobil Biotechnol 2006;34:305–22.

[168] Fruijtier-Pölloth C. Safety assessment on polyethylene glycols (PEGs) and their derivatives as used in cosmetic products. Toxicology 2005;214:1–38.

[169] Working PK, Newman MS. Safety of the poly(ethylene glycol) and poly(ethylene glycol) derivatives. Poly(ethylene glycol); 1997.

[170] Prentice DE, Majeed SK. Oral toxicity of polyethylene glycol (PEG 200) in monkeys and rats. Toxicol Lett 1978;2:119–22.

[171] Shaffer CB, Critchfield FH. The absorption and excretion of a liquid polyethylene glycol. J Am Pharm Assoc Am Pharm Assoc 1950;39:340–4.

[172] Richter AW, Akerblom E. Polyethylene glycol reactive antibodies in man: titer distribution in allergic patients treated with monomethoxy polyethylene glycol modified allergens or placebo, and in healthy blood donors. Int Arch Allergy Appl Immunol 1984;74:36–9.

[173] Ganson NJ, Kelly SJ, Scarlett E, Sundy JS, Hershfield MS. Control of hyperuricemia in subjects with refractory gout, and induction of antibody against poly(ethylene glycol) (PEG), in a phase I trial of subcutaneous PEGylated urate oxidase. Arthritis Res Ther 2006;8:R12.

[174] Armstrong JK, Hempel G, Koling S, Chan LS, Fisher T, Meiselman HJ, et al. Antibody against poly(ethylene glycol) adversely affects PEG-asparaginase therapy in acute lymphoblastic leukemia patients. Cancer 2007;110:103–11.

[175] Sroda K, Rydlewski J, Langner M, Kozubek A, Grzybek M, Sikorski AF. Repeated injections of PEG-PE liposomes generate anti-PEG antibodies. Cell Mol Biol Lett 2005;10:37–47.

[176] Sundy JS, Ganson NJ, Kelly SJ, Scarlett EL, Rehrig CD, Huang W, et al. Pharmacokinetics and pharmacodynamics of intravenous PEGylated recombinant mammalian urate oxidase in patients with refractory gout. Arthritis Rheum 2007;56:1021–8.

[177] Scagnolari C, Trombetti S, Soldà A, Milella M, Gaeta GB, Angarano G, et al. Development and specificities of anti-interferon neutralizing antibodies in patients with chronic hepatitis C treated with pegylated interferon-α. Clin Microbiol Infec 2011;18:1033–9.

[178] Tillmann H, Ganson NJ, Patel K, Thompson AJ, Abdelmalek M, Moody T, et al. High prevalence of pre-existing antibodies against polyethylene glycol (PEG) in hepatitis C (HCV) patients which is not associated with impaired response to PEG-Interferon. J Hepatol 2010;52:S129–9.

[179] Armstrong JK, Leger R, Wenby RB, Meiselman HJ, Garratty G, Fisher TC. Occurrence of an antibody to poly(ethylene glycol) in normal donors. Blood 2003:556A.

[180] Liu Y, Reidler H, Pan J, Milunic D, Qin D, Chen D, et al. A double antigen bridging immunogenicity ELISA for the detection of antibodies to polyethylene glycol polymers. J Pharmacol Toxicol Methods 2011;64:238–45.

[181] Richter AW, Akerblom E. Antibodies against polyethylene glycol produced in animals by immunization with monomethoxy polyethylene glycol modified proteins. Int Arch Allergy Appl Immunol 1983;70:124–31.

[182] Cheng TL, Wu PY, Wu MF, Chern JW, Roffler SR. Accelerated clearance of polyethylene glycol-modified proteins by anti-polyethylene glycol IgM. Bioconjugate Chem 1999;10:520–8.

[183] Scott MD, Murad KL. Cellular camouflage: fooling the immune system with polymers. Curr Pharm Des 1998;4:423–38.

[184] Graham ML. Pegaspargase: a review of clinical studies. Adv Drug Deliv Rev 2003;55:1293–

302.

[185] Veronese FM, Mero A. The impact of PEGylation on biological therapies. BioDrugs 2008;22:315–29.

[186] Immordino ML, Dosio F, Cattel L. Stealth liposomes: review of the basic science, rationale, and clinical applications, existing and potential. Int J Nanomedicine 2006;1:297.

[187] Allen C, Santos Dos N, Gallagher R, Chiu GNC, Shu Y, Li WM, et al. Controlling the physical behavior and biological performance of liposome formulations through use of surface grafted poly(ethylene glycol). Biosci Rep 2002;22:225–50.

[188] Orive G, Hernández RM, Gascón AR, Calafiore R, Chang TMS, De Vos P, et al. Cell encapsulation: promise and progress. Nat Med 2003;9:104–7.

[189] Gonen-Wadmany M, Goldshmid R, Seliktar D. Biological and mechanical implications of PEGylating proteins into hydrogel biomaterials. Biomaterials 2011;32:6025–33.

[190] Wang D, Toyofuku WM, Chen AM, Scott MD. Induction of immunotolerance via mPEG grafting to allogeneic leukocytes. Biomaterials 2011;32:9494–503.

[191] Mizouni SK, Lehman JM, Cohen B. Viral modification with methoxypoly(ethylene glycol): Implications for gene therapy and viral inactivation. Blood 1998;92:379.

[192] Yun Lee D, Hee Nam J, Byun Y. Functional and histological evaluation of transplanted pancreatic islets immunoprotected by PEGylation and cyclosporine for 1 year. Biomaterials 2007;28:1957–66.

[193] Lee DY. Islet surface PEGylation attenuate the instant blood-mediated inflammatory reaction in intrahepatic islet transplantation. J Genet 2011;19:904–10.

[194] Brooks DE, Norris-Jones R. [2] Preparation and analysis of two-phase systems. Methods Enzymol, vol. 228, Elsevier; 1994, pp. 14–27.

[195] Bradley AJ, Murad KL, Regan KL, Scott MD. Biophysical consequences of linker chemistry and polymer size on stealth erythrocytes: size does matter. Biochim Biophys Acta 2002;1561:147–58.

[196] Bradley AJ, Scott MD. Separation and purification of methoxypoly(ethylene glycol) grafted red blood cells via two-phase partitioning. J Chromatogr B Analyt Technol Biomed Life Sci 2004;807:163–8.

[197] Van Kampen EJ, Zijlstra WG. Standardization of hemoglobinometry II. The hemiglobincyanide method. Clin Chim Acta 1961;6:538–44.

[198] Wang D, Kyluik DL, Murad KL, Toyofuku WM, Scott MD. Polymer-mediated immunocamouflage of red blood cells: effects of polymer size on antigenic and immunogenic recognition of allogeneic donor blood cells. Sci Chi Life Sci 2011;54:589–98.

[199] Branch DR, Gallagher MT, Mison AP, Sy Siok Hian AL, Petz LD. In vitro determination of red cell alloantibody significance using an assay of monocyte-macrophage interaction with sensitized erythrocytes. Br J Haematol 1984;56:19–29.

[200] Rampersad GC, Suck G, Sakac D, Fahim S, Foo A, Denomme GA, et al. Chemical compounds that target thiol-disulfide groups on mononuclear phagocytes inhibit immune mediated phagocytosis of red blood cells. Transfusion 2005;45:384–93.

[201] Gallagher MT, Branch DR, Mison A, Petz LD. Evaluation of reticuloendothelial function in autoimmune hemolytic anemia using an in vitro assay of monocyte-macrophage interaction with erythrocytes. Exp Hematol 1983;11:82–9.

[202] Crew VK, Poole J, Long S, Warke N, Colavecchia C, Burton N, et al. Two MER2-negative individuals with the same novel CD151 mutation and evidence for clinical significance of anti-MER2. Transfusion 2008;48:1912–6.

[203] Arndt PA, Garratty G. A retrospective analysis of the value of monocyte monolayer assay results for predicting the clinical significance of blood group alloantibodies. Transfusion 2004;44:1273–81.

[204] Nance SJ, Arndt P, Garratty G. Predicting the clinical significance of red cell alloantibodies using a monocyte monolayer assay. Transfusion 1987;27:449–52.

[205] Grebe KM, Potter TA. Enumeration, phenotyping, and identification of activation events in conjugates between T cells and antigen-presenting cells by flow cytometry. Sci STKE 2002;2002:pl14.

[206] Tang MLM, Hale LPL, Steeber DAD, Tedder TFT. L-selectin is involved in lymphocyte migration to sites of inflammation in the skin: delayed rejection of allografts in L-selectin-deficient mice. J Immunol 1997;158:5191–9.

[207] Cosimi AB, Colvin RB, Burton RC, Winn HJ, Rubin R, Goldstein G, et al. Immunologic monitoring with monoclonal antibodies to human T-cell subsets. Transplant Proc 1981;13:1589–93.

[208] Adu D, Cockwell P, Ives NJ, Shaw J, Wheatley K. Interleukin-2 receptor monoclonal antibodies in renal transplantation: meta-analysis of randomised trials. BMJ 2003;326:789–9.

[209] Nakakura EK, McCabe SM, Zheng B, Shorthouse RA, Scheiner TM, Blank G, et al. Potent and effective prolongation by anti-LFA-1 monoclonal antibody monotherapy of non-primarily vascularized heart allograft survival in mice without T cell depletion. Transplantation 1993;55:412–7.

[210] Wells AD, Walsh MC, Bluestone JA, Turka LA. Signaling through CD28 and CTLA-4 controls two distinct forms of T cell anergy. J Clin Invest 2001;108:895–903.

[211] Bromley SK, Iaboni A, Davis SJ, Whitty A, Green JM, Shaw AS, et al. The immunological synapse and CD28-CD80 interactions. Nat Immunol 2001;2:1159–66.

[212] Bayer AL, Baliga P, Woodward JE. Transferrin receptor in T cell activation and transplantation. J Leukoc Biol 1998;64:19–24.

[213] Ware CF, Sanchez-Madrid F, Krensky AM, Burakoff SJ, Strominger JL, Springer TA. Human lymphocyte function associated antigen-1 (LFA-1): identification of multiple antigenic epitopes and their relationship to CTL-mediated cytotoxicity. J Immunol 1983;131:1182–8.

[214] Barclay AN, Brown MH, Law S, McKnight AJ. The leucocyte antigen factsbook. 2nd ed. San Diego: Academic Press; 1997.

[215] Shaw AS, Dustin ML. Making the T cell receptor go the distance: a topological view of T cell activation. Immunity 1997;6:361–9.

[216] Sun Z-YJ, Kim ST, Kim IC, Fahmy A, Reinherz EL, Wagner G. Solution structure of the CD3εδ ectodomain and comparison with CD3εγ as a basis for modeling T cell receptor topology and signaling. Proc Natl Acad Sci USa 2004;101:16867–72.

[217] Wang M, He H-J, Turko IV, Phinney KW, Wang L. Quantifying the cluster of differentiation 4 receptor density on human T lymphocytes using multiple reaction monitoring mass spectrometry. Anal Chem 2013;85:1773–7.

[218] Janes PW, Ley SC, Magee AI. Aggregation of lipid rafts accompanies signaling via the T cell antigen receptor. J Cell Biol 1999;147:447–61.

[219] Harder T, Scheiffele P, Verkade P, Simons K. Lipid domain structure of the plasma membrane revealed by patching of membrane components. J Cell Biol 1998;141:929–42.

[220] Nichols BJ. GM1-containing lipid rafts are depleted within clathrin-coated pits. Curr Biol 2003;13:686–90.

[221] Friedman RS, Beemiller P, Sorensen CM, Jacobelli J, Krummel MF. Real-time analysis of T cell receptors in naive cells in vitro and in vivo reveals flexibility in synapse and signaling dynamics. J Exp Med 2010;207:2733–49.

[222] Nobile C, Lind M, Miro F, Chemin K, Tourret M, Occhipinti G, et al. Cognate CD4+ T-cell-dendritic cell interactions induce migration of immature dendritic cells through dissolution of their podosomes. Blood 2008;111:3579–90.

[223] Miller MJ. Two-photon imaging of lymphocyte motility and antigen response in intact lymph node. Science 2002;296:1869–73.

[224] Jayo A, Conde I, Lastres P, Jiménez-Yuste V, González-Manchón C. Possible role for cellular FXIII in monocyte-derived dendritic cell motility. Eur J Cell Biol 2009;88:423–31.

[225] Dustin ML, Bromley SK, Kan Z, Peterson DA, Unanue ER. Antigen receptor engagement delivers a stop signal to migrating T lymphocytes. Proc Natl Acad Sci USa 1997;94:3909–13.

[226] Negulescu PA, Krasieva TB, Khan A, Kerschbaum HH, Cahalan MD. Polarity of T cell shape, motility, and sensitivity to antigen. Immunity 1996;4:421–30.

[227] O'Shaughnessy MJ, Vogtenhuber C, Sun K, Sitcheran R, Baldwin AS, Murphy WJ, et al. Ex vivo inhibition of NF-kappaB signaling in alloreactive T-cells prevents graft-versus-host disease. Am J Transplant 2009;9:452–62.

[228] Peters VA, Joesting JJ, Freund GG. IL-1 receptor 2 (IL-1R2) and its role in immune regulation. Brain Behav Immun 2013;32:1–8.

[229] Le Y. Immunocamouflage: the biophysical and biological basis of immunoprotection by grafted methoxypoly (ethylene glycol). University of British Columbia, 2010.

[230] Röpke C, Gladstone P, Nielsen M, Borregaard N, Ledbetter JA, Svejgaard A, et al. Apoptosis following interleukin-2 withdrawal from T cells: evidence for a regulatory role of CD18 (beta 2-integrin) molecules. Tissue Antigens 1996;48:127–35.

[231] Claret E, Renversez JC, Zheng X, Bonnefoix T, Sotto JJ. Valid estimation of IL2 secretion by PHA-stimulated T-cell clones absolutely requires the use of anti-CD25 monoclonal antibody to prevent IL2 consumption. Immunol Lett 1992;33:179–85.

[232] Mankelow TJ, Satchwell TJ, Burton NM. Refined views of multi-protein complexes in the erythrocyte membrane. Blood Cells Mol Dis 2012;49:1–10.

[233] Lillemeier BF, Mörtelmaier MA, Forstner MB, Huppa JB, Groves JT, Davis MM. TCR and Lat are expressed on separate protein islands on T cell membranes and concatenate during activation. Nat Immunol 2010;11:90–6.

[234] Damodaran VB, Fee CJ, Ruckh T, Popat KC. Conformational studies of covalently grafted poly(ethylene glycol) on modified solid matrices using X-ray photoelectron spectroscopy. Langmuir 2010;26:7299–306.

[235] Heuberger M, Drobek T, Spencer ND. Interaction forces and morphology of a protein-resistant poly(ethylene glycol) layer. Biophys J 2005;88:495–504.

[236] Rex S, Zuckermann MJ, Lafleur M, Silvius JR. Experimental and Monte Carlo simulation studies of the thermodynamics of polyethyleneglycol chains grafted to lipid bilayers. Biophys J 1998;75:2900–14.

[237] Van Der Meulen FW, De Bruin HG, Goosen PC, Bruynes EC, Joustra-Maas CJ, Telkamp HG, et al. Quantitative aspects of the destruction of red cells sensitized with IgG1 autoantibodies: an application of flow cytofluorometry. Br J Haematol 1980;46:47–56.

[238] Garratty G, Nance SJ. Correlation between in vivo hemolysis and the amount of red cell-bound IgG measured by flow cytometry. Transfusion 1990;30:617–21.

[239] Garratty G. Effect of cell-bound proteins on the in vivo survival of circulating blood cells. Gerontology 1991;37:68–94.

[240] Bradley AJ, Scott MD. Immune complex binding by immunocamouflaged [poly (ethylene glycol) grafted] erythrocytes. Am J Hematol 2007;82:970–5.

[241] Emlen W, Carl V, Burdick G. Mechanism of transfer of immune complexes from red blood cell CR1 to monocytes. Clin Exp Immunol 1992;89:8–17.

[242] Scott MD, Chen AM. Beyond the red cell: pegylation of other blood cells and tissues. Transfus Clin Biol 2004;11:40–6.

[243] Russell PS, Oliaro J. Compartmentalization in T-cell signalling: membrane microdomains and polarity orchestrate signalling and morphology. Immunol Cell Biol 2006;84:107–13.

[244] Yokosuka T, Sakata-Sogawa K, Kobayashi W, Hiroshima M, Hashimoto-Tane A, Tokunaga M, et al. Newly generated T cell receptor microclusters initiate and sustain T cell activation by recruitment of Zap70 and SLP-76. Nat Immunol 2005;6:1253–62.

[245] Viola AA, Schroeder SS, Sakakibara YY, Lanzavecchia AA. T lymphocyte costimulation mediated by reorganization of membrane microdomains. Science 1999;283:680–2.

[246] Schneider H, Smith X, Liu H, Bismuth G, Rudd CE. CTLA-4 disrupts ZAP70 microcluster formation with reduced T cell/APC dwell times and calcium mobilization. Eur J Immunol 2008;38:40–7.

[247] Mossman KD, Campi G, Groves JT, Dustin ML. Altered TCR signaling from geometrically repatterned immunological synapses. Science 2005;310:1191–3.

[248] Klammt C, Lillemeier BF. How membrane structures control T cell signaling. Front Immunol 2012;3:291.

[249] Gunzer M, Schäfer A, Borgmann S, Grabbe S, Zänker KS, Bröcker EB, et al. Antigen presentation in extracellular matrix: interactions of T cells with dendritic cells are dynamic, short lived, and sequential. Immunity 2000;13:323–32.

[250] Gijzen K, Tacken PJ, Zimmerman A, Ben Joosten, de Vries IJM, Figdor CG, et al. Relevance of DC-SIGN in DC-induced T cell proliferation. J Leukoc Biol 2007;81:729–40.

[251] Crabtree GR, Clipstone NA. Signal transmission between the plasma membrane and nucleus of T lymphocytes. Annu Rev Biochem 1994;63:1045–83.

[252] Altman A, Coggeshall KM, Mustelin T. Molecular events mediating T cell activation. vol. 48. Elsevier; 1990.

[253] Bonnefoy-Berard N, Verrier B, Vincent C, Revillard JP. Inhibition of CD25 (IL-2R alpha) expression and T-cell proliferation by polyclonal anti-thymocyte globulins. Immunology 1992;77:61–7.

[254] Bunting K, Wang J, Shannon MF. Control of interleukin-2 gene transcription: a paradigm for inducible, tissue-specific gene expression. Vitam Horm 2006;74:105–45.

[255] Stepkowski SM. Molecular targets for existing and novel immunosuppressive drugs. Expert Rev Mol Med 2000;2:1–23.

[256] Robinson MR, Korman BD, Korman NJ. Combination immunosuppressive therapies: the promise and the peril. Arch Dermatol 2007;143:1053–7.

[257] Kitchens WH, Larsen CP, Ford ML. Integrin antagonists for transplant immunosuppression: panacea or peril? Immunotherapy 2011;3:305–7.

[258] Barz M, Luxenhofer R, Zentel R, Vicent MJ. Overcoming the PEG-addiction: well-defined alternatives to PEG, from structure–property relationships to better defined therapeutics. Polym Chem 2011;2:1900–0.

[259] McMurtrey C, Lowe D, Buchli R, Royer D, Cate S, Osborn S, et al. Profiling class II HLA alloantibodies in transplant patient sera (P2222). J Immunol 2013;190:69.49.

[260] Powell JD, Pollizzi KN, Heikamp EB, Horton MR. Regulation of immune responses by mTOR. Ann Rev Immunol 2012;30:39–68.

[261] Delgoffe GM, Pollizzi KN, Waickman AT, Heikamp E, Meyers DJ, Horton MR, et al. The kinase mTOR regulates the differentiation of helper T cells through the selective activation of signaling by mTORC1 and mTORC2. Nat Immunol 2011;12:295–303.